Neuroprotective effects of heat shock proteins in experimental ischaemia: an MRI study

Romina Aron Badin

Thesis submitted for the Degree of Doctor in Philosophy

October 2005

Royal College of Surgeons Unit of Biophysics

Medical Molecular Biology Unit

Institute of Child Health

University of London

ProQuest LLC
789 East Eisenhower Parkway
P.O. Box 1346
Ann Arbor, MI 48106-1346

"We must never cease from exploration.
And the end of all our exploring
will be to arrive where we began
and to know the place
for the first time"

T.S. Elliot

Abstract

Heat shock proteins (HSPs) are molecular chaperones with essential roles in cellular function such as modulating the proteolytic machinery and accelerating cell repair. HSP overexpression has been observed *in vitro* and *in vivo* under stresses including heat, nutrient deprivation and ischaemia. Experiments in *in vivo* models of stroke indicate that transgenically overexpressed or virally delivered HSPs can enhance cell survival but cannot always reduce lesion size. This study aims to assess the protective effects of HSPs in a rat model of reversible focal cerebral ischaemia using magnetic resonance imaging (MRI) techniques to measure cerebral blood flow and lesion size.

The experiments described used three different herpes simplex virus (HSV) constructs: two potentially therapeutic vectors, HSV-HSP27 and HSV-HSP70, and an HSV-LacZ control vector. Initially, the localization and duration of expression from the viral vector used to deliver the HSP genes into the rat brain was assessed. Subsequently, the effect of pre-ischaemic intra-striatal microinjections of HSV-HSP27 and HSV-HSP70 was evaluated in a middle cerebral artery occlusion (MCAO) model of stroke. Finally, the effect of delivering the same HSPs 30 minutes after ischaemia was assessed. Behavioural tests were carried out in the latter study up to a month after MCAO in order to determine whether HSP treatment induced functional recovery as well as reduction in lesion size.

Results suggest that intracerebral microinjections with HSV-HSP27 have a neuroprotective effect *pre*-and *post*-ischaemia. Multislice T_2-weighted images show that HSP27 treatment results in a significant reduction in lesion size after MCAO, whereas HSP70 treatment does not affect lesion size compared to controls. Western blots confirm that virally-induced overexpression of both HSP27 and HSP70 is achieved in treated animals. For the first time, non–invasive MRI techniques were used to demonstrate the neuroprotective effect of HSP27 and not HSP70 in a rat model of reversible focal cerebral ischaemia.

Acknowledgements

I would like to thank my supervisors, Professor David S Latchman and Dr Mark F Lythgoe not only for their unconditional support and ideas but especially for their trust and vision that three years ago gave me the opportunity to undertake this great challenge. Professor David Gadian, has been a supervisor at heart and deserves special mention for his constant guidance, contagious critical drive to high scientific standards and for setting an inspirational scientific and human example.

I would also like to thank the people in the Department of Biophysics who have enriched my daily life and made my PhD pleasurable. In particular, Dr Martin King, for his simple brilliance and analytical expertise, Sally Dowsett, for her unconditional kindness and generosity, Mankin Choy for his sense of humour, friendship and advice, and Dr Ted Proctor, for the privilege of sharing his unique passion for science and life with me. I am grateful to Dr Miratul Muqit, Dr Samantha Alsbury and Dr Alexandra Zourlidou not only for their support but also for their help and teaching on cell lines, viruses and histology at the initial stages of my training. I am deeply indebted to Dr Mike Modo for his experimental advice, patience, teaching and availability at the final stages of my PhD. The completion of this project would have been impossible without the endless cups of coffee and pints shared with Dr Fernando Calamante, whose friendship came as an invaluable and unexpected gift. Needless to mention my family, friends and partner who silently accompanied me through this journey and without whom great achievements like this one would be worthless.

Declaration

All the experiments presented in this thesis are the work of Romina Aron Badin.

Publications

- Aron Badin R, Lythgoe M, van der Weerd L, Thomas D, Gadian D, Latchman D (2005). Neuroprotective effects of virally delivered HSPs in experimental stroke. *Journal of Cerebral Blood Flow and Metabolism* (in press).

- van der Weerd L, Lythgoe M, Aron Badin R, Valentim L, Akbar T, de Belleroche J, Latchman D, Gadian G (2005). Neuroprotective effects of HSP70 overexpression after cerebral ischaemia - An MRI study. *Experimental Neurology*, **195**:257-266.

- Bustamante J, Bersier G, Aron Badin R, Cymeryng C, Parodi A, Boveris A (2002). Sequential NO Production by Mitochondria and Endoplasmic Reticulum during Induced Apoptosis. *Nitric Oxide* **6**(3):333-341.

- Houseman MJ, Jackson AP, Al-Gazali LI, Aron Badin R, Roberts E, Mueller RF (2001). A novel mutation in a family with non-syndromic sensorineural hearing loss that disrupts the newly characterized *OTOF* long isoforms. *Journal of Medical Genetics* **38**:E25.

- Bustamante J, Bersier G, Romero M, Aron Badin R, Boveris A (2000). Nitric Oxide Production and Mitochondrial Dysfunction during Rat Thymocyte Apoptosis. *Archives of Biochemistry and Biophysics* **376**:239-247.

Abbreviations

AAV, adeno-associated virus

ADC, apparent diffusion coefficient

ADP/ ATP, adenosin diphosphate/ triphosphate

AIF, apoptosis inducing factor

Apaf-1, apoptotic protease activating factor-1

APS, ammonium persulfate

Ask-1, apoptosis signal-regulated kinase-1

ASL, arterial spin labelling

BBB, blood brain barrier

bp, base pairs

BHK, baby hamster kidney

BSA, bovine serum albumin

CA1/ CA3, cornu amonis 1/ 3 neurones

CASL, continuous arterial spin labelling

CBF, cerebral blood flow

CCA, common carotid artery

cDNA, complementary DNA

CMC, carboxymethyl cellulose

CMV, cytomegalovirus

CNS, central nervous system

CSF, cerebral spinal fluid

ddH_2O, double distilled H_2O

DMEM, Dulbecco's modified Eagle's medium

DMSO, dimethyl sulphoxide

DNA, deoxyribonucleic acid

DRG, dorsal root ganglion

DWI, diffusion weighted imaging

E, early genes

ECG, electrocardiogram

ECL, enhanced chemoluminescence

EPI, echo planar imaging

FADD, Fas-associated protein with death domain

FCS, foetal calf serum

FGM, full growth medium

G6PDH, glucose-6-dehydrogenase

GDNF, glial derived neurotrophic factor

GFP, green fluorescent protein

HBSS, Hank's balanced salt solution

HCF, host cell factor

HIV, human immunodeficiency virus

HP, hippocampal neurone

HSP, heat shock protein

HSV, herpes simplex virus

ICP, infected cell polypeptide

IE genes, immediately early genes

JNK, c-jun N-terminal kinase

L, late genes

LAT, latency associated transcript

MAP, mitogen-activated protein

MAPK, mitogen-activated protein kinase

MCA, middle cerebral artery

MCAO, middle cerebral artery occlusion

MOI, multiplicity of infection

MRI, magnetic resonance imaging

mRNA, messenger ribonucleic acid

MRS, magnetic resonance spectroscopy

NF-kB, nuclear factor kappa B

NMR, nuclear magnetic resonance

OD, optical density

PBS, phosphate buffered saline

PFA, paraformaldehyde

pfu, plaque forming unit

PKCdelta, protein kinase C delta

RF, radiofrequency

RG, retinal ganglion

ROS, reactive oxygen species

rpm, revolutions per minute

RT, room temperature

rt-PA, recombinant tissue plasminogen activator

SDS, sodium dodecyl sulphate

SE, spin echo

s.e.m., standard error of the mean

TE, echo time

TEMED, N,N,N',N'-tetramethyl-ethylenediamine

Tg, transgenic

TI, inversion time

TIA, transient ischaemic attack

TN, trigeminal nerve

TNF, tumour necrosis factor

TR, repetition time

TTC, 2,3,5-triphenyltetrazolium chloride

Tween 20, polyoxyethylene-sorbitan monolaurate

U_L/ U_S, unique long/ unique short

vhs, virion host shut-off protein

VP16, virion protein 16

X-gal, 4-Cl,5-bromo,3-indolyl-β-galactosidase

Table of Contents

Index of Tables & Figures

Chapter 1

Chapter 2

Chapter 3

Chapter 4

Chapter 5

Chapter 6

INTRODUCTION

Introduction Overview

The work presented in this thesis investigates the protective effects of overexpressing heat shock proteins (HSPs) *in vivo* in a rat model of cerebral ischaemia. Heat shock proteins are overexpressed through recombinant herpes simplex virus (HSV) type 1 vector-mediated transgene delivery to the brain prior to and after ischaemic insult respectively.

The general introduction of this thesis is divided into sections dealing with various aspects of this project. The first section will discuss the biology of heat shock proteins and the role of heat shock proteins in stress. The second section deals with pathological changes occurring during ischaemia and the use of magnetic resonance imaging (MRI) as a predictive, diagnostic and follow-up tool. The final part deals with the choice of vector and issues about gene delivery to the brain.

Chapter 1 *The biology of Heat Shock Proteins*

1.1 Introduction

Heat shock proteins were discovered in 1962 as part of an endogenous protective mechanism by which cells respond to environmental stress (Ritossa, 1962). Their name was initially derived from the observation that their expression was enhanced upon exposure to high temperatures that led to protein denaturation. In fact, "puffing" in the chromosomes of *Drosophila* salivary gland cells was noticed shortly after elevating the temperature to 37°C. Such changes in the DNA were due to increased expression of HSP70 and HSP26 (Tissieres *et al.*, 1974). It was later shown that HSPs were upregulated in many organisms, from yeast and bacteria to mammalian cells. Interestingly, the temperatures that triggered such induction varied according to the organisms' natural environment: from 28°C in trout and salmon, to 38°C in mammals and 60°C in thermophilic bacteria (for review see Lindquist, 1986; Lindquist and Craig, 1988; Feder & Hofmann, 1999). This phenomenon was observed not only after heat shock but also after a series of different insults such as ischaemia, nutrient deprivation and hypoxia, in keeping with the idea that raising HSP levels can protect cells from stress. This is why the term "stress proteins" was believed to be more appropriate than "heat shock proteins" when referring to this group. Without any specific knowledge of their function in the cell, their importance is highlighted by the fact that their expression is an immediate emergency response to stress and that the HSP protein coding domains have been conserved across prokaryotic and eukaryotic species throughout evolution (Latchman, 2001).

HSPs are in fact cellular chaperones that assist in protein folding of nascent polypeptides or proteins that have been denatured due to environmental stress. The generic mechanism by which they act involves binding to the exposed hydrophobic domains of nascent or misfolded polypeptides, thus avoiding undesired and/or potentially damaging interactions with other proteins or with themselves. Under

normal conditions many HSPs are constitutively expressed to ensure proteins achieve their correct 3D structure and functional conformation. They are also responsible for the localization of nascent polypeptides, by aiding protein targeting and translocation within different cellular compartments. They are sometimes involved in antigen presentation, steroid receptor function, intracellular trafficking of proteins to different organelles, multiprotein complex assembly, nuclear receptor binding and apoptosis amongst other housekeeping functions (Jakob *et al.*, 1993; Ehrnsperger *et al.*, 2000; Richter-Landsberg & Goldbaum, 2003; Latchman, 2004; Katschinski, 2004). Accelerating cell repair after stress is related not only to the abovementioned chaperoning activities but also to their ability to present denatured proteins to the proteasome for degradation and to their anti-apoptotic functions, which will be discussed later (see section 1.5).

The large HSP family consists of proteins with different sub-cellular anatomical and temporal distributions and functions and is divided into subfamilies named according to their molecular weight in kilo-Daltons (kDa) (Latchman, 1998). Some of the most studied HSPs include ubiquitin, HSP27, HSP56, HSP70 and HSP90 (Table 1.1). Certain HSPs, like HSP70, have been found to bind to co-chaperones in order to enhance their activity in the cell. Although these proteins have variable roles, it is clear that they are essential for the maintenance of cell viability. The following sections will only review the roles of HSP27 and HSP70 in detail because these are the only HSPs used in this study and the main ones investigated in neuroprotective experiments.

Heat shock protein	Known functions
HSP100/104	ATPase activity, tolerance to severe stress (yeasts), protein refolding
HSP90/94	Protein refolding, degradation & transport, steroid receptor binding, hormone signalling, cell cycle control, cooperates with HSP70
HSP70/72 GRP78/Bip	Oligomer dissociation, clathrin uncoating, protein trafficking & refolding, ATPase activity, nascent protein folding, prevents aggregation, anti- and pro-apoptotic, neuroprotective.
HSP60	Mitochondrial chaperonin, protein folding & unfolding (mycobacteria), organelle translocation
HSP40	Protein refolding, interacts with HSP70
HSP27	Cytoskeleton stabilization, protein solubilization, refolding and targeting for degradation, anti-apoptotic, redox control, neuroprotective
HSP10	Co-chaperone, mitochondrial

Table 1.1. HSP families and main known functions.

1.2 The heat shock protein 70 family

HSP70 is one of the largest and probably most studied families of chaperones. They are highly conserved proteins among eukaryotes and prokaryotes, the human HSP70 sharing more than 70% of its amino acid sequence with *Drosophila* and 50% with *E.coli* (Lindquist, 1986). As mentioned before, the degree of conservation throughout evolution reflects the importance of the biological functions performed by these groups of proteins. Moreover, the functional differentiation of this HSP family suggests that it has amplified and diversified throughout evolution (Feder & Hoffman, 1999; Taylor & Benjamin, 2005). Understanding their structure has provided some clues towards their mechanism of action in cells. They all work in an ATP-dependent fashion in that they require ATP hydrolysis in order to release bound proteins. In fact, ATP binding to HSP70 promotes conformational rearrangements in the molecule that increase its affinity to the substrate and stabilize their interaction (reviewed in Wegele *et al.*, 2004). These chaperones therefore carry a characteristic 44 kDa ATPase domain at their N-terminus and an 18 kDa domain which works as a protein binding site (Mallouk *et al.*, 1999). In fact, ATP binding to the N-terminus of HSP70 induces a conformational change in the chaperone that allows it to bind to other proteins (Giffard & Yenari, 2004). The C-terminus contains a 10 kDa domain with a characteristic terminal sequence that allows binding to specific co-factors in all eukaryotic cells. There is also some evidence that the carboxy-terminal domain is able to inhibit the ATPase activity of HSP70 in the absence of substrate (Wegele *et al.*, 2004). These structural characteristics ensure that all HSP70 members function as molecular chaperones regardless of their intracellular location, which ranges from the cytoplasm to the mitochondria and the endoplasmic reticulum.

Recent findings have shown that human HSP70 has a ribosomal docking site equivalent to the ones previously characterized in yeast and eubacteria (Huang *et al.*, 2005). HSP70 is recruited to the ribosome via Mpp11 and can interact optimally with nascent polypeptide chains as they are being formed, thus ensuring they do not aggregate and they are kept in the correct conformation for folding (Hundley *et al.*,

2005). Thus, chaperones provide a link between protein translation and folding, acting at a co-translational level.

An interesting hypothesis on the mechanisms of action of HSP70 suggests that it can exert its role passively or actively. In the latter case, the binding and releasing of substrates without refolding simply reduces the amount of free soluble proteins and thus prevents their aggregation. Alternatively, this chaperone can bind the substrate to correct its conformation in an energy-dependent fashion by unfolding a stretch of protein and refolding it (Mayer & Bukau, 2005). Because misfolded proteins have a tendency to aggregate, it is important that HSP70 is able to "dissolve" such aggregates in order to refold the proteins. Experiments in *E.coli* have confirmed that HSP70 can solubilize small protein aggregates of heat denatured G6PDH enzyme (dimers or trimers), whereas it relies on its cooperation with HSP40 and HSP104 for larger aggregates. Based on this evidence, the authors propose two mechanisms of action. Several HSP70 molecules acting simultaneously could locally unfold parts of the aggregates in repeated cycles of binding and dissociation to allow for disaggregation and correct refolding of the proteins to their native state. The unfolding of the substrate would occur by Brownian motion in random directions of many HSP70s acting synergistically to pull the misfolded protein open. Alternatively, less HSP70 molecules could be needed if disaggregation was facilitated by the misfolded substrate being held in a multichaperone complex (Ben-Zvi *et al.*, 2004).

The presence of co-chaperones is important for HSP70 function. From an evolutionary perspective it also implies that more functional differentiation is achieved if the chaperone can interact with and be modulated by a range of co-factors. It has been shown that certain co-chaperones can increase HSP70's affinity in binding substrates, enhancing its ATPase activity and thus accelerating the rate of protein binding, refolding and release. An example of this is HSP40 which was hsown to aid protein release from HSP70 in *E.coli* (Liberek *et al.*, 1991; Freeman *et al.*, 1995). Co-chaperones can also be involved in recruiting chaperones in specific cellular compartments or in large protein complexes. For example, the interaction of several chaperones and co-factors including HSP56, Hop, HSP70 and HSP90, has been shown to enhance steroid receptor function by inhibiting its translocation to the

nucleus (Edwards *et al.*, 1992). HSP70 collaborates with HSP90 in a well described cycle (figure 1.1): the substrate bound to HSP70 and HSP40 is presented to HSP90, in turn bound to a Hop co-factor to form an intermediate complex. Then, HSP70 and HSP40 dissociate to allow p23 binding and the substrate is appropriately processed (Wegele *et al.*, 2004). Moreover, HSP70 and HSP90 chaperone families also collaborate in targeting proteins for degradation in the proteasome (Young *et al.*, 2004). It is important to understand that co-chaperones can modify the function of a chaperone, determining whether proteins will be folded or degraded. This will be mentioned later in relation to overexpression of chaperones *in vivo* upon stress and possible competition for binding of co-chaperones modulating cellular response.

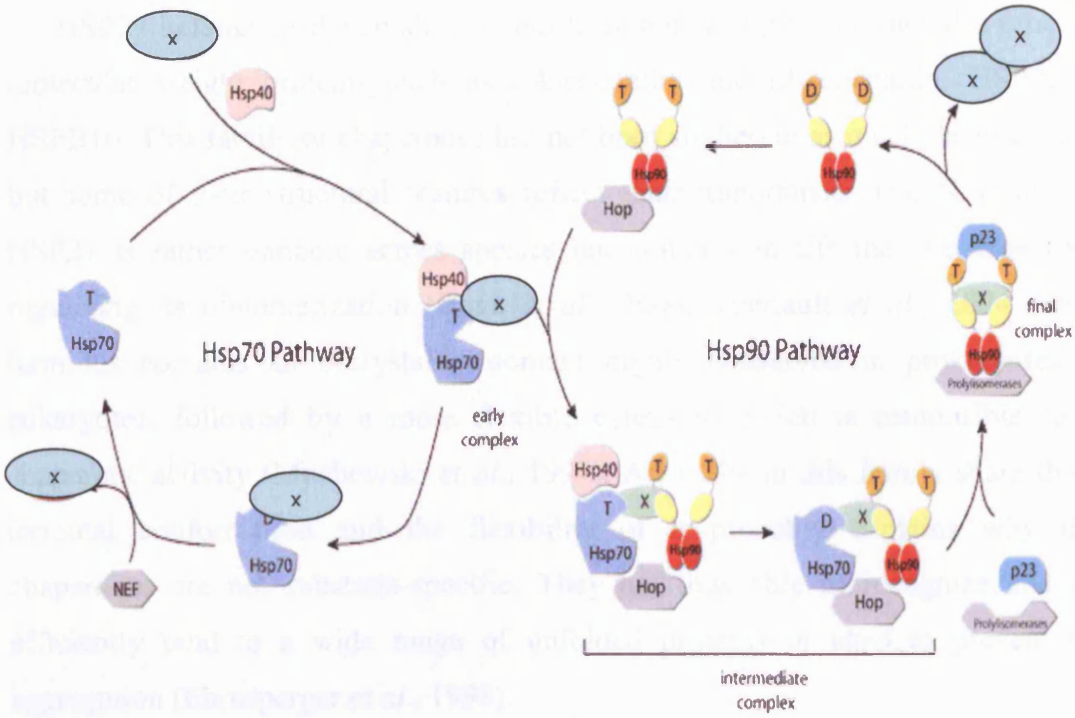

Figure 1.1. HSP70 and HSP90 protein folding cycle. HSP40 delivers the newly synthesized or denatured protein (x) to the HSP70 complex. HSP70 can then process the substrate (x) on its own through an ATP/ADP hydrolysis cycle involving the nucleotide exchange factor (NEF). Alternatively, the HSP40-HSP70-x protein complex binds to the scaffold protein Hop and enters the HSP90 pathway. This intermediate complex in turn binds to p23 and prolylisomerases as the HSP70 complex dissociates. The folded substrate is then released from this final complex. After binding to Hop, HSP90 is able to reenter the cycle. T, ATP-bound form; D, ADP-bound form. (Adapted from Wegele *et al.*, 2004).

1.3 The heat shock protein 27 family

HSP27 belongs to the small heat shock protein group which includes other low molecular weight proteins such as αA-crystallin and αB-crystallin, HSP22 and HSPB10. This family of chaperones has not been studied in as much detail as others but some of their structural features reflect their importance. The N-terminus of HSP27 is rather variable across species but contains motifs that are essential in regulating its oligomerization (Bova *et al.*, 2000; Theriault *et al.*, 2004). Its C-terminus contains an α-crystallin domain highly conserved in prokaryotes and eukaryotes, followed by a more flexible extension which is responsible for its chaperone activity (Muchowski *et al.*, 1997). All HSPs in this family share this C-terminal conformation and the flexibility of it probably explains why these chaperones are not substrate-specific. They are thus able to recognize and very efficiently bind to a wide range of unfolded proteins *in vitro* to prevent their aggregation (Ehrnsperger *et al.*, 1998).

Oligomerization and phosphorylation state are two key features when considering HSP27 function. Under normal conditions, HSP27 is found in large multimeric aggregates of high molecular weight (600-800 kDa). Phosphorylation upon stress causes dissociation of this chaperone into monomers and dimers (Lambert *et al.*, 1999; Rogalla *et al.*, 1999). Recent studies have shown that mutations in the 141 cysteine residue of HSP27 prevent dimerization of this chaperone and significantly reduce its ability to protect cells from stress-induced apoptosis. Thus, dimerization of HSP27 heavily relies on its only cysteine residue (C141) and is essential for chaperone activity *in vivo* (Diaz-Latoud *et al.*, 2005). The same laboratory has shown that the C terminus of HSP27 is crucial for its protective activity. Other studies have determined that protein kinase D is responsible for phosphorylation of a serine residue in HSP27 that also modulates oligomerization and therefore chaperone activity (Doppler *et al.*, 2005). The role of oligomerized HSP27 appears to be biologically important too. Early studies suggest that large HSP27 aggregates can bind denatured proteins and by keeping them soluble, prevent their aggregation and misfolding (Ehrnsperger *et al.*, 1997). Thus, dimers bind to proteins damaged after

stress and then oligomerize to generate larger molecules in an ATP-independent fashion (Ehrnsperger *et al.*, 1997; Arrigo *et al.*, 2005).

1.4 The role of HSPs in stress and apoptosis

A series of experiments on thermotolerance followed the discovery of HSPs in 1962. Subsequent experiments *in vitro* and *in vivo* have established that these proteins are naturally upregulated during a variety of stresses and that artificial overexpression confers protection (Lindquist & Craig, 1988; Higashi *et al.*, 1994; Wagstaff *et al.*, 1996; Ehrnsperger *et al.*, 1997; Feder & Hofmann, 1999). Such evidence will be discussed in detail for HSP27 and HSP70 in sections 1.5 and 1.6 respectively. Table 1.2 summarizes all known up-to-date neuronal studies.

All these experiments assess either the role of HSPs during stress, the effect of overexpressing HSPs before and after stress or the effect of the absence of HSPs during stress. This section aims to highlight the two main consequences of stress for the cell, necrosis or apoptosis, since it is these pathways that HSPs will interfere with in order to promote cell stability.

Depending on the nature and length of the insult, the cell will experience different degrees of energetic and metabolic impairment that could eventually lead to apoptosis or necrosis. Denaturing stresses such as ischaemia cause proteins to unfold or misfold. Such proteins have a tendency to aggregate due to their exposed hydrophobic segments and it is these aggregates that damage cells (Taylor *et al.*, 2002). Inducible HSPs can enhance cell survival by binding to and keeping denatured proteins soluble, thus preventing their misfolding or aggregation with other proteins. Their other main role is refolding aberrant proteins or targeting them for degradation in the proteasome (Kiang & Tsokos, 1998; Hershko & Ciechanover, 1998; Sharp *et al.*, 1999; Latchman, 2004).

A different but equally important mechanism of protection of HSPs is their role in preventing programmed cell death. Because ischaemia causes necrosis and,

more importantly, apoptosis, it is useful to briefly review the pathways that lead to the latter form of cell death. This will provide a framework for understanding the anti-apoptotic functions of HSPs discussed in the following section (see section 1.5). There are several pathways leading to apoptosis. In the intrinsic pathway, stressed mitochondria release cytochrome *c* that binds to Apaf-1 (Apoptotic protease-activating factor 1) and this complex recruits pro-caspase 9. This leads to the formation of the apoptosome where pro-caspase 9 is cleaved and active caspase 9 activates caspases 3 and 7. This results in proteolysis and cell death. In the extrinsic pathway, activation of death domain receptors such as FADD (Fas-associated protein with death domain) leads to the recruitment of pro-caspase 8. Activated caspase 8 can then trigger other downstream effector caspases. Caspase-independent pathways can lead to apoptosis via release of AIF (apoptosis inducing factor) from mitochondria. Alternatively, FADD interacts with Daxx protein and this complex recruits the apoptosis signal-regulated kinase 1 (Ask1). When activated, Ask1 can trigger the stress-activated protein kinase 1/ Jun N-terminal kinase (SAPK1/JNK) pathways of cell death. The protective role of HSP27 and HSP70 in apoptosis will be reviewed for each chaperone individually in the next section. Figure 1.2 illustrates some of the interventions of HSP27 in the apoptotic pathway.

	Cell type	HSP	Vector	Stress	Effect	Reference
In vitro	DRG/Glia	70	plasmid	heat	✓	Uney *et al.*, 1993
	DRGs/ND7	70	plasmid	heat	✓	Mailhos *et al.*, 1994
		70	plasmid	apoptosis	X	Mailhos *et al.*, 1994
	DRGs	70	plasmid	heat/ischaemia	✓	Amin *et al.*, 1996
	TNs	70	plasmid	heat	✓	Wyatt *et al.*, 1996
	Astrocytes	70	retrovirus	O_2+Glu removal	✓	Papadopoulos *et al.*, 1996
	HPs	70	hsv	heat	✓	Fink *et al.*, 1997
		70	hsv	apoptosis	✓	Fink *et al.*, 1997
	Astrocytes	70	retrovirus	Glucose removal	✓	Xu & Giffard 1997
	HPs	70	adenovirus	heat	✓	Beaucamp *et al.*, 1998
	Neuronal	27	plasmid	apoptosis	✓	Rogalla *et al.*, 1999
	DRGs/ND7	70	hsv	heat/ischaemia	✓	Wagstaff *et al.*, 1999
		27	hsv	heat/ischaemia	✓	Wagstaff *et al.*, 1999
	DRGs	27	hsv	serum removal	✓	Wagstaff *et al.*, 1999
		70	hsv	serum removal	X	Wagstaff *et al.*, 1999
		27	hsv	apoptosis	✓	Wagstaff *et al.*, 1999
		70	hsv	apoptosis	X	Wagstaff *et al.*, 1999
		27	adenovirus	serum removal	✓	Lewis *et al.*, 1999

	Astrocytes	70	retrovirus	Glucose removal	✓	Lee *et al.*, 2001a
		70	Tg	Glucose removal	✓	Lee *et al.*, 2001a
		70	Tg	Glutamate	✓	Lee *et al.*, 2001a
		70	Tg	O_2+Glu removal	✓	Lee *et al.*, 2001a
	HPs	70	Tg	O_2+Glu removal	✓	Lee *et al.*, 2001a
		70	Tg	Glutamate+Fe^{2+}	✓	Kelly *et al.*, 2001a
	DRGs	27	hsv	serum removal	✓	Benn *et al.*, 2002
	Astrocytes	70	retrovirus	O_2+Glu removal	✓	Giffard *et al.*, 2004
		70	Tg	H_2O_2	✓	Giffard *et al.*, 2004
	ND7	27	hsv	ischaemia	✓	Zourlidou *et al.*, 2004
		70	hsv	ischaemia	X	Zourlidou *et al.*, 2004
		27	hsv	staurosporine	✓	Zourlidou *et al.*, 2004
		70	hsv	staurosporine	X	Zourlidou *et al.*, 2004
		70	hsv	serum removal	X	Zourlidou *et al.*, 2004
		27	hsv	serum removal	✓	Zourlidou *et al.*, 2004
	DRGs/ND7	70	hsv	apoptosis	✓	Patel *et al.*, 2005
		27	hsv	apoptosis	✓	Patel *et al.*, 2005
	RG	27	plasmid	ischaemia	✓	Whitlock *et al.*, 2005

In vivo	rat	70	hsv	ischaemia	✓	Yenari *et al.*, 1998
	rat	70	hsv	ischaemia	✓	Hoehn *et al.*, 2001
	rat	70	adenovirus	ischaemia	✓	Kelly *et al.*, 2001b
	rat	70	hsv	ischaemia	✓	Kelly *et al.*, 2002
	rat	27	hsv	kainic acid	✓	Kalwy *et al.*, 2003
	mouse	70	Tg	ischaemia	✓	Plumier *et al.*, 1997
	mouse	70	Tg	ischaemia	✓	Rajdev *et al.*, 2000
	mouse	70	Tg	ischaemia	X	Lee *et al.*, 2001a
	mouse	70	Tg	ischaemia	✓	Kelly *et al.*, 2001a
	mouse	70	Tg	ischaemia	✓	Lee *et al.*, 2001b
	mouse	27	Tg	kainic acid	✓	Akbar *et al.*, 2003
	mouse	70	Tg	ischaemia	✓	Tsuchiya *et al.*, 2003
	mouse	70	Tg	kainic acid	✓	Tsuchiya *et al.*, 2003
	mouse	70	Tg	ischaemia	✓	van der Weerd *et al.*, 2005
	mouse	27	Tg	ischaemia	✓	van der Weerd (p.c.)

Table 1.2. Summary of all *in vitro* and *in vivo* studies assessing neuroprotection (✓) of HSP27 and HSP70 against different insults. (DRGs, dorsal root ganglion neurones; RG, retinal ganglion cells; HPs, hippocampal neurones; TNs, trigeminal nerve neurones; Tg, transgenics; hsv, herpes simplex virus; Glu, glucose; p.c., personal communication)

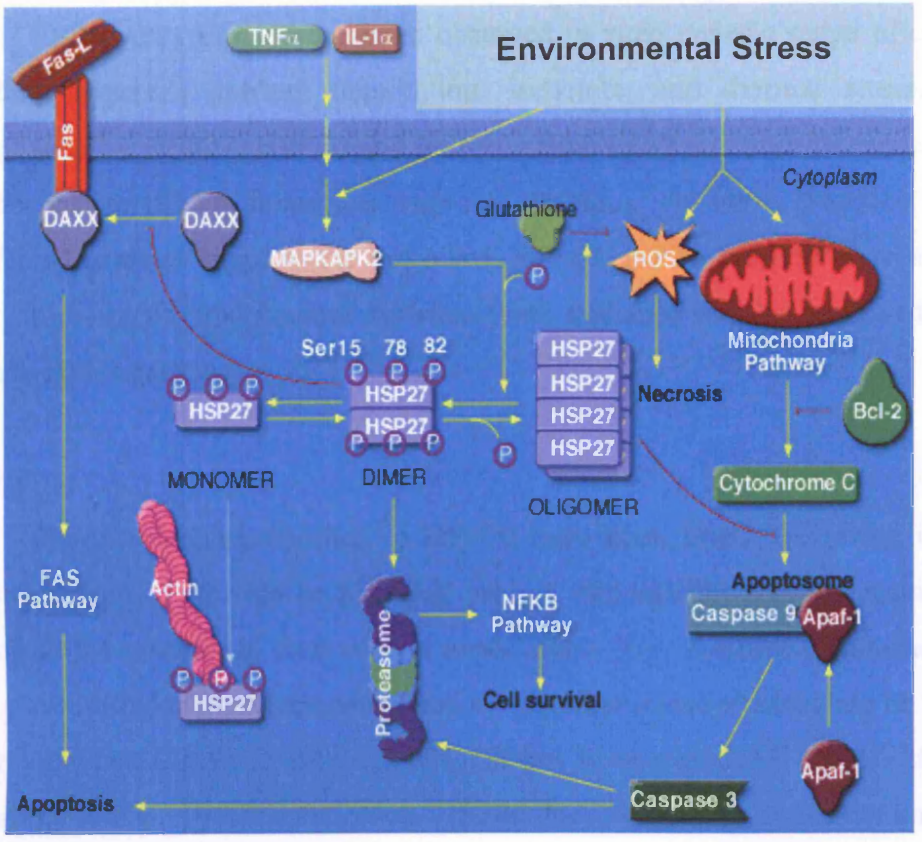

Figure 1.2. The anti-apoptotic functions of HSP27. Overview of the targets of HSP27 in the cell upon stress (adapted from www.biocarta.com). TNFα, tumour necrosis factor alpha; IL-1α, interleukin-1alpha; MAPK, mitogen activated kinase; ROS, reactive oxygen species; NFkB, nuclear factor kappa B; Apaf, apoptosis inducing factor-1.

1.5 HSPs and the stress response in neurones *in vitro*

HSP overexpression has been observed *in vitro* under a range of conditions including hypoxia, nutrient deprivation, ischemia, and thermal stress. Briefly, upregulation of HSP27, HSP70 and HSP90 mRNA and protein after several insults has been detected in numerous neuronal cultures. *In vitro* evidence of HSP-transfected neurons supports the protective role of HSP27 and HSP70 to a different extent in different experimental systems. Such evidence will be discussed in detail for each HSP separately.

HSP70

The chaperone properties of HSP70 have been briefly reviewed in section 1.2, in relation to its role in blocking protein aggregation and promoting protein folding in the cytosol. In fact, several experiments have confirmed this chaperone's ability to refold denatured enzymes such as ornithine transcarbamoylase or luciferase (for review see Mayer & Bukau, 2005). It has been estimated that 10-20% of all bacterial protein synthesis relies on HSP70 for correct 3D conformation of new peptides and that this percentage should be greater in eukaryotes and even greater after stress (Hartl & Hayer-Hartl, 2002). The importance of the ATPase domain of HSP70 has also been highlighted since it is responsible for clathrin uncoating and binding to and releasing unfolded proteins. Interestingly, recent *in vitro* experiments have shown that the Hdj-2 co-chaperone, a member of the HSP40 family, is also needed to mediate protein binding to HSP70. However, Hdj-2 on its own was found to protect cells regardless of the levels of HSP70, suggesting that this co-chaperone might have a crucial effect (Giffard *et al.*, 2004). The relevance of co-factors becomes more obvious when we consider that their binding can change the fate of unfolded proteins and promote either their refolding or their degradation.

The neuroprotective role of overexpression of HSP70 has been established by numerous *in vitro* systems. Neuronal cell lines isolated from transgenic overexpressing mice or transfected with engineered viruses have shown enhanced viability after a range of stresses but protection was not always conferred against apoptosis (for reviews see Kiang and Tsokos, 1998; Yenari *et al.*, 1999; Feder & Hofmann, 1999; Kelly & Yenari, 2002; Richter-Landsberg & Goldbaum, 2003).

Early experiments by Uney and colleagues showed that HSP70 transfected dorsal root ganglion (DRG) neurones are protected from heat shock (Uney *et al.*, 1993). ND7 cells and trigeminal ganglion neurones stably transfected with HSP70 were protected from heat shock but not from serum removal induced apoptosis (Mailhos *et al.*, 1994; Wyatt *et al.*, 1996). Similarly, DRG neurones transfected with HSP70 were protected against thermal and ischaemic lethal stresses (Amin *et al.*, 1996). Moreover, addition of antisense oligonucleotides against HSP70 to primary hippocampal rat neurones significantly decreased cell survival after heat shock (Sato *et al.*, 1996).

Viruses engineered to overexpress HSP70 have been used to infect neuronal cell cultures and test the protective effect of this chaperone against a range of stresses. Thus, transfection of hippocampal neurones with HSV expressing HSP70 (HSV-HSP70) has been shown to enhance their resistance to heat shock but not to glutamate or 3-nitropropionic acid (NP-3) exposure (Fink *et al.*, 1997). Similarly, adenovirus infected primary hippocampal neurones were protected against thermal stress (Beaucamp *et al.*, 1998). Survival of astrocytes in culture to either glucose or both oxygen and glucose deprivation was significantly enhanced when transfected with HSP70 expressing retroviruses (Papadopoulos *et al.*, 1996; Xu & Giffard, 1997). In contrast to these studies, it has been shown that HSV-HSP70 infected ND7 cells and DRG neurones are protected from thermal and ischaemic stress but not from apoptosis induced by serum removal and retinoic acid addition (Wagstaff *et al.*, 1999).

Kelly and colleagues observed neuroprotection against glutamate and oxidative stress in primary hippocampal neurone cultures from *Lmo*-1 promoter-mediated inducible HSP70 transgenic mice (Kelly, *et al.*, 2001*a*). Primary astrocytes and pure neuronal cell cultures were isolated from transgenic HSP70 mice and subjected to a range of insults. Astrocytes and pure hippocampal neuronal cultures were more protected from oxidative stress than glucose and oxygen-glucose deprivation whereas pure cortical neuronal cultures were not protected from either oxygen-glucose deprivation or glutamate exposure (Lee *et al.*, 2001*a*).

As far as its role in apoptosis is concerned, HSP70 has been shown to protect cells against both necrosis and caspase-dependent as well as caspase-independent apoptotic death pathways. There is evidence suggesting that HSP70 regulates both upstream events by inhibiting the formation of the apoptosome, and downstream events by binding either the apoptosome complex or the effector caspases. In fact, HSP70 can bind to different components of this complex, such as Apaf-1 (Beere *et al.*, 2000; Saleh *et al.*, 2000), cytochrome *c* (Tsuchiya *et al.*, 2003; Mosser *et al.*, 2000; Creagh *et al.*, 2000; Steel *et al.*, 2004) and dATP. If the apoptosome complex forms, it then binds to pro-caspase 9 and activates a downstream cascade of effector caspases such as caspase 3. Beere and colleagues have shown that HSP70 prevents the binding of pro-caspase 9 to the apoptosome complex upon cytochrome *c* release (Beere *et al.*, 2000). Some studies demonstrate that HSP70 is unable to prevent cytochrome *c* release from mitochondria but it can inhibit activation of caspase 3 or act downstream of the caspase cascade by downregulating cytosolic phospholipase activity (Jaattela *et al.*, 1998; Li *et al.*, 2000*a*). There is also some evidence that this chaperone can bind to the apoptosis inducing factor (AIF) and stop its release from mitochondria (Ravagnan *et al.*, 2001), whereas other groups suggest that inhibition of apoptosis occurs via the JNK/SAPK pathway (Gabai *et al.*, 1997; Meriin *et al.*, 1999).

It is widely recognized that HSP70 is a powerful chaperone, with anti-apoptotic activity, as well as providing a link between denatured proteins and the proteasome degradation machinery. Certain *in vitro* studies have, however, shown the potentially harmful effects of this chaperone. There is evidence that increased levels of HSP70 can be detrimental to neurones by binding to survival elements that could otherwise block TNF-induced apoptosis (Ran *et al.*, 2004). It is important to note that, in contrast, HSP27 can protect cells from TNF-induced apoptosis (see below; Mehlen *et al.*, 1997). *In vitro* evidence of protection with HSP70, however, remains extremely dependent on the type and severity of insult and the susceptibility to different environmental insults of the cell population affected (Amin *et al.*, 1996; Jaattela *et al.*, 1998; Lee *et al.*, 2001*a*; Ran *et al.*, 2004; Latchman, 2004).

HSP27

HSP27 has been shown to protect cells *in vitro* by interfering with the stress-triggered apoptotic cascades. Numerous experiments have confirmed the anti-apoptotic effects of this chaperone after exposure to a range of toxic stimuli such as staurosporine (Zourlidou *et al.*, 2004; Patel *et al.*, 2005), FAS/Apo-1 (Arrigo *et al*, 1998; Melhen *et al.*, 1996), etoposide (Samali *et al.*, 1996, 1999), NGF withdrawal (Lewis *et al.*, 1999; Zourlidou *et al.*, 2004; Patel et al., 2005), doxorubicin (Garrido *et al.*, 1997; Hansen *et al.*, 1999), cisplatin (Garrido *et al.*, 1997), actinomycin D and others (see Paul *et al*, 2002; Latchman, 2004). Primary sensory and motor neurons benefit from the upregulation of HSP27 after nerve injury induced apoptosis (Costigan *et al.*, 1998; Tandrup *et al.*, 2000) whereas HSP27 knockdowns show increased cell death (Benn *et al.*, 2002).

It has been suggested that HSP27 can interfere with both caspase-dependent and caspase-independent apoptotic pathways. TNF-α induced cell death can be prevented by expression of HSP27, decreasing the levels of reactive oxygen species (ROS) and reducing the activation of NF-κB, lipid peroxidation and protein oxidation. In has been proposed that the chaperone increases glutathione content in the cells, which is in charge of scavenging ROS like TNFα in mitochondria (Melhen *et al.*, 1997). Virally transfected HSP27-overexpressing ND7 and DRG cell lines are more resistant to heat shock, ischaemia and serum withdrawal with retinoic acid addition (Wagstaff *et al.*, 1999). Garrido and colleagues have shown that HSP27 prevents procaspase 9 activation without interfering with cytochrome *c* release (Garrido *et al.*, 1997 & 1999). Other studies have shown that HSP27 overexpression can sequester cytochome *c* after release from the mitochondria and prevent its binding to the apoptosome (Bruey *et al.*, 2000). Cytochrome *c* release can also be delayed by HSP27 and in turn delay caspase activation (Paul *et al.*, 2002). Similarly, sequestration of cytochrome *c* and binding to procaspase 9 can inhibit apoptosis (Concannon *et al.*, 2001). Several experiments show that this protein is able to block caspase-3 activation after ischaemia (Pandey *et al.*, 2000; Whitlock *et al.*, 2005). Interestingly, replacing HSP27 in rat neurons with a caspase blocking agent does not prevent cytotoxicity suggesting that in addition to caspase-3 blockage, HSP27 must exert chaperoning functions that prevent necrosis and caspase-independent events

(Whitlock *et al.*, 2005). Moreover, recent findings suggest that HSP27 overexpression can reduce stress-triggered membrane translocation of PKCdelta, an upstream molecule in the activation of the p38 MAP kinase pathway, which leads to ROS formation and mitochondrial-induced caspase-dependent apoptosis (Lee *et al.*, 2005). Overexpression of HSP27 can also decrease the amount of AIF, which is released by mitochondria in the caspase-independent pathway of cell death (Rashmi *et al.*, 2003). This chaperone can also interact with Daxx to prevent caspase-independent apoptosis (Charette *et al.*, 2000).

Other possible mechanisms of protection by this HSP could be related to its chaperone functions. Some experiments have linked cytoskeleton stability to mitochondria and apoptosis. They suggest that HSP27 acts further upstream and prevents cytochrome *c* release via Bid relocalization which is in turn associated with F-actin filaments modulated by this chaperone (Paul *et al.*, 2002). Previous studies had shown that HSP27 could stabilize F-actin microfilaments and intermediate microfilaments during stress (Lavoie *et al.*, 1993, Guay *et al.*, 1997). It has more recently been found that phosphorylated and unphosphorylated HSP27 binds actin and tubulin filaments and can promote axonal growth and regeneration after injury (Costigan *et al.*, 1998; Williams *et al.*, 2005). Finally, recent studies have shown that although HSP27 cannot prevent thermal denaturation of F-actin, it translocates to the cytoskeleton upon stress and binds to its denatured form to prevent aggregates. Protection is conferred by solubilization of denatured F-actin, in order for it to be refolded or degraded (Pivovarova *et al.*, 2005).

In contrast to other HSPs including HSP70, HSP27 has the ability of binding partially or completely denatured proteins in an ATP-independent fashion, which could be crucial in preserving cellular stability during the metabolic depletion caused by ischaemia (Rogalla *et al.*, 1999; Garrido, 2002). Early experiments have demonstrated translocation of HSP27 into the nucleus upon stress signals where it can stabilize mRNAs and limit denaturation of proteins involved in transcription (Carper *et al.*, 1997). Since protein synthesis is impaired by cerebral ischaemia, protection may work by enabling accelerated recovery of protein synthesis rate after stress.

Mehlen and colleagues have proposed that large HSP27 aggregates are able to regulate production of reactive oxygen species and TNF alpha damage in cells (Mehlen *et al.*, 1997). Arrigo and colleagues have proposed a mechanism of protection where HSP27 decreases intracellular iron levels thus preventing free radical generation and reducing the levels of oxidized proteins within cells. Moreover, such proteins are also actively recruited by HSP27 chaperones and presented to the proteasome for degradation (Arrigo *et al.*, 2005).

1.6 HSPs and stress response in neurones *in vivo*

The temporal expression pattern of several HSPs including HSP27, HSP56, HSP60, HSP70, and HSP90 after cerebral ischaemia in rodents has been extensively studied. Both mRNA and protein levels of HSP27, HSP70 and HSP60 were significantly increased at 2, 4, 8 and 24 hours after stroke although mRNA levels seemed higher than protein levels (Wagstaff *et al.*, 1996). Higashi and colleagues looked at HSP27, HSP47, HSP70 and HSP90 and determined that HSP70 mRNA expression increased 4 hours after focal ischaemia adjacent to the lesion core, whereas HSP27 expression peaked at 24 and 48 hours and was more widespread (Higashi *et al.*, 1994). Other studies used northern blot or in situ hybridization to determine a timecourse of HSP70 mRNA expression increase upon stress. Rabbit glial cells in the forebrain region were enriched in HSP70 mRNA at 1, 2 and 3 hours after hyperthermia. It is interesting to note that in that study it is oligodendrocytes and microglial cells and not neurones or astrocytes that strongly upregulate HSP70 (Foster & Brown, 1997). However, ischaemic insult induced HSP70 expression in astrocytes and neurons in the periphery of the infarct whereas only endothelial cells were seen to express it near the core of the lesion (Kinouchi *et al.*, 1993). Cortical regions seem to upregulate HSP70 mRNA at higher levels than the caudate in rats, possibly delineating an area where protein synthesis is recovering (Abe *et al.*, 1992). Interestingly, gerbil CA1 neurons minimally induce HSP70 compared to CA3 cells and the former die 48 hours after transient ischaemia (Kawagoe *et al.*, 1993). Further ischaemia experiments in rats suggest there might be an imbalance in the amount of constitutive and stress-induced HSP70 mRNA that renders CA1 neurons more

susceptible to ischaemia (Kawagoe *et al.*, 1992*a*, 1992*b*, 1993). It has however more recently been shown that striatum and cortex are highly immunopositive for HSP70 after transient focal ischaemia in rats (Rebel *et al.*, 2005).

The distribution of HSP70 in the brain after thermal stress was also studied by Pavlik and colleagues. Their experiments revealed high levels of this chaperone in glial and vascular cells 1.5 hours after heat shock, with expression peaking at 4 hours. They detected high expression in the cortex and white matter areas whereas neuronal staining was more discrete, localizing in amygdala and hypothalamus. They were also able to show that nuclear translocation of HSP70 occurred as early as 1.5 hours after hyperthermia and relocation to the cytoplasm took place 4 to 5 hours later (Pavlik *et al.*, 2003).

These and other studies suggest that although there are similarities in expression patterns of HSP27 and HSP70 after stress in the brain, the levels and location of such expression depends on the severity and length of the insult and can also be specific to cell populations.

Overexpression experiments in *in vivo* models of epilepsy and stroke have yielded different results. Transgenically overexpressed or virally delivered HSP70 was not always able to reduce lesion size but was able to enhance cell survival. HSP70 transgenics showed no reduction in lesion size but decreased damage in hippocampal neurons after permanent focal cerebral ischaemia (Plumier *et al.*, 1997). Similar results were obtained by one other study after permanent middle cerebral artery occlusion (Lee *et al.*, 2001*a*). In contrast to these findings, transgenic mouse models of transient global and focal ischaemia and kainic-acid induced seizures showed reduced lesion volume and decreased neuronal damage and apoptosis in the hippocampus respectively (Tsuchiya *et al.*, 2003). Reduction in lesion size was also found by two further studies in permanent focal ischaemia models in mice (Rajdev *et al.*, 2000; van der Weerd *et al.*, 2005). A slightly different approach involved knockout mice carrying deletions in HSP70. Permanent focal cerebral ischaemia induced a much larger infarct size in these animals than in wild type mice, supporting the idea that HSP70 is neuroprotective (Lee *et al.*, 2001*b*). Giffard and colleagues have examined the protective role of HSP70, where its overexpression was able to

reduce protein aggregation in CA-1 neurons in an *in vivo* model of global ischaemia (Giffard *et al.*, 2004). Kelly and colleagues created an inducible HSP70 transgenic mouse line where expression was not pan-neural but more discrete and driven to specific hippocampal populations. These animals showed reduced neuronal damage after 25 minutes of bilateral carotid artery occlusion, although the HSP70 protein levels were no different in transgenics and wild type controls subjected to ischaemia (Kelly, *et al.*, 2001*a*).

Viral overexpression of HSP70 has been attempted in four studies, three of which used stereotaxic intracerebral microinjections of herpes simplex virus as a vector in rats whilst the fourth one used adenovirus in mice. None of these experiments provide any evidence of reduction in lesion size due to treatment with HSP70. All of them, however, report that the morphology of stressed neurones is improved in the presence of this chaperone reflecting its neuroprotective effect. It is interesting to note that improving the cell's appearance is apparently not directly related to an enhancement of the cell's viability and therefore has no consequences in the final lesion area. Yenari and colleagues showed that pre-ischaemic delivery of HSP70-expressing virus improved neuronal survival in the striatum and in the hippocampus after focal ischaemia and kainic acid induced seizures respectively (Yenari *et al.*, 1998). Post-ischaemic injection of the viral transgene improved neuronal survival in the striatum when delivered at 0.5 and 2 hours but not at 5 hours after stroke (Hoehn *et al.*, 2001). Similarly, CA1 hippocampal neurones were protected from global ischaemia when the vector was delivered 12 hours before insult (Kelly *et al.*, 2002). Finally, engineered adenovirus microinjected two weeks before the insult protected mice from 20 minutes of global ischaemia. It is interesting to mention that the control vector, an adenovirus carrying enhanced green fluorescent protein, also protected striatal neurones so no differences were found between treated and controls (Kelly *et al.*, 2001*b*).

The great majority of these studies have involved HSP70 whilst the protective effect of HSP27 *in vivo* has been less investigated. Transgenic mice overexpressing HSP27 presented a significant decrease in hippocampal neuron death in a kainic-acid model of epilepsy (Akbar *et al.*, 2003). This study showed a significant 50% reduction in mortality of the animals, less toxicity and less caspase 3 induction,

which correlates with an anti-apoptotic effect of HSP27. In agreement with these findings, a reduction in lesion size was seen in transgenic mice 24 hours after permanent focal ischaemia (van der Weerd, personal communication). Only one study to date has attempted viral delivery of HSP27 and shown enhancement of cell survival in a model of kainate-induced cell death in the hippocampus (Kalwy *et al.*, 2003).

1.7 Summary

This first chapter has addressed several aspects of the biology of heat shock proteins, focussing on the main chaperones induced in the brain, HSP27 and HSP70. A brief account of their structure was also given in an attempt to understand the way these chaperones bind to other proteins in the cell. Subsequently, an overview of *in vitro* and *in vivo* studies reporting known functions of HSP27 and HSP70 was presented. Although the exact mechanisms of protection are still under investigation, the overall importance of HSPs as molecular chaperones under normal and stress conditions is clear. The cell's proteolytic machinery relies on chaperones for its correct functioning. A newly formed protein has several fates: it can remain unfolded, fold to the appropriate conformation or misfold and either be refolded or degraded. The interaction of HSPs and other co-factors is thus crucial in modulating cell survival.

Chapter 2 *Cerebral ischaemia*

2.1 Introduction

Stroke continues to be a major cause of death and disability in the western world and industrialized nations. It has been estimated that on average, one person suffers a stroke every 45 seconds in the United States alone (Nudo & Nelson, 2003). Incidence figures indicate that 5.5 million people died from stroke around the world in 1999, leaving stroke as the third most common cause of death after heart infarction and cancer (Lo *et al.*, 2003). Approximately 25% of all strokes lead to death, but about 80% of those surviving experience motor weakness and 30% result in long term chronic disability (in Dijkhuizen *et al.*, 2001). The term encompasses a range of conditions of vascular origin, including total or partial obstruction of a vessel, haemorrhage and less often a total lack of blood supply to the brain due to cardiac arrest. Excluding this last example, the pathology can manifest itself in two main forms: as the thrombotic occlusion of a cerebral artery or as a vessel rupture leading to haemorrhage. Symptoms are usually abrupt, reflecting the sudden interruption of blood supply to a region of the brain, and persist for at least 24 hours after onset. Of the two existing types of stroke, haemorrhagic and ischaemic, the latter accounts for approximately 85% of all clinical cases. The patient's outcome is strongly dependent on the type and duration of the stroke. The spectrum ranges from transient ischaemic attacks (TIAs), in which small neurological deficit resolves completely in a relatively short period of time, to longer periods of ischaemia that might leave permanent damage, or even death. Ultimately, the common feature is that brain cells will die and some will remain dysfunctional, leading to variable neurological deficit depending on the location of the specific brain regions affected by the ischaemic event and extent of the damage.

2.2 Animal models of cerebral ischaemia

The use and development of experimental brain ischaemia models is justified by the need to expand treatment options. In fact, thrombolytic therapy has been the only available option for stroke patients for over 10 years, and even if it is moderately effective, it is limited by the need for intervention within a very narrow therapeutic window (~3 hours post-treatment). Different animal models of stroke have been developed over the years in order to study the evolving pathophysiology and assess the effect of different treatments. In these models, the duration of the ischaemic event determines whether the stroke is transient (where the flow is eventually restored), or permanent (where no tissue reperfusion takes place). It is also important to distinguish whether the stroke is global, affecting the brain overall, or focal, affecting a specific region. Some examples of different animal stroke models will be briefly reviewed in the next two sections.

2.2.1 Global cerebral ischaemia

Rodent global models have been used to mimic cardiac arrest in humans but can be even more useful in studying the death of certain neuronal populations. Decapitation has been used to reproduce this global reduction in blood flow without reperfusion (Hossmann, 1998). Other examples are the four-vessel occlusion model in rats and the bilateral forebrain ischaemia in gerbils (Small & Buchan, 2000; Lythgoe & Gadian, 2000; Lythgoe *et al.*, 2003). In the former, permanent bilateral occlusion of the vertebral arteries is obtained by cauterization and both common carotid arteries (CCAs) are ligated for at least 10 and up to 30 minutes before reperfusion (Pulsinelli & Brierley, 1979). Transient bilateral occlusion of the CCAs on its own can induce global ischaemia in gerbils. This is due to an abnormality in their circle of Willis, namely a lack of communicating arteries connecting the posterior and anterior circulations (Levine & Payan, 1966). The type of cell death produced by this model of forebrain ischaemia is delayed and selective: 10 minutes of occlusion can damage CA1 hippocampal neurones, whereas longer periods can affect or striatal and cortical neurones. It has recently been reported, however, that

this type of cell death is not strictly "delayed" but the result of a gradual process that can be monitored through the reduction in water diffusion in the affected tissue after reperfusion (Lythgoe *et al.*, 2005).

2.2.2 Focal cerebral ischaemia

Focal models are thought to more closely correlate with clinical situations than global models. This type of stroke causes a gradient of reduction in cerebral blood flow (CBF) across the tissue, so that the focal lesion typically has an unsalvageable core and is surrounded by tissue at risk that is partially perfused by collaterals and is therefore potentially salvageable. Commonly, focal models involve occlusion of the middle cerebral artery (MCA) in a transient or permanent fashion. Some of the techniques used for the latter are cauterisation, photochemical thrombolysis after injection of rose bengal dye, injection of blood clots into the common carotid artery or intraluminal occlusion of the MCA (Small & Buchan, 2000; Lythgoe *et al.*, 2003). Some groups have attempted to increase the reproducibility of the lesion size by combining the MCA occlusion with permanent occlusion of the CCA or by subjecting the animal to hypotension for a short period of time (Brint *et al.*, 1988; Chen *et al.*, 1986; van Bruggen *et al.*, 1992; Lythgoe & Gadian, 2000). Occlusion of the MCA by electrocoagulation usually generates a large lesion in the cortex and caudate putamen (Tamura *et al.*, 1981). Some of these methods have the advantage of avoiding craniotomy but not all of them can be specific about the location of the infarct.

Transient models may sometimes be less reproducible than models involving permanent occlusion but they allow investigation of the fate of the tissue after reperfusion (Longa *et al.*, 1989). MCA occlusion is normally performed via clips, ligature or intraluminal thread. In the original method described by Shigeno and colleagues, a ligature was loosely placed around the MCA and the blood flow was interrupted by pulling and releasing the thread around the artery (Shiegno *et al.*, 1985). In other models, clips are used to distally obstruct the artery, giving rise to a cortical lesion only (Kaplan et al., 1991). Embolic models are thought to better

resemble clinical stroke (Busch *et al.*, 1997; Mayzel-Oreg *et al.*, 2004). The intraluminal method is the least invasive but can yield variable sized infarcts; some groups have attempted to reduce the variability by perfecting the suture. In the first model proposed by Koizumi and colleagues, a rubber cylinder attached to a thread was used to block the MCA via the internal carotid (Koizumi *et al.*, 1986). Nylon monofilaments with a blunted tip were later used (Longa *et al.*, 1989). It was then noticed that the size, the length, the material and the degree of coating of the suture affected lesion size and reproducibility (Garcia *et al.*, 1993). This limitation is intrinsic to the method because the thread needs to be positioned correctly to completely block the origin of the MCA as it branches from the internal carotid artery. Otherwise, partial reduction of flow will lead to smaller lesion size. However, unlike some of the listed models, this method is specific about the location of the lesion and the size of the lesion can be varied according to the duration of the occlusion. Among the other advantages, the surgery does not involve craniotomy and is therefore less invasive than abovementioned models. Thus, this method allows the study of dynamic changes occurring immediately after occlusion and/or reperfusion of the ischaemic area.

2.2.3 Pathophysiology of brain tissue during ischaemia

Cellular damage upon ischaemia involves a range of events including exitotoxicity, ionic imbalance, oxidative stress and programmed cell death. The degree of damage will depend on the duration and extent of interruption of blood flow to the tissue, and this will in turn determine whether the damage is reversible or not. After prolonged ischaemia, the centre of the lesion is the most damaged, eventually proceeding to pan-necrosis of neurones, glia and endothelial cells resulting in infarction. In more peripheral, compromised areas, cells die at a slower rate by active cell mechanisms of gene activation that cause apoptosis (Garcia *et al.*, 1995; Dirnagl *et al.*, 1999; Lee *et al.*, 2002; see section 1.4).

One of the first consequences of cerebral ischaemia is energy failure. ATP is the main source of energy in the brain and is crucial in maintaining ion pump

activity. The conversion of ADP to ATP is an oxidative process, and therefore heavily relies on constant oxygen and glucose supply and is therefore compromised during ischaemia. As a consequence, ion pumps including the Na^+/ K^+ pump fail, causing the disruption of ion gradients across the cellular membrane leading to their depolarization. There is a rapid intracellular accumulation of Na^+, Ca^{++} and Cl^- ions and an efflux of K^+ ions, which osmotically obliges an influx of water from the extracellular to the intracellular compartment. This results in the phenomenon known as cytotoxic oedema or cell swelling (Hansen, 1985).

An inflammatory response is triggered as a result of cytotoxic oedema which is mediated by signalling molecules including cytokines, chemokines and immediate early genes (*c-fos*, *c-jun*). Release of neurotransmitters such as glutamate promotes Ca^{++} influx and triggers a cascade of events that result in release and activation of reactive oxygen species (ROS), endonucleases and proteases such as matrix metalloproteinases and plasminogen activators from astrocytes and microglia. These proteins are able to disrupt tight junctions in endothelial cells of the blood vessels, thus degrading the matrix and disrupting the blood brain barrier (BBB). The excess of serum/fluid leaking from the blood into the tissue results in vasogenic oedema (Klatzo, 1987). This phenomenon involves an increase in interstitial water content and overall tissue swelling and is a direct consequence of blood vessel proteolysis. As the pathology progresses, cells in this area die by necrosis, are reabsorbed by glial tissue and a fluid filled cavity remains.

2.3 MRI and its applications to animal models of stroke

In order to understand how MRI can provide useful information about the healthy and diseased brain, it is necessary to describe some of its fundamental biophysical properties. This technique is concerned with imaging the hydrogen nuclei present in water molecules, which constitute 70-80 % by weight of neuronal tissue. A variety of parameters that will be detailed in the following sections can describe macroscopic and microscopic motions of water and how its distribution is altered by diseases such as stroke. Thus, MRI can report not only on alterations in blood flow (perfusion) due to an ischaemic event, but also on metabolic changes

associated with the distribution of water between intracellular and extracellular compartments (diffusion) and in tissue structure due to cytotoxic and vasogenic oedema.

2.3.1 Basic theory

Nuclear magnetic resonance is widely used as a diagnostic and research tool. Two distinct fields of NMR are concerned with either the detection of metabolites by magnetic resonance spectroscopy (MRS), or the characterization of tissue structures using magnetic resonance imaging (MRI). For the purpose of this study, only the latter will be reviewed. The technique is based on the concept that each nucleus possesses a nuclear spin and an associated magnetic moment. The most widespread analogy used to describe this phenomenon is thinking of each atom as a small bar magnet. The "behaviour" of this small magnet will be affected by the magnetic field it experiences: in the absence of a field, the spins will be randomly distributed; in the presence of an external field, the spins will align with or against the main magnetic field (B_0), although slightly more will be aligned with the field than against it. The resulting net magnetization can be represented by a vector aligned with B_0, and its magnitude is directly proportional to the spin density (figure 2.1). Moreover, the individual spins will precess around B_0 at a specific frequency, the Larmor frequency (ω_0), which is directly proportional to the strength of the main magnetic field. This relationship is described by the equation: $\omega_0 = \gamma B_0$, where γ is the gyromagnetic ratio of the nucleus.

In order to detect this net magnetization (M_Z), it is necessary to disturb its longitudinal alignment and flip the magnetization towards the perpendicular (x-y) plane. A radiofrequency pulse at the resonant (Larmor) frequency of the protons can be applied for this purpose. A 90° pulse can be used to tilt the magnetization vector into the x-y plane. This transverse magnetization gradually decays and returns to its original position at equilibrium, longitudinally aligned with the main magnetic field B_0 (figure 2.2).

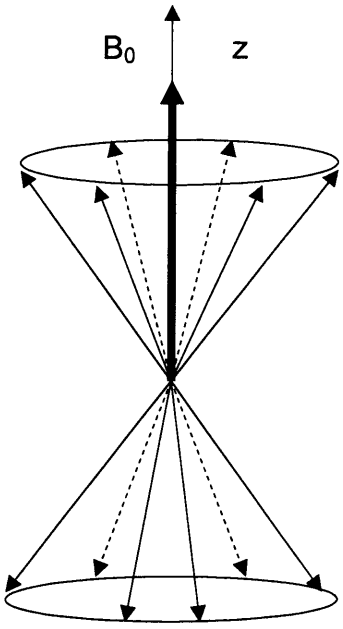

Figure 2.1. Spins align with or against the B_0 field. The thick arrow represents the net magnetization vector along the direction of the field (z axis).

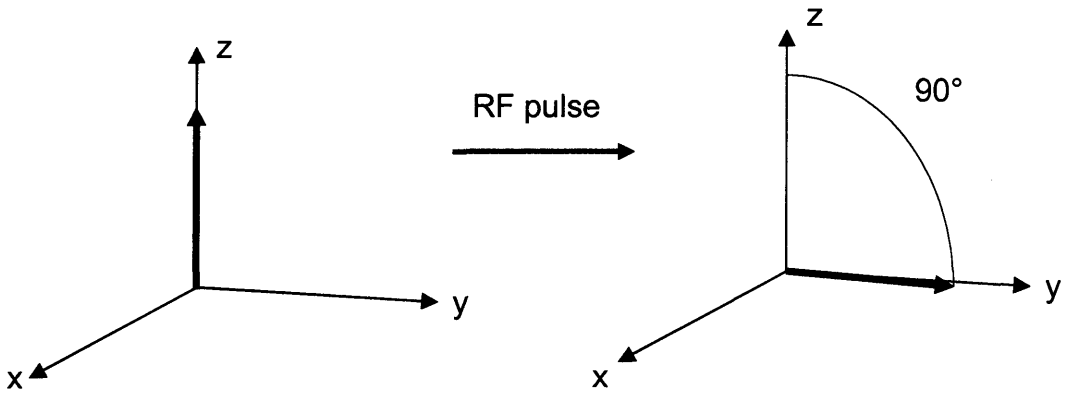

Figure 2.2. Schematic representation of the effect of a radiofrequency (RF) pulse on the net magnetization vector. Prior to the application of the 90° pulse, the vector is aligned to the z axis. After the application of the pulse, the vector is tilted onto the x-y plane.

2.3.2 T_1 and T_2 relaxation in cerebral ischaemia

The loss of transverse magnetization in the x-y plane over time is characterized by the transverse relaxation time T_2. T_1 on the other hand is a time constant that describes the recovery of net magnetization in the longitudinal direction along B_0. The relaxation rate is affected by a number of factors including molecular mobility. T_1 or spin-lattice relaxation describes an energy exchange between the excited protons and their molecular environment, which is facilitated by the presence of macromolecules and tissue structures in the immediate surroundings. T_2 relaxation is also called spin-spin relaxation, reflecting the interactions between neighbouring nuclear spins rather than with the lattice.

Free water, such as CSF, has long T_1 and T_2 relaxation times compared to water in brain tissue due to its high mobility. In contrast, water molecules bound to macromolecules in the tissue will tumble at slower rates and this causes shortening of T_1 and more obviously T_2. Thus, variations rates of relaxation will occur between different tissues. T_1 and T_2 can therefore yield information not only about different structures in the brain but more importantly for this study, about pathological states associated with differences in tissue water properties. As mentioned before, ischaemia causes shifts of water from the extracellular to the intracellular compartment. Diffusion-weighted imaging (DWI) is sensitive to such microscopic alterations and has been extensively used in stroke to detect acute changes in cellular energetics that can predict final lesion size and identify areas of salvageable tissue (Calamante *et al.*, 1999*a*; Shen *et al.*, 2004). Pioneering experiments by Moseley and colleagues established that changes in the apparent diffusion coefficient (ADC) of water occur minutes after ischaemia onset due to the formation of cytotoxic oedema and consequent relocation of water from the extracellular to the intracellular compartment (Moseley *et al.*, 1990). Electrophysiology and spectroscopy studies later confirmed that the timecourse of events following cell swelling is directly related to the decrease in the ADC of water (Hossmann *et al.*, 1994; van der Toorn *et al.*, 1996). Moreover, the relationship between energy failure, ADC and cerebral blood flow thresholds after ischaemia was also studied in gerbil models and embolic rat models, indicating that all these parameters are interdependent (Busza *et al.*,

1992; Busch *et al.*, 1998). Although DWI is a very powerful technique, this study is not concerned with acute phase of ischaemia and other MRI sequences were used instead.

Vasogenic oedema, leads to an increase in overall water content in the lesion area due to BBB breakdown, which causes an increase in the T_1 and T_2 relaxation rates of the affected tissue. Changes in the relaxation times are important in determining contrast in the acquired image. In practice, T_1 and T_2 changes have been accurately correlated to histological areas of tissue damage (Pierpaoli *et al.*, 1993). However, T_2-weighted images are most frequently used to delineate lesion areas because of more apparent changes in T_2 relaxivity (Van Bruggen *et al.*, 1994). Early studies have used T_2-weighted images to evaluate lesion size at 24 hours after permanent MCA occlusion in rats and found strong correlations with histology (Allegrini & Sauer, 1992). Another study followed changes in the ischaemic lesion after 7 hours of permanent middle cerebral artery occlusion in rats. ADC reduction was highest in the core of the lesion (60% of control) and was larger in area than the areas of increased relaxation times during the first 2 hours of occlusion. Later measurements showed a 29% change in T_1 within the lesion and a much higher 51% increase in T_2 (Hoehn-Berlage *et al.*, 1995).

Changes in ADC, CBF and T_2 have been measured in embolic MCA occlusion models in rats subjected to recombinant tissue plasminogen activator (rt-PA) intervention and untreated controls. Immediately after occlusion, changes were seen in CBF and ADC values as expected, while a small increase in T_2 was detected only 4 hours after stroke induction (Jiang *et al.*, 1998). T_2 signal enhancement was maximal at 24 and 48 hours in untreated controls and rt-PA treated rats respectively. These values declined at 1 week but remained higher than baseline in both groups. In fact, the reduction in lesion size in treated animals due to thrombolysis is reflected by the increase in CBF and ADC and by the lower T_2 values at 24 hours compared to untreated controls. Similarly, T_1, T_2, perfusion and diffusion measurements have been made in reversible MCA occlusion models in rats. Van Lookeren and colleagues used diffusion and T_2 weighted imaging to establish the degree of damage following different occlusion times, ranging from 20 to 90 minutes. Moreover, the changes in T_2 and ADC were correlated with histology. Short periods of ischaemia

(< 20mins) resulted in no changes in either ADC, T_2 or tissue morphology. After 90 minutes of occlusion on the other hand, a significant decrease in ADC and increase in T_2 relaxation time were observed 6 hours after reperfusion (van Lookeren *et al.*, 1999). More importantly, these changes were accompanied by major signs of necrosis on histological sections indicating that the tissue was irreversibly damaged. That study also demonstrated that the volume of tissue with increased T_2 relaxation time was maximal at 3 days in animals occluded for 30-45 minutes and at 24 hours in rats occluded for 90 minutes. This suggests that the expansion of cerebral oedema is related to the duration of the initial insult and can be measured in T_2-weighted images. Further support for this hypothesis comes from a focal transient stroke model in rats, where a 2.5 hour occlusion caused the maximum amount of signal change at 48 hours compared to 30 minutes and 1 hour occlusion times. Moreover, this increase in T_2 relaxation was correlated with an increase in lesion volume in histological sections as well as an increase in the duration of the ischaemic event (Neumann-Haefelin *et al.*, 2000).

Another study used MRI and histology to investigate the effect of 10 and 30 minutes of middle cerebral artery occlusion in rats (Li *et al.*, 2000*b*). A temporal profile of T_2 changes showed that values remained equal pre- and post-occlusion in animals subjected to 10 minutes of ischaemia and there were no differences between ipsilateral (ischaemic) and contralateral (non-ischaemic) hemispheres up to 72 hours after stroke induction. The 30 minute group, on the other hand, showed significant hyperintensity in the lesion area at 12 hours, with T_2 values peaking at 48 hours after tissue reperfusion. In agreement with the MRI data, histology on brain sections revealed 17% of neurones were necrotic in the infarct core of the 10 minute transient ischaemia group compared to 95% pannecrosis in the 30 minute group (Li *et al.*, 2000*b*). Similarly, a comparison between the 60 and 90 minutes duration of MCA occlusion in rats shows that the increase in T_2 is highest for the longer occlusion time and continues rising after reperfusion as measured at 4.5 hours. The initial changes found upon ischaemic onset followed the timecourse described for permanent occlusion, with a rapid reduction in diffusion of water and a more progressive increase in T_1 and T_2 relaxation times (van Dorsten *et al.*, 2002). As for models of permanent occlusion, T_2 increase was more pronounced and correlated with areas of decreased ADC, suggesting the evolution of vasogenic oedema.

Interestingly, some experiments have indicated that changes in the relaxation properties of the tissue can be influenced by factors other than vasogenic oedema, such as changes in the oxygenation state of haemoglobin or the exchange of magnetization between free and bound water (Ogawa *et al.*, 1990; Ordidge *et al.*, 1991). Changes in T_1 and T_2 have been observed at early stages of ischaemia in rats at high magnetic field (8.5 T). Remote occlusion of the MCA allowed for immediate simultaneous acquisition of diffusion, perfusion, T_1 and T_2 and allowed for comparison between pre- and post-occlusion values. These experiments showed that alongside the expected decrease in ADC, a decrease in T_2 and an increase in T_1 were also observed (Calamante *et al.*, 1999*a*).

2.3.3 Cerebral blood flow (CBF)

Blood is the constant source of nutrients for the brain. The exchange of oxygen, nutrients and waste between blood circulating at the capillary level and tissue is reflected by the extent of perfusion, i.e. the rate at which blood is delivered to the capillaries in the tissue (figure 2.3). This parameter is therefore conventionally measured as the amount of blood in millilitres per mass of tissue in grams per time i.e. ml/100g/min. A distinction has to be made between measuring blood at the capillary level that exchanges with the tissue, and blood flowing in main arteries and vessels that is simply being transported to and out of the brain. Capillaries are narrow and have semi-permeable vessel walls that facilitate nutrient exchange. Also, blood velocity is much slower than in arteries. Thus, one aim of perfusion techniques is to identify alterations in the rate of such exchange in haemodynamically compromised tissue.

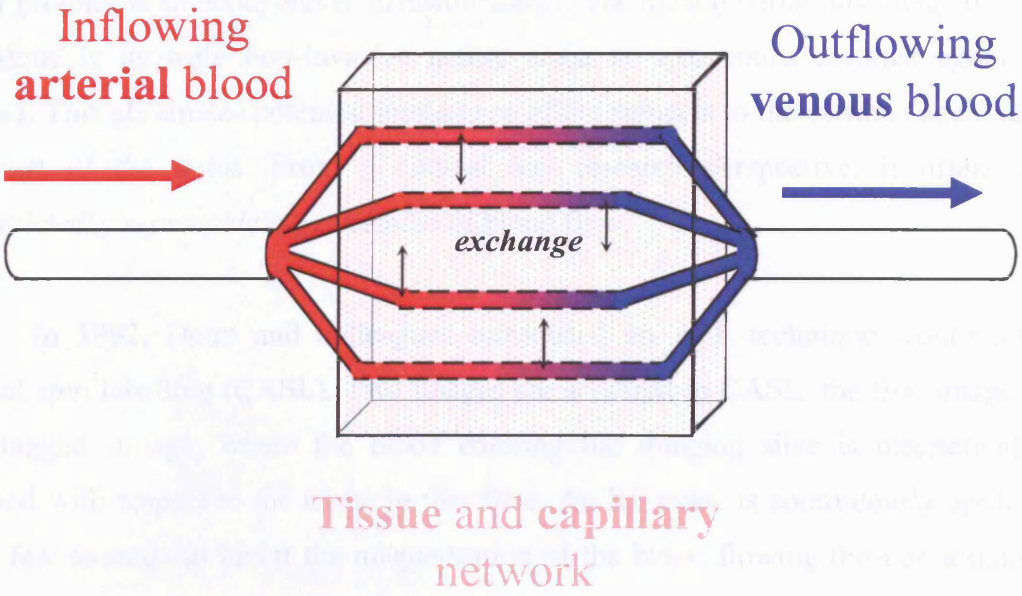

Figure 2.3. Schematic representation of tissue perfusion.

The two main MRI perfusion techniques used to measure CBF are bolus tracking and arterial spin labelling (ASL). The former is widely used in the clinical setting and involves the intravenous injection of an exogenous tracer, a gadolinium based contrast agent. ASL techniques, on the other hand, are based on the use of water protons as an endogenous diffusible tracer. The most obvious advantage of this technique is its truly non-invasive nature since no exogenous contrast agent is needed. This eliminates potential intolerance of the subjects to the contrast agent and the cost of the bolus. From a clinical and research perspective, it offers an unrestrictedly *repeatable* measurement of blood flow.

In 1992, Detre and colleagues introduced an ASL technique, continuous arterial spin labelling (CASL). Two images are acquired in CASL: the first image is the 'tagged' image, where the blood entering the imaging slice is magnetically labelled with respect to the tissue in that slice. An RF pulse is continuously applied for a few seconds to invert the magnetisation of the blood flowing through a major vessel supplying the brain. The inversion slice is commonly placed in the neck so that the water in the blood inflowing to the brain becomes magnetically tagged. Thus, the labelled spins in blood travel into the brain and exchange with tissue water at the capillary bed, altering the magnetization of the perfused tissue in the imaging slice (figure 2.4). In the second image, the control image, inflowing blood is not labelled and thus can be subtracted from the labelled image to reflect the level of perfusion of the tissue (Detre, 1992). Quantification of CBF is, however, not straightforward and several parameters, including the blood-brain partition coefficient of water (λ), the rate of longitudinal relaxation T_1, the efficiency of spin inversion (α) and the steady state vs fully relaxed magnetization per unit mass of brain tissue, need to be considered in order to obtain flow values (Herscovitch & Raichle, 1985; Roberts *et al.*, 1996; Zhang *et al.*, 1995; Alsop & Detre, 1996; Calamante *et al.*, 1999*b*).

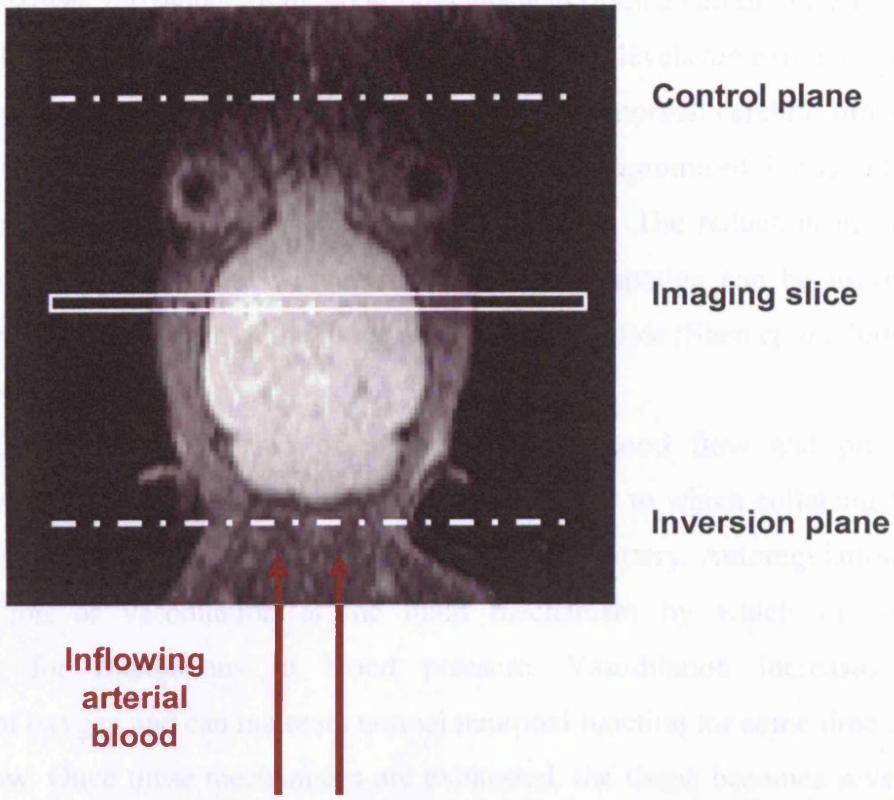

Figure 2.4. Representation of the continuous arterial spin labelling (CASL) technique. Axial scan of the rat brain showing the position of the imaging, control and labelling planes. Blood inflowing from the neck is magnetically labelled when passing though the inversion plane. The site of the inversion slice was chosen in each animal by locating the coordinates for end of the cerebellum. The control plane was chosen by default to be equidistant to the imaging slice in the opposite direction.

2.3.4 CBF thresholds and pathology

The term cerebral ischaemia broadly refers to the interruption of blood flow to the brain. However, the reduction in blood flow needs to reach a certain threshold for the tissue to become infarcted. In the latter case, blood flow levels are extremely low, affecting tissue structure and metabolic rates and impairing normal cerebral function. If the reduction in flow is milder, the tissue is certainly compromised, but is defined as oligaemic rather than ischaemic (Lythgoe *et al.*, 2000). The reduction in blood flow can be heterogeneous after ischaemia and CBF estimation can be useful in classifying the metabolic state of the tissue and therefore its fate (Shen *et al.*, 2004).

Immediately after occlusion of an artery, both blood flow and pressure decrease. Blood flow will then be determined by the extent to which collateral flow and alternative arterial routes compensate for the occluded artery. Autoregulation via vasoconstriction or vasodilation is the main mechanism by which the body compensates for fluctuations in blood pressure. Vasodilation increases the availability of oxygen and can maintain normal neuronal function for some time after a drop in flow. Once these mechanisms are exhausted, the tissue becomes severely compromised and can become infarcted via processes already detailed in section 2.2.3 (Powers *et al.*, 1991).

Several groups have determined cerebral blood flow thresholds in different animal species and through different methods. Experiments in rats and gerbils have determined that protein synthesis starts to be compromised when CBF levels drop to 55 ml/100g/min, which corresponds to oligaemic perfusion (Astrup *et al.*, 1981; Xie *et al.*, 1989; Mies *et al.*, 1991; Hossmann *et al.*, 1994). Lactate accumulation, tissue acidosis and excitatory amino acid release occur at values of about 35 ml/100g/min (Obrenovitch *et al.*, 1988; Allen *et al.*, 1993). A 25-20 ml/100g/min threshold exists, below which metabolic dysfunction is severe, causing ATP and glucose decrease (Mies *et al.*, 1991; Allen *et al.*, 1993). Because brain tissue has no oxygen stores, it is unable to sustain brain activity. In fact, it has been shown that below 15 ml/100g/min electrical activity in neurones disappears: failure of the ion pumps on cell membranes

leads to disturbances of ionic gradients and cell depolarization (Astrup *et al.*, 1981; Hossmann *et al.*, 1994).

Moreover, early experiments by Busza and colleagues established a relationship between CBF thresholds and ADC decrease in a gerbil model of forebrain ischaemia (Busza *et al.*, 1992). Only when flow values were lower than 20 ml/100g/min did the decrease in ADC become significant. This threshold was found to be higher in rat models of focal ischaemia where flows of 30-35 ml/100g/min were sufficient to correlate with ADC changes (Kohno *et al.*, 1995). In fact, these experiments found a further relationship with the duration of the insult whereby the CBF threshold increases in a time dependent manner (reviewed in Thomas *et al.*, 2000). Combined analysis of ADC changes, CBF values and ATP levels has been useful in classifying different territories within the ischaemic lesion: normal tissue is defined as a region of normal perfusion and diffusion, whereas hypoperfused regions can present normal diffusion but decreased CBF values and severely compromised tissue at the core of the lesion tends to exhibit abnormal perfusion and diffusion values (Hoehn-Berlage *et al.*, 1995; Kohno *et al.*, 1995; Calamante *et al.*, 1999*a*; Shen *et al.*, 2004). These studies have helped in the investigation of the penumbra, the hypoperfused border region of the lesion that can potentially lead on to infarction.

2.4 Summary

This chapter has aimed to briefly review the pathophysiological changes occurring in cerebral ischaemia. The brain has high energetic demands and needs a continuous supply of oxygen and nutrients from blood. A reduction or suppression in flow can severely and irreversibly damage neurones. This is, however, a complex phenomenon encompassing a series of gradual events that lead to cell death and infarct formation. Even if the pathophysiology of the lesion evolution has been characterized over a number of years, there is still a need for further therapeutic study. Animal models of stroke are therefore essential for the development of neuroprotective strategies that can reduce the brain's vulnerability to an ischaemic

event. The application of MRI techniques has been crucial in studying stroke because it allows non-invasive and repeatable image acquisition on the same animals over time. This enables the design of longitudinal studies while significantly reducing the number of animals required. Moreover, it is possible to simultaneously obtain multiparametric data reflecting the consequences of ischaemia at a cellular level, reporting on changes in energy status, metabolism, function and morphology along with perfusion alterations that underlie the pathology. Furthermore, the longitudinal, multiparametric data sets acquired can then be integrated with end point histological analysis.

Chapter 3 *Gene delivery to the brain*

3.1 Introduction

Gene therapy was initially conceived as the replacement of defective genes causing a particular disease with functional ones. However, this concept has now been extended to other pathologies in which symptoms can be relieved by expressing or overexpressing certain genes even if the disease has no genetic aetiology. Several systems have therefore been developed to incorporate foreign genes and deliver them into specific cell types, often to determine whether overexpression of a particular protein has any impact on an ongoing biological process. This is of great value for both research and medical applications. This chapter will discuss the desirable features of a viral vector, concentrating on the herpes simplex virus vector used in this study, its applications to gene delivery to the central nervous system and the relevance of gene therapy for cerebral ischaemia.

3.2 Gene delivery methods

Gene therapy relies on the efficient delivery of genes *in vivo*. Numerous laboratories have attempted this via two main approaches: *ex vivo* and *in vivo* gene introduction using either DNA plasmids or engineered viral vectors. *Ex vivo* gene therapy involves transfection of cells with the gene of interest via plasmids or viruses *in vitro*, followed by grafting of the cultured cells into the tissue. For example, fibroblasts and myoblasts have been used for the treatment of Parkinson's disease in animal models: the grafted cells were engineered to express tyrosine hydroxylase and their transplantation reduced rotational behaviour in a 6-hydroxydopamine rat model of the disease (Fisher *et al.*, 1991). Some of the limitations of this method are the finite duration of expression of the transgene and the potential tumorigenic effects of transplanting tumour derived cell lines.

Direct injection of DNA in a plasmid vector has proved rather unsuccessful in the brain, probably due to the rapid degradation of the foreign nucleic acid upon entry into the host. In an attempt to refine this simple method, the nucleic acid was coated with a cationic liposome that facilitated entry to the cell (Tsuda & Imaoka, 1996). *In vivo* injections to the mouse brain have yielded low numbers of transfected cells and astrocytes were more often transfected than neurones (Imaoka *et al.*, 1995). These and other studies suggest that gene delivery efficiency and specificity are still too low to envisage its applications to therapeutics.

Viruses, on the other hand, are natural and highly efficient nucleic acid delivery systems. A straightforward strategy is to use such viruses to directly and efficiently deliver therapeutic genes to the nervous system. The main concern, however, is the potential toxicity of the vector to the host. Several laboratories have attempted to engineer disabled or attenuated viruses that are safe whilst retaining their efficiency of transfer. The range of viruses now available for research purposes makes choosing the right vector for the study more difficult, although adenoviruses, herpesviruses and retroviruses such as lentiviruses are the most commonly used. Hence, the advantages of the herpes virus chosen for this study will be briefly reviewed in the next section.

3.3 Choice of vector

Several issues need to be considered when using viruses for gene therapy. Firstly, the vector should have no cytopathic effects in order to cause minimum or no toxicity to the host. Secondly, it should be efficient in delivering the transgene, which implies it should have high infectivity. Moreover, it should be able if possible to selectively infect the target cells. These properties will in turn determine how many cells need to be infected to achieve the desired result. The insert capacity of the vector should also be taken in to account since it will determine the allowed size of the transgene. Lastly, viral expression should be sustained for a considerable period of time depending on the aim of the study. Most of the vectors available for gene therapy are derived from common human pathogens and tend to be able to infect

more than one cell type. This is important when considering that the brain contains a variety of cells, and targeting a specific sub-group can be difficult.

The method of delivery of the transgene should be as safe as possible. In the case of viruses this is a key factor because of their pathogenicity. They enter the nucleus and use the cell's own machinery to replicate their nucleic acid and form new virion particles. This cycle results in lysis and death of the cell as the new viruses accumulate in the cytoplasm to be released. There are several mechanisms that the virus interferes with in order to survive in the cell, like avoiding an immune reaction from the host or entering the nucleus and shutting down the cell's protein synthesis to establish its own. It is therefore important to know the entry routes for each specific virus and how they replicate in the specific cell type. This is the only way of introducing disabling mutations in the viral vector that will impede its replication, thus rendering it non-toxic but allowing it to stably infect the cell and express the inserted transgene.

A generic division is helpful in understanding the mechanisms of entry to the cell. Capsid virions like adenovirus and adeno-associated virus (AAV) have their nucleic acid surrounded by a protein structure, whereas enveloped virions like herpes simplex virus and retroviruses have a lipid bilayer surrounding the capsid. Adenoviruses, for example, enter the cell by binding to specific receptors and integrins on the plasma membrane and become temporarily enclosed in an endosome. This process is known as receptor mediated endocytosis. Enveloped viruses, on the other hand, use their glycoproteins to attach to the cell's membrane and diffuse along it until they encounter receptors that enable penetration (Frampton *et al.*, 2005). After the envelope fuses with the cell surface, the viral capsid is released directly into the cytosol where it binds to dynein proteins associated to microtubules and is transported to the nucleus (Davidson & Breakefied, 2003).

Similarly, the mechanism of entry to the nucleus can vary. Small viruses, like parvoviruses, are able to enter the nucleus directly through the nuclear pore without being modified. Adenoviruses induce rupture of the endosomal membrane and release the viral DNA for nuclear entry. Retroviruses wait until the cell undergoes division and take advantage of the nuclear membrane reorganization during mitosis

to associate with chromatin and integrate to a newly assembled nucleus. This implies that the infectivity of retroviruses depends largely on the rate of division of the specific cell type in question and that they are unable to infect non-dividing neurones (Whittacker *et al.*, 2000). On the other hand, certain retroviruses like lentiviruses are able to infect non-dividing cells and have the advantage of being non-immunogenic and not very toxic to the host. However, the main disadvantage of retroviruses is the fact that their DNA is incorporated into the host genome and genes can be mutated in this process. Similarly, adenoviruses carrying deletions in essential early genes that control replication have been found to sometimes express late viral genes leading to cytotoxicity. Such "leaky" gene expression results in the stimulation of an immune response by the host *in vivo* (Yang *et al.*, 1994). Several mutations have been introduced to the herpesvirus genome and this will be reviewed in the next section.

The size of the genome is also very important in determining the choice of vector. Table 3.1 lists some of the most commonly used viruses and their size in base pairs (bp). Adenoviruses and adeno-associated viruses are often used but have small genomes and therefore very limited cloning capacity of 8 and 4.5 kb respectively (Bett *et al.*, 1994). Attempts to overcome such limitations resulted in the generation of "gutless" adenoviruses in which the viral genome is provided in *trans* by a cell line or helper virus, thus potentially extending the cloning capacity to 37 kb (Mitani *et al.*, 1995). Similarly, the disadvantage of adeno-associated virus is that it needs co-transfection with a helper virus in order to replicate. Herpesviruses in contrast have a large genome size and the fact that many non-essential genes can be deleted without impairing viral replication processes allows it to accommodate a large amount (~30-40 kb) of foreign DNA (Latchman, 2002). This is important for therapeutic purposes, since it is feasible that more than one gene may need to be delivered, possibly therapeutic genes acting together or even in combination with a marker gene. An example of the benefits of large transgene capacity is an experiment by Haase and colleagues where two separate adenoviral vectors carrying neurotrophin-3 and ciliary neurotrophic actor respectively were delivered simultaneously to alleviate motor neurone disease in mice (Haase *et al.*, 1997).

The duration of transgene expression is determined by more than one factor. Retroviruses ensure long term expression because they integrate to the cell's

genome. Some experiments have in fact demonstrated β-galactosidase transgene expression six months after inoculation using an HIV-based lentiviral vector in neurons *in vivo* (Blomer *et al.*, 1997). However, as stated before, this also represents an inherent mutation or inactivation risk for the host. Herpesviruses are the only pathogens that naturally establish a latent asymptomatic infection in human neurones. The reasons for this will be discussed in detail in the next section but suffice to say it possesses latency associated transcripts (LAT) that can potentially be engineered for long term expression.

This study uses herpes simplex virus type-1 (HSV-1) because it meets many of the abovementioned demands. The vector has a large transgene capacity and is able to infect neurones *in vivo* thus ensuring high infectivity and efficiency of gene delivery into the brain. Other advantages that make this virus very suitable for gene therapy are that it can be manipulated to enter long-term stable asymptomatic latency in the infected cells and its genome remains episomal, thus reducing the risk of insertional inactivation or mutation of host genes (Fink *et al.*, 1996; Wolfe *et al.*, 1999; Latchman, 2001). Overall, this viral vector appears to be more suitable for investigating the effect of heat shock protein expression before and after ischaemia than others reviewed. The next sections will describe the way HSV enters the cell, the genetic controls of its replication cycle and the mutations that have been introduced in order to maximize its safety as a vector.

Virus Type	Genome size (kb)
Adenovirus	35
Adeno-associated virus	8.5
Lentivirus	10
Herpesvirus	152

Table 3.1. Genome sizes of the viruses most commonly used for gene therapy.

3.4 The biology of HSV type 1

HSV is a double stranded DNA virus consisting of two unique DNA segments, the unique long (U_L) and unique short (U_S), each flanked by a pair of inverted repeats (I_R) (figure 3.1). The nucleic acid is surrounded by an icosahedral capsid composed of four different proteins. Between this capsid and the external glycoprotein lipid envelope lies the tegument, a layer attached to the capsid that contains a range of proteins with diverse functions. The genome's size is 152 kb and it encodes for more than 80 different genes with characteristic temporal expression patterns upon infection: immediately early genes (IE) are followed by early (E) and late (L) genes respectively (Wagner *et al.*, 1995; Stingley *et al.*, 2000).

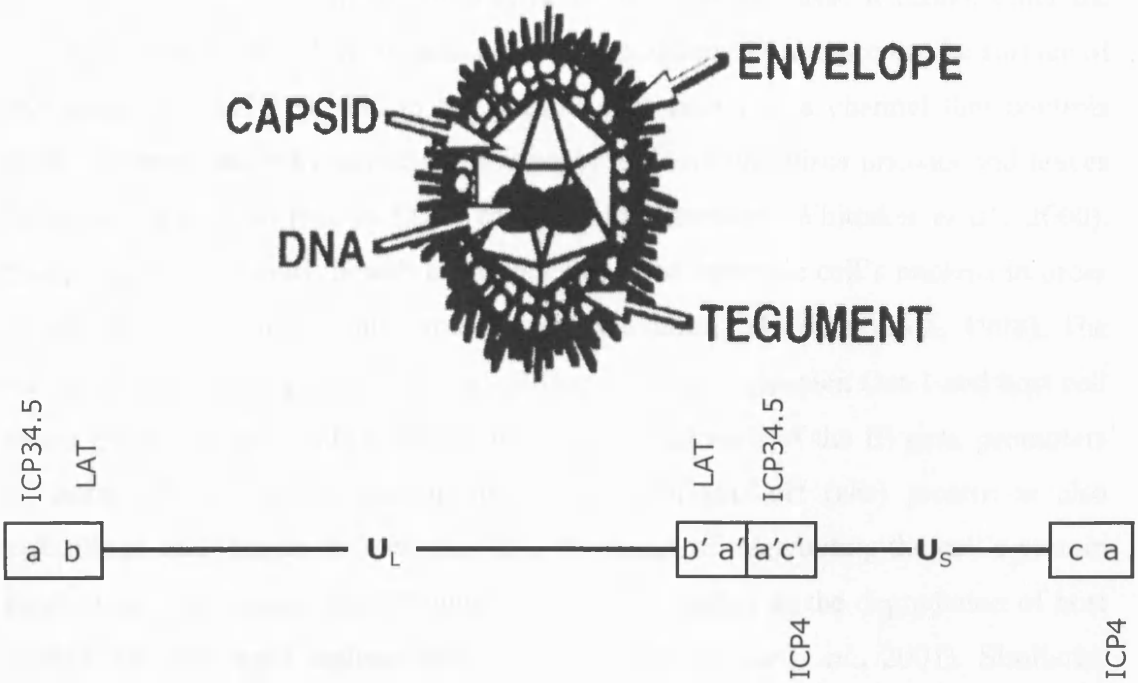

Figure 3.1. Schematic representation of the herpes simplex virus structure and genome (adapted from Fink *et al.*, 1996).

The infection cycle begins with fusion of the viral envelope to the plasma membrane of the host cell. Because HSV is such a large virus, it cannot enter the nucleus directly. Instead, it contains a nuclear localization sequence on the surface of the capsid that helps it bind to the nuclear pore complex, a channel that controls traffic between the cytosol and the nucleoplasm. Here, the virus uncoats and leaves its capsid behind so that its DNA can enter the nucleus (Whittaker *et al.*, 2000). Some tegument proteins detach from the capsid and enter the cell's nucleus in order to mediate viral genome entry and IE gene activation (Morrison *et al.*, 1998). The virion trans-activator protein VP16 in particular forms a complex Oct-1 and host cell factor (HCF), which binds to the promoter region of each of the IE gene promoters (O'Hare, 1993). Another protein, the virion host shut-off (*vhs*) protein is also essential at early stages of infection and is in charge of interrupting the cell's protein production. *Vhs* triggers endoribonuclease activity leading to the degradation of host mRNA and the rapid replacement with viral mRNA (Lu *et al.*, 2001). Similarly, gamma 34.5 is involved in preventing shut-down of protein synthesis by the host at late stages in the infection cycle (He *et al.*, 1997).

There are five IE genes in HSV-1 that are expressed in the absence of *de novo* protein synthesis: infected cell polypeptide 0 (ICP0), ICP4, ICP22, ICP27 and ICP47. Overall, IE genes are responsible for orchestrating viral replication. ICP4 and ICP27 regulate E and L gene expression at the transcriptional and post-transcriptional level and have been shown to be crucial for lytic viral replication *in vitro* and *in vivo* (reviewed in Weir, 2001). E genes encode for important enzymes that produce nucleotide pools and initiate viral DNA synthesis, such as thymidine kinase and DNA polymerase. L gene products include structural proteins of the capsid, tegument and envelope and do not become activated until the newly synthesized DNA is cleaved to the right length and ready to package. The "a" sequence within the short IR is used as a packaging signal. The envelope is acquired as the particle exits the cell through a modified patch of the nuclear membrane that expresses viral glycoproteins (for reviews see Roizman & Sears, 1996; Fink *et al.*, 1996; Whittaker *et al.*, 2000; Weir, 2001).

HSV has the ability to infect a range of cell types but is naturally neurotropic (Roizman & Sears, 1987; Latchman, 1990). After infecting and replicating in epithelial cells, it migrates up nerve processes to cell bodies via retrograde axonal transport. Once in the neurone, HSV can undergo lytic replication or remain latent. If the virus establishes such silent infection, it remains in the sensory neurones that innervate the peripheral skin cells originally infected without expressing most genes or disrupting the host cell. This dormant state can be disrupted by stress and the virus can reactivate to enter the lytic cycle. The fact that the virus can transport away from nerve termini, remain latent in neurones, reactivate and transport again to the peripheral epithelial cells explains the patterns seen in the pathology it causes. The initial skin infection gives rise to cold sores or genital sores that tend to disappear but are characteristically recurrent. It is important to note that the infection does not cause damage to the neurone or its processes and is entirely asymptomatic. These characteristics already address some of the issues raised by gene therapy: permanence in the neurone with minimal toxicity. It should, however, be noted that direct injection of the virus to the brain could potentially lead to encephalitis if the attenuated virus reverted to wild type. The virus can potentially be engineered for long term gene expression but during its latency period, viral gene expression almost completely shuts down and the virus remains silent (Roizman & Sears, 1987). Hence, transfected genes will also be silenced and the therapeutic effect is lost. Latency associated transcripts (LATs), however, are the few genes still active during latency. Many laboratories have attempted to use the promoters for such genes to drive long term expression of exogenous genes, by either inserting the transgene close to the LAT region or linking the LAT promoter to a different part of the genome where the foreign gene lies (for review see Latchman, 2002). Some of these experiments have been successful in producing long term expression both *in vitro* and *in vivo*, indicating that, in this respect, HSV is more advantageous than other viruses for gene therapy (Ho & Mocarski, 1989; Goins *et al.*, 1994; Coffin *et al.*, 1998; Palmer *et al.*, 2000).

3.5 Disabled HSV-1 vectors

Two different HSV-1 types of vector are currently available for central nervous system gene delivery, amplicon vectors and recombinant viruses. Amplicon systems involve introducing the transgene into a plasmid containing an HSV origin of replication and packaging signal ("a"). This is grown in bacterial cells and transfected into cell lines together with a deficient HSV helper virus. The plasmid replicates into concatamers with the aid of the helper virus and is packaged into viral particles (reviewed in Fink *et al.*, 1996). The alternative system still involves the insertion of the gene of interest in a plasmid but this time flanked by specific HSV sequences. Cells are then co-transfected with plasmid and HSV and homologous recombination leads to insertion of the transgene directly into the viral genome (Coffin *et al.*, 1996; Freese *et al.*, 1996). Reporter genes such as green fluorescent protein (GFP) or LacZ can then be used to select recombinant versus non-recombinant viruses. This in turn renders quantification by titration and plaque assay easier. Although both amplicon and recombinant viral systems are currently in use, this study used the latter and it will therefore be the only one discussed.

A lot of effort has been focused on improving the efficiency of gene transfer and, more importantly, the degree of disability of the vector without compromising its ability to grow in culture. The simplest way of making viral vectors safe to their host is to render them avirulent by deleting some of the key immediately early genes involved in the lytic growth cycle. Viruses lacking ICP4 and or ICP27 have in fact been constructed to impair lytic replication in all cell types and eliminate the risk of encephalitis after injection to the brain (Chiocca *et al.*, 1990; Dobson *et al.*, 1990; Howard *et al.*, 1998). Deletion of ICP0 or ICP22, on the other hand, does not impair replication completely but reduces titre and therefore some of its toxicity (Post & Roizman, 1981; Sacks & Schaffer, 1987). Some of these mutations, like deletion of ICP4 or ICP27, require that the defective virus is grown in complementing cell lines engineered to express the missing gene in order to allow replication to occur. Special care should be taken so that the gene sequence in the cell line and the ones remaining in the virus do not overlap so that no recombination can take place that could revert the virus to wild type. Losing avirulence of the vector could obviously have

disastrous consequences to the host in terms of toxicity and could lead to encephalitis *in vivo*.

Reversion to virulence by homologous recombination with genes added to the cell line can be avoided through different strategies. Some have attempted the deletion of ICP34.5, a viral gene needed for replication in non-dividing cell types only. This mutation does not affect growing of the virus in dividing cells *in vitro* and therefore does not require a complementing cell line, but it prevents lytic growth after brain delivery *in vivo* (Maclean *et al.*, 1991; Robertson *et al.*, 1992; Coffin *et al.*, 1996). Another target protein is vmw65 or VP16 which is involved in transactivating IE gene promoters at early stages of infection. Mutations in it vastly reduce IE gene expression and such vectors have been used for *in vivo* delivery of β-galactosidase to dorsal root ganglion neurones (Ecob-Prince *et al.*, 1995; Thomas *et al.*, 1999).

Alternatively, deletion of more than one gene for viral attenuation is a more efficient strategy since it reduces the chances that all deleted genes required for viral replication will be recombined at once. Even if this approach is technically more laborious, it has been widely applied when developing new viral vectors in order to increase safety. The ICP34.5 disabled virus has been used as a platform for developing other vectors. Howard and colleagues combined deletions in this gene and ICP27 to guarantee no lytic replication in either dividing or non-dividing cell types in the rodent brain *in vivo*. The double mutant was less damaging to cells and more efficient in delivering the LacZ transgene than a vector with a single ICP34.5 mutation (Howard *et al.*, 1998). Similarly, a virus deleted for ICP4, ICP22 and ICP27 stops synthesizing DNA transiently and safely expresses the transgene in primary neurones *in vivo* for over three weeks (Krisky *et al.*, 1998). Other vectors used have combined mutations in vmw65 and ICP4 or ICP27, which are unable to undergo lytic growth and efficiently express the desired transgene but require further modifications to grow in culture even when using complementing cell lines (Thomas *et al.*, 1999; Lilley *et al.*, 2001). Moreover, viruses carrying deletions in ICP34.5 and inactivating mutations in vmw65 are successful in delivering the LacZ transgene to dorsal root ganglion (DRG) neurones in mice (Coffin *et al.*, 1996). Such constructs have been further engineered by inserting the transgene under the control of LAT

promoter in order to improve long term β–galactosidase gene expression in DRG neurones after footpad inoculation (reviewed in Palmer *et al.*, 2000).

Overall, there is sufficient evidence to suggest that different alterations to the HSV genome can be made in order to optimize efficient and safe gene delivery to the brain. This encouraging work has been essential in the development of the vector used in this study, a recombinant HSV-1 vector disabled for lytic replication by deletions in ICP25, ICP34.5 and vmw65.

3.6 Applications to the CNS

Gene therapy for neurological diseases has yielded some promising results but is still in its infancy. The use of viruses for gene delivery provides an important tool to address key issues about the aetiology and molecular biology of such disorders. Viral vectors have been developed to efficiently introduce therapeutic proteins *in vivo* and assess their effects (see Wolfe *et al.*, 1999; Burton *et al.*, 2002; Verma & Weitzman, 2005). HSV in particular has been used in several models of neurodegenerative disease since its latency state can be exploited for long term gene expression. One of the main concerns with HSV is that being such a common human pathogen its incidence in the population is high and the latent virus could revert the attenuated one to wild type. However, animal experiments and to some extent human clinical trials suggest this is not very likely (reviewed in Latchman, 2002).

HSV vectors have been used to deliver GDNF, a glial derived neurotrophic factor, to prevent dopaminergic cells in the substantia nigra from dying in a rodent model of Parkison's disease (Choi-Lundberg *et al.*, 1997). Viruses expressing GDNF or tyrosine hydroxylase cause a reduction in rotational behaviour in 6-hydroxydopamine rat models of Parkinson's disease (Latchman & Coffin, 2000). Similarly, viral driven overexpression of Bcl-2 was shown to prevent death of dopaminergic neurones *in vivo* (Yamada *et al.*, 1999). HSV has also been used to deliver the Brn-3a transcription factor where it promoted neuronal survival after sciatic nerve injury (Smith *et al.*, 2001).

Applications of gene therapy to stroke are fewer but promising. Many studies have preferentially used HSV-based vectors for reasons stated before. Overexpression of Bcl-2 before or after a 1 hour ischaemic insult is able to significantly protect striatal neurones (Lawrence *et al.*, 1996; Lawrence *et al.*, 1997). This protein is able to block cytochrome *c* release and therefore interrupt the downstream cascade of events leading to apoptosis. Pre-ischaemic delivery of the glucose transporter gene Glut-1 was found to protect neurones against ischaemia in rats (Lawrence *et al.*, 1996). It is thought that glutamate overexpression can improve energy availability to compromised cells in the penumbra and increase the ATP levels needed for cellular functions. A different strategy is to reduce the amount of intracellular Ca^{++} in order to prevent cytotoxic oedema and consequent cell death following ischaemia. HSV-driven calbindin D28K expression in the striatum has improved neuronal survival after MCA occlusion in rats by acting as a calcium buffer (Yenari *et al.*, 2001). Other experiments have shown that pre- and post-ischaemic delivery of HSP70 can protect the brain from stroke, possibly through its chaperone properties and by reducing the effect of reactive oxygen species (Yenari *et al.*, 1998; Hoehn *et al.*, 2001).

Although the feasibility of such experimental evidence directly correlating to successful clinical trials is low, investigating gene and cell therapy in animal models can yield important information. Because stroke, like any other pathology, involves a complex series of events, it might be necessary to address each of these events individually or through combined therapies. An excellent review by Szentirmai and Carter highlights the fact that delivery of a single gene or pharmacological agent at an acute stage is unlikely to prevent or ameliorate the damaging consequences of stroke. The authors suggest that cell and gene therapy might in fact be more useful in enhancing the recovery of the tissue by restoring cellular architecture and helping cells to regain their functionality (Szentirmai & Carter, 2004). This, in combination with neuroprotective strategies and targeting of the ongoing pathology in penumbral areas, might prove a more effective strategy.

3.7 Summary

This chapter has concentrated on how viruses can be exploited for gene delivery if appropriate modifications are engineered into them in order to avoid lytic growth and toxicity. The application of viral vectors, and in particular herpes simplex virus, to animal models of disease has also been reviewed, paying particular attention to the relevance of gene therapy for cerebral ischaemia. Such issues are crucial in the context of this study since the effect of pre- and post-ischaemic viral delivery of therapeutic genes is assessed.

Project Aims

The overall aim of this project is to use MRI techniques to assess the neuroprotective effect of heat shock protein (HSP) overexpression in a rat model of stroke. Three different experiments have been designed in order to investigate such effect:

a) intracerebral microinjections with herpes simples virus vector carrying LacZ (HSV-LacZ) control protein in order to determine viral expression levels and regional distribution in the rat brain (Chapter 4);

b) pre-ischaemic delivery of HSV engineered to express HSP27 (HSV-HSP27), HSP70 (HSV-HSP70) and control protein (HSV-LacZ) into the rat striatum, using MRI to determine changes in the ischaemic lesion size (Chapter 5);

c) post-ischaemic intrastriatal microinjection of HSV-HSP27, HSV-HSP70 and HSV-LacZ virus, using MRI to measure the effect of therapy on lesion size and behavioural tests to assess functional recovery up to 1 month after stroke (Chapter 6).

VIRAL MICROINJECTIONS

Chapter 4 *Viral microinjections*

4.1 Aims

The purpose of this study was to assess viral expression *in vitro* and *in vivo*. Although this construct has been previously used, it was necessary to verify that the vector was effective in expressing the transgene. Viral stocks were grown on a large scale and the infectivity of the HSV-LacZ virus was tested initially *in vitro*. Once β-galactosidase expression was verified, the efficiency of the construct was investigated *in vivo* by intracerebral microinjection in 18 rats. These were divided into 5 sub-groups which were sacrificed at 6 different time points following microinjection: 3 days, 5 days, 1 week, 2 weeks, 3 weeks, 4 weeks (see schematic representation below). Spatial distribution and expression levels of the LacZ transgene in the brain were assessed by X-gal staining.

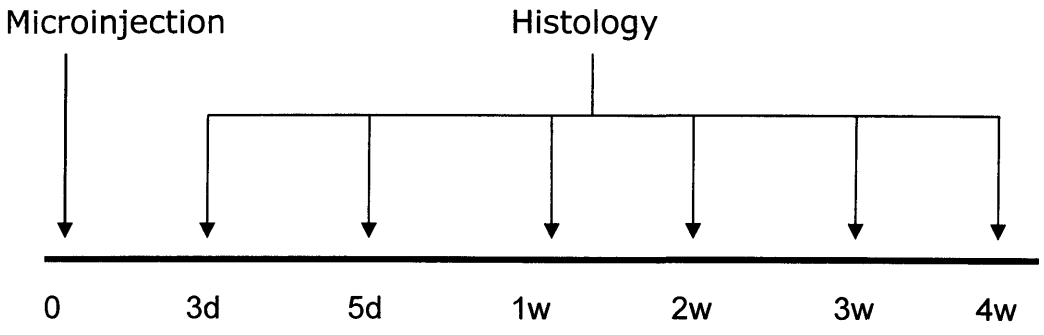

Figure 4.1. Schematic representation of the experimental design. Animals were microinjected with HSV-LacZ and sacrificed at different timepoints to confirm viral transgene expression *in vivo*.

4.2 Methods

4.2.1 Tissue culture

4.2.1.1 *Reagents and solutions*

All solid chemicals were dissolved in either ddH_2O or autoclaved phosphate buffered solution (x1 PBS). General laboratory chemicals were of analytical grade and purchased from either: Sigma Chemical Company Ltd, U.K; Life Technologies, U.K., or Amersham Biotechnologies, UK. General disposable plasticware was supplied by Sterilin unless otherwise stated. General solutions were prepared as follows:

Phosphate buffered saline (PBS), stock concentration (x10): 104mM sodium, 1.8mM potassium chloride, 5.4mM disodium orthophosphate dihydrate, 1.25mM potassium dihydrogen orthophosphate (pH7) in ddH_2O.

Paraformaldehyde (PFA): 4% w/v in sterile PBS.

Full growth medium (FGM): 10% Foetal Calf Serum (FCS) in Dulbecco's modified Eagel's medium (DMEM).

Selection medium: 10% FCS-DMEM, G418 (Geneticin) as 64mg x 100ml medium, Zeocin as 700µl x 100ml medium.

Virus medium: 20% FCS-DMEM + 2 x HMBA (2.8ml of HMBA x 100mls of medium).

HMBA: 2% w/v solution = 1g in 50mls of DMEM (filter sterilized).

CMC solution: 1.6% w/v carboxymethyl cellulose (CMC) in water.

Freezing medium: 30% FCS-DMEM and 8% DMSO.

Cresyl violet stain: 0.1% w/v cresyl violet in 20% ethanol.

4.2.1.2 *Growth conditions for mammalian cell lines*

A laminar flow safety cabinet was used to perform all tissue culture and viral preparations in order to ensure sterility and safety conditions. A baby hamster kidney (BHK) cell line, B130/2, was modified to stably express the zeocin resistance gene and the ICP27 gene from HSV-1 strain 17+ under the control of an ICP27 promoter. The cells were grown in Dulbecco's modified Eagel's medium (DMEM), containing 10% foetal calf serum (FCS). B130/2 cells were selected by adding 500μg of Geneticin or G418 sulphate per ml to the growth media. Cells were grown from frozen stocks at 37°C/ 5% CO_2, seeded, allowed to reach confluence (48-72 hours approximately) and passaged as many times as required for infection. Stocks of cells were frozen down for repeated use.

4.2.1.3 *Thawing BHK B130/2 cells*

Cells were removed from -80°C and quickly placed at 37°C. Once thawed, the cells were rapidly pipetted onto 10mls of pre-warmed DMEM and spun down at 1000rpm for 5 minutes. The supernatant was discarded and the pellet resuspended in 0.5mls of medium. The cells were then plated onto a medium or large flask and incubated at 37°C/ 5%CO_2 for at least three days or until confluent.

4.2.1.4 *Freezing BHK B130/2 cells*

Once cells reached 80-90% confluence, they were passaged by washing with 10mls of Hank's Balanced Salt Solution (HBSS) and trypsinizing. This was achieved by incubating the monolayer for 1 or 2 minutes with 4mls of a detergent solution containing 10% trypsin in versene. Once the monolayer was disrupted, 6mls of 10% FCS-DMEM were added and mixed thoroughly. The cells were then centrifuged in 15ml tubes at 1000rpm for 5 minutes. Most of the supernatant was then very carefully removed and discarded. The pellets were resuspended in 4mls of freezing

medium, consisting of 30% FCS-DMEM and 8% DMSO. Cells needed to be counted in a hemocytometer and freezing medium was added in order to adjust the final concentration, until 1-2 million cells per vial was achieved. Vials were wrapped in paper roll and placed in a polystyrene cup, covered with aluminium foil at -80°C for at least 24 hours. The vials were transferred into liquid nitrogen for long term storage.

4.2.2 Infection of mammalian cell lines with recombinant virus

4.2.2.1 *Creating a virus stock*

A 6 well plate of B130/2 cells was grown by splitting a large flask ($175cm^2$) of confluent cells as detailed before (i.e., wash with 10mls of Hank's Buffer; trypsinize with 4mls of trypsin-versene, add 6mls of full growth medium and mix). An aliquot of 1.25mls out of the resulting 10mls of cells and medium was used for each plate, i.e. 200µl of cells per well. Each well was topped up with selection medium for a total final volume of 2mls per well. The solution was thoroughly mixed and incubated at 37°C/ 5% CO_2 for 24 hours or until confluent. All the medium was carefully discarded and replaced with 500µl of DMEM + 5µl of virus. The plates were gently rocked sideways in order to completely cover the cells with the viral suspension. After incubating at 37°C/ 5% CO_2 for 1 hour, the wells were overlaid with 500µl of viral medium (20% FCS-DMEM + 2 x HMBA) and incubated at 37°C for 48 hours. Once most cells had lysed, the edges of the plate were sealed with parafilm very carefully and placed at -80°C at least overnight before using.

4.2.2.2 *Large scale viral culture*

A 6 well plate was initially grown and each of the wells was harvested and used to seed a $175cm^2$ tissue culture flask as detailed in the previous sections. Once

the flasks were fully confluent, all supernatant was removed and enough serum free DMEM was added in order to cover the cells (6mls approximately). The 6 well plate of viral stock was thawed and one well of solution was added to each flask. The cells and virus were mixed gently and incubated at 37°C/ 5% CO_2 for 1 hour. Then, each flask was overlaid with 10mls of virus medium and incubated at 37°C/ 5% CO_2 for 48 hours. Once most cells had lysed, the large flasks were frozen at -80°C before further use.

Once again, 10 large flasks of cells were grown until fully confluent and split so that each flask contained 10mls of cells and medium. Each of these 10mls was placed in an 850cm^2 disposable roller bottle (Corning Glass Works, Corning, New York, U.S.A.) and 40mls of FGM were added for a total volume of 50mls per bottle. The bottles were supplemented with 5% CO_2 in 95% air through a double filtered gas line in a laminar flow cabinet thoroughly sprayed with 70 % ethanol for sterility. The lids were then closed tightly and the bottles incubated for approximately three days until fully confluent at 37°C in a roller bottle incubator rotating at 0.5rpm. Once the cells were fully confluent, the bottles were infected by removing all medium and replacing it with 25mls of a mixture of virus and medium prepared as: 12.5mls of thawed virus stock (i.e., the large flasks infected and stored at -80°C) and 12.5mls of fresh serum free DMEM. The bottles were incubated at 37°C for 1 hour and a further 25mls of virus solution was added to each bottle for a total volume of 50mls. CO_2 gas was added to each bottle before incubating at 37°C for a further 48 hours.

As infection progressed, the medium started acidifying and changing colour, and most cells appeared dead under the microscope (i.e. rounded and floating instead of in a monolayer). The virus was harvested by shaking and collecting all the media from the bottles into 50ml falcon tubes. This solution was frozen at -80°C at least overnight and then thawed at room temperature in order to lyse any remaining intact cells and maximize the amount of virus available.

4.2.2.3 *Large scale viral concentration and filtration*

The falcon tubes containing virus were thawed slowly at room temperature or in a 37°C water bath for 1.5 to 2 hours approximately. Once completely defrosted, the falcons were centrifuged at 3500rpm at 4°C for 45 minutes in order to eliminate cell debris. All pellets were discarded and the supernatants filtered through a 0.22μm filter on ice. The filtered viral solution was transferred to 250mls autoclaved centrifuge vials on ice. The tubes were weighed in order to distribute the volumes evenly before centrifuging in a Beckman J2-21 at 12000rpm at 4°C for 2 hours.

All supernatant was carefully discarded and the tubes placed upside down, resting on their lids to further drain supernatant. The pellets were resuspended in 350μl of either DMEM or autoclaved PBS. Although these pellets are extremely hard to resuspend, a small volume was chosen in order to obtain a more concentrated final viral solution. Once all pellets had been resuspended, they can be transferred to an eppendorf and sonicated in a sonicating water bath for 10 seconds at a time, placing the sample on ice for 30-40 seconds in between each sonication to avoid overheating the viral solution. The virus was then aliquoted and stored at -80°C before using.

4.2.3 Titration of virus on complementing cells

A confluent 6 well plate of BHK B130/2 complementing HSV-ICP27 cells was obtained as described before. The wells were infected with 1:10 serial dilutions of virus from $1x10^{-2}$ to $1x10^{-11}$. The initial solution was made up as 10μl of virus with 100μl of DMEM mixed thoroughly for a final 10^{-2} dilution factor. 10μl of this mix was added to 100μl of DMEM for 10^{-3}, mixing thoroughly every time and changing tip for every 10μl that were mixed into the following well. Before infection, the medium was removed from the 6 well plates and replace with 500μl of fresh DMEM. The prepared serial dilutions of virus are added to each well, from lowest to highest concentration. Special care was taken not to squirt the liquid onto the fragile monolayers of cells. The plates are carefully mixed and placed in the incubator at 37°C/ 5% CO_2 for 1 hour. After this incubation period, the medium was

discarded and replaced with 2mls of 1:2 CMC:FGM with 1 x HMBA and placed in the incubator for 48 hours. The wells were washed twice in 1ml PBS and fixed for 10 minutes in 4% paraformaldehyde (PFA). After rinsing the PFA off with PBS, the wells were covered with cresyl violet stain for a few minutes. Plaques can be visualized and counted under a light microscope. The infection titre of the virus was defined by multiplicity of infection (MOI), as the number of plaque forming units per cell.

4.2.4 Intracerebral microinjections

Adult male Sprague-Dawley rats (250-300g, n=18) were anaesthetized with 2% isoflurane in 100% oxygen and secured by a bite bar and ear bars in a stereotaxic frame (Korf, Germany). A midline incision was made on the head and the skin and dura were retracted to locate bregma. This reference point was used to calculate the coordinates for the striatum defined as anterior-posterior = +0.10cm; lateral =-0.35cm; ventral = -0.50cm. A burr hole was made on the right side of the skull at these coordinates. The virus was delivered using a 33' gauge stainless steel cannula attached to a 25µl Hamilton syringe under the control of a microsyringe pump (UltraMicroPump II, WPI, UK) at a rate of 0.25µl/min. The syringe was left in place for 10 minutes after the microinjection was completed to minimize dispersion of the virus through the needle tract. A total of 2.5µl of $1x10^6$ pfu/µl of HSV-LacZ viral suspension was injected. The needle was retracted and the wound closed with a mersilk braided non-absorbable suture (Ethicon, Ethylon, UK).

4.2.5 Detection of transgene expression

LacZ expression patterns following HSV delivery were investigated using X-Gal staining to detect β-galactosidase enzymatic activity.

In vitro assays were carried out on 6 well plates in duplicate. BHK B130/2 cells were grown until 80% confluent as described in section 4.2.2.1. The cells were infected with HSV-LacZ recombinant virus as previously detailed. The virus medium was washed twice with PBS and the cells were incubated with 1ml of fixing solution (0.05% glutaraldehyde in PBS) for 10 minutes at room temperature. The plates were rinsed with PBS twice again and overlaid with 3mls of X-gal solution consisting of:

x1 PBS
1mM $MgCl_2$
150mM NaCl
5mM potassium ferricyanide ($K_3Fe(CN)_6$)
5mM potassium ferrocyanide ($K_4Fe(CN)_6$)
0.1% NP40 or Igepal
150 μg/ml 5'bromo-4chloro-3indolyl-B-Dgalactopyranoside (X-gal) in di-methyl-sulfonamide (DMSO)

The plate was incubated at 37°C/ 5% CO_2 in the dark for at least 2 hours or more depending on the intensity of the staining. The wells were then examined under a light microscope and blue viral plaques were identified as sites of β-galactosidase activity and therefore LacZ expression. The buffer was then discarded and the wells rinsed with water and overlaid with 2mls of 70% glycerol for long term storage.

For *in vivo* detection, 3 rats were killed at each timepoint investigated. Animals were deeply anaesthetized with 3-5% halothane in O_2 and transcardially exanguinated with 0.9% saline followed by ice cold 4% paraformaldehyde (PFA). Brains were extracted, kept in PFA overnight at 4°C and embedded in 3% agarose. A vibrotome was used to slice the brains into 250μm thick coronal slices which were collected in PBS. Sections were rinsed in PBS twice and stained free floating with the following X-gal solution:

x1 PBS
1mM $MgCl_2$
0.2% Igepal in PBS

100mM potassium ferricyanide

100mM potassium ferrocyanide

40 mg/ml X-gal in DMSO

The slices were incubated at 37°C for at least 6 hours in the dark or overnight, depending on the desired staining intensity. The plates were rinsed twice in PBS to dilute the solution and stop the enzymatic reaction in order to inspect the slices under the microscope. Pictures were captured and slices discarded.

4.3 Results

4.3.1 LacZ expression *in vitro*

The aim of this experiment was to verify that the disabled HSV virus was able to express the transgene in culture. To this purpose, the BHK B130/2 complementing cell line was infected with a recombinant disabled HSV-1 vector lacking ICP27 and engineered to carry LacZ. The assay was prepared by titration of the virus in serial dilutions of 1:10 on 6 well plates seeded with B130/2 cells. After 48 hours of infection the cells were stained with X-gal solution to detect β-galactosidase enzymatic activity as described in section 4.2.5. Consistent with other *in vitro* work from this laboratory, blue stained plaques were seen under light microscopy and this staining suggested that the virus was efficiently expressing the transgene (data not shown). Thus, this simple assay re-confirmed that the construct was suitable for applications *in vivo*.

4.3.2 LacZ expression *in vivo*

The ability of the virus to express the LacZ gene in adult rat brain was tested by intracerebral microinjection followed by X-gal staining of 250μm fixed brain slices. The purpose of this study was not to characterize the vector's ability to infect

different neuronal populations *in vivo* or its expression levels. This work has already been published and established HSV-1 and this recombinant vector in particular as a suitable for gene delivery to the brain (see sections 3.5 and 3.6 for references). However, determination of the regional distribution of the virus was necessary ground work for the subsequent gene therapy study that will be described in chapter 5. This allowed a direct comparison between the area of viral expression and the area affected by middle cerebral artery occlusion.

LacZ expression was observed in all 18 rats at 6 different timepoints (n=3), ranging from 3 days to 1 month after infection. Figure 4.2 clearly reveals blue staining in the striatum of a rat 3 days after microinjection. An overall view of the stained region in slices from front to back of the brain is presented in figure 4.2a. The same distribution and signal intensity was observed throughout all timepoints tested. In fact, all animals presented strong blue signal in the striatum but none showed staining in the cortex with the exception of some traces of expression along the needle tract (figure 4.2c). Protein expression was strongest at 3 days but was sustained below peak levels for at least 1 month after injection although no later timepoints were tested (figure 4.3). Some blood traces and mild β-galactosidase expression was detected along the needle tract in the cortex at early timepoints, but this disappeared within a maximum of 10 days (figure 4.2b).

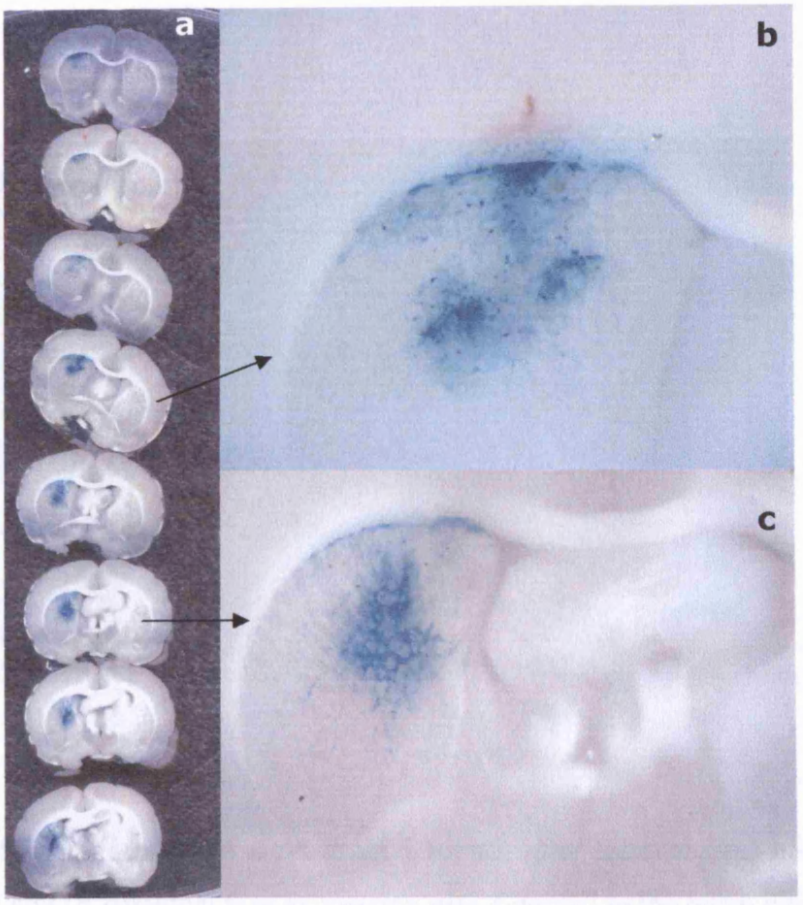

Figure 4.2. LacZ expression in the basal ganglia peaks 3 days after HSV microinjection. a) X-gal assay showing HSV-LacZ spatial distribution and expression levels at 72 hours after intracerebral microinjection in 250µm slices from front to back of the rat basal ganglia. b) Detail of traces of blood seen 3 days after microinjection. c) Detail of LacZ expression in the basal ganglia.

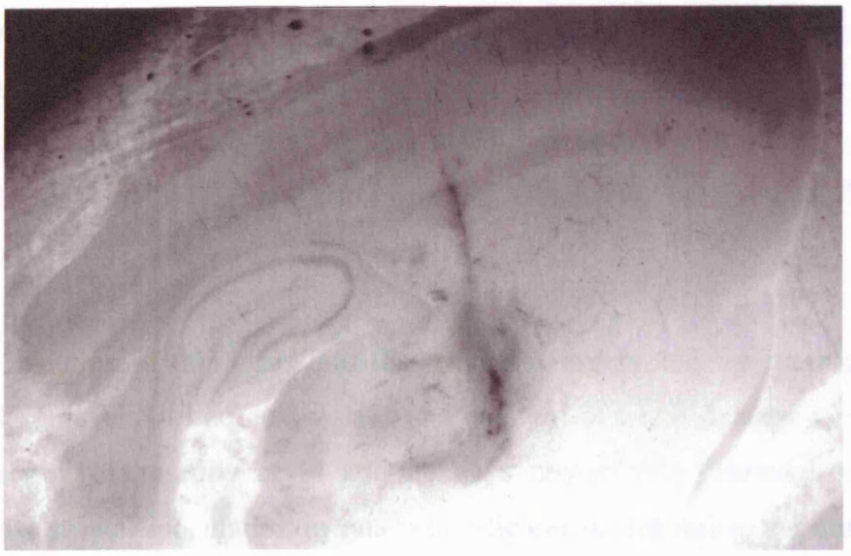

Figure 4.3 Sagittal section of a rat brain 1 month after intracerebral microinjection with HSV-LacZ. β-galactosidase expression was detected in the basal ganglia.

4.4 Conclusions

The β-galactosidase enzyme is the product of the LacZ gene and is often used as a reporter gene to verify gene expression *in vitro* and *in vivo*. This transgene has been recombined into several HSV vectors to assess their efficiency in delivering a foreign gene. The vector used in this study has been tested *in vitro* and *in vivo* following delivery to ND7 and DRG neurones (Wagstaff *et al.*, 1998, 1999; Kalwy *et al.*, 2003).

Injection of this virus into the rat motor cortex and the marmoset striatum shows high levels of LacZ expression and no signs of tissue damage as seen on light and electron microscopy at 14 and 28 days respectively (Howard *et al.*, 1998). Similarly, striatal inoculation in rats was efficient in delivering the transgene for 1 week and the virus exhibited retrograde transport to the substantia niagra, but expression dramatically declined 1 month after injection (Lilley *et al.*, 2001). Following footpad inoculation or direct inoculation into the nerve, animals were sacrificed at different timepoints and DRG neurones fixed and stained. Virally-driven expression of β-galactosidase was detected up to 1 month after injection (Palmer *et al.*, 2000).

Since the infectivity, efficiency of transgene expression and safety of the disabled virus has already been established, this study was concerned with the distribution of the virus after intrastriatal microinjection. The reasons for this will become more apparent in the next two chapters, where this vector is used to deliver therapeutic proteins and the LacZ protein to the brain following middle cerebral artery occlusion. In views of these studies it was important to:

- verify the vector was able to efficiently and safely deliver the gene *in vivo* as suggested by previous experiments;

- asses the regional distribution of the gene following intrastriatal microinjection;

- asses the timecourse of expression.

The experiments described confirm previous findings about the recombinant HSV-1 vector used, and establish that its expression coincides with the areas affected by focal ischaemia. Moreover, although LacZ expression was not quantified, intense blue signal was still detected up to one month after inoculation. Since the same viral backbone and promoter are used, the studies detailed in chapters 5 and 6 assume that the expression *profile* of the virus carrying heat shock protein 27 (HSP27) and HSP70 is the same as that of the HSV-LacZ vector. However, HSP27 and HSP70 protein expression *levels* were later quantified via end point histology in microinjected rats *in vivo* (chapter 5).

PRE-ISCHAEMIC THERAPY

Chapter 5 *Pre-ischaemic viral delivery of heat shock proteins in vivo*

5.1 Aims

The experiments reported in this chapter examine the neuroprotective effect of pre-ischaemic gene therapy with two heat shock proteins (HSPs) in an experimental model of stroke.

Aims were therefore:

- to deliver HSPs into the central nervous system using engineered herpes simplex virus type-1 (HSV-1) as a vector;

- to use MRI to assess the neuroprotective effects of pre-ischaemic viral delivery of HSPs on lesion size in a rat model of reversible focal cerebral ischaemia.

5.2 Introduction

Heat shock proteins are part of a natural mechanism of cell defence to environmental stress in all living organisms. Following the initial thermotolerance study in Drosophila, many *in vitro* and *in vivo* experiments have established that these proteins are upregulated during a variety of stresses in different species (Lindquist & Craig, 1988; Higashi *et al.*, 1994; Wagstaff *et al.*, 1996; Ehrnsperger *et al.*, 1997; Feder & Hofmann, 1999). HSPs can enhance cell survival by binding to denatured proteins to prevent their misfolding or aggregation with other proteins. They are also responsible for refolding aberrant proteins or targeting them for disposal into proteasomes (Kiang & Tsokos, 1998; Sharp *et al.*, 1999; Latchman, 2004). HSP27 and HSP70 have been specifically, although not exclusively, linked to protection in the CNS and extensive *in vitro* and *in vivo* evidence has been detailed in chapter 1.

Endogenous HSP27 and HSP70 have been shown to be upregulated upon transient focal ischaemia in rats (Wagstaff *et al.*, 1996). Moreover, the *in vitro* and *in vivo* evidence suggests that overexpression of these chaperones has a neuroprotective effect (chapter 1). The hypothesis here tested is that viral overexpression of heat shock proteins can enhance protection upon stroke. An intraluminal middle cerebral artery (MCA) occlusion model of transient focal cerebral ischaemia was used because it is currently retained to be the least invasive and most relevant to clinical stroke cases (chapter 2). The lesion induced typically has an unsalvageable core that is surrounded by hypoperfused, compromised but potentially salvageable tissue.

The choice of delivery method was based on a rich literature supporting viruses as efficient vectors (chapter 3). A disabled herpes virus engineered to carry HSP27, HSP70 or LacZ was used. The viruses were delivered three days prior to induction of ischaemia because viral expression of the LacZ transgene was previously established to peak at this timepoint (chapter 4). The method of assessing the consequences of therapy was non-invasive magnetic resonance imaging combined with end point histology. As described in chapter 2, MRI techniques enable the measurement of lesion size and cerebral blood flow and have been

extensively used in experimental stroke models to describe the evolution of the lesion after occlusion and/or reperfusion. Gene therapy studies with HSPs to date have exclusively used histological techniques to evaluate the effects of therapy. The novelty of the study presented here is the use of non-invasive MRI to determine changes in lesion size due to pre-ischaemic delivery of HSP27 and HSP70 to the brain. Moreover, it is the first time that therapeutic intervention with HSP27 has been assessed in a rat model of stroke.

5.2 Materials and Methods

5.2.1 Experimental design

All animal care and procedures were carried out in accordance with the UK Animals (Scientific Procedures) 1986 Act. This experiment involved 3 different studies, A, B and C, all using adult male Sprague-Dawley rats (220-250 g, Charles Rivers):

Study A: 18 rats were divided into 3 sub-groups microinjected with HSV-HSP27 (n=6), HSV-HSP70 (n=6), or HSV-LacZ as a control (n=6). All rats underwent occlusion of the middle cerebral artery (MCA) 3 days after microinjection and MRI scanning 24 hours later was used to assess CBF and lesion size.

Studies B and C: 2 different groups of rats were divided into sub-groups microinjected with HSV-HSP27 (n=4), HSV-HSP70 (n=4), or HSV-LacZ as a control (n=4). All rats underwent middle cerebral artery occlusion (MCAO) 3 days after microinjection. T_2-weighted multislice scans were run 24 hours later not to determine lesion volume but to confirm the presence of a lesion. 48 hours after MRI, brains were extracted for immunohistochemistry (study B, n=12) or Western blotting (study C, n=12) respectively. A schematic representation of the experimental design is included below (figure 5.1).

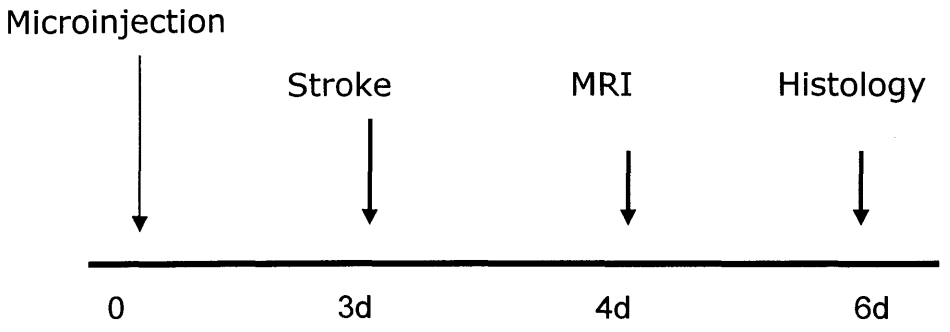

Figure 5.1. Schematic representation of the experimental design. Animals were subjected to viral microinjection three days prior to stroke induction. Rats were scanned 24 hours later and sacrificed 48 hours later for end point histology.

5.2.2 Virus growth

This procedure has been described in detail in chapter 4. Herpes simplex virus strains 4+/27-/pR19-HSP27, 4+/27-/pR19-HSP70, 4+/27-/pR19-LacZ have been previously described (Coffin *et al.*, 1996; Wagstaff *et al.*, 1999; Wolfe *et al.*, 1999; Latchman, 2001; Lilley *et al.*, 2001). Briefly, the HSV-1 backbone 1764/4+/27-/RL1 was attenuated by a disabling mutation in Vmw65 and deletion of ICP34.5. An expression cassette containing cDNA inserts from either Chinese hamster HSP27, inducible human HSP70 or β-galactosidase under the control of a cytomegalovirus immediate early promoter was inserted into the backbone via the p19/20.5/UL43 vector by homologous recombination. Replication of such incompetent viruses was obtained in the complementing B130/2 BHK cell line (stably over-expressing ICP27 gene of HSV-1). Viruses were extensively grown; the cell lysates were initially centrifuged at 3500rpm for 45 minutes and the supernatant further clarified by filtration through a 0.22μm filter. The resultant medium was centrifuged (2 hours at 12500rpm in a Beckman J2-21 centrifuge) and the virus pellet resuspended in sterile phosphate buffered solution (PBS). Concentrated virus was titrated by counting plaque formation on B130/2 BHK cells. Titres of $1\text{-}2x10^{10}$ plaque forming units (pfu) were routinely obtained.

5.2.3 Intracerebral microinjections

Rats were anaesthetized with 2% isoflurane in 100% oxygen. All rats in studies A, B and C were stereotaxically microinjected with 2.5μl of $1x10^{6}$ pfu/μl of HSV-LacZ, HSV-HSP70 and HSV-HSP27 respectively. The virus suspensions were introduced into the right rat striatum (Bregma coordinates: AP= +0.10; L =-0.35; V= -0.50) using a 33' gauge stainless steel cannula attached to a 25μl Hamilton syringe under the control of a microsyringe pump (UltraMicroPump II, WPI, UK) at a rate of 0.25μl/min. Animals were allowed to recover for three days before being subjected to focal reversible MCAO.

5.2.4 Middle cerebral artery occlusion

All rats in studies A, B and C were anaesthetized with 2% isoflurane in a 70:30 N_2O:O_2 delivered by a nose cone. The origin of the right MCA was occluded with an intravascular suture as described elsewhere (Longa *et al.*, 1989). Briefly, the common, internal and external carotid arteries were exposed by a cervical midline incision. A 3/0 monofilament suture (Monocryl, Ethicon, UK) with an araldite (Sil-Mid, UK) coated rounded tip was used. This 290μm suture was introduced into the lumen of the right common carotid artery up to the carotid bifurcation and advanced approximately 17mm into the internal branch of the carotid artery to block the origin of the MCA. The embolus was secured by sutures at two points: first, to the common carotid artery at the base of the neck and then further up on the same artery and before its branching. An arterial clip was also placed further up from the second suture just before the carotid bifurcation into internal and external carotid arteries. The artery was carefully nicked and the intraluminal suture pushed through, until the clip; then the second upper suture was tightened and the clip removed. The animals remained occluded for a total of 30 minutes after which they were carefully reperfused by retracting the embolus and securing both sutures at either side of the nick. The cutaneous wound was then sutured and cleaned. Rectal temperature was maintained at 37±1°C via a heating blanket controlled by a thermocouple. The whole procedure took 1.5 hours and the animals were left to recover for 24 hours before scanning with free access to food and water.

5.2.5 Magnetic Resonance Imaging

Animals in studies A, B and C were anaesthetized with 2% halothane in a 70:30 N_2O:O_2 mix delivered via nose cone and placed on a probe with bite and ear bars securing the head to minimize movement artefacts (figure 5.2). The change in anaesthetics for the scanning sessions was based on the fact that halothane has vasodilating properties that were convenient when acquiring perfusion data. All scans were performed on a 2.35 Tesla horizontal bore magnet (Oxford Instruments, UK) interfaced to a SMIS console (Guilford, UK). Physiological monitoring

included electrocardiography (ECG) recordings and rectal temperature, which was maintained at 37±1°C using an air warming system.

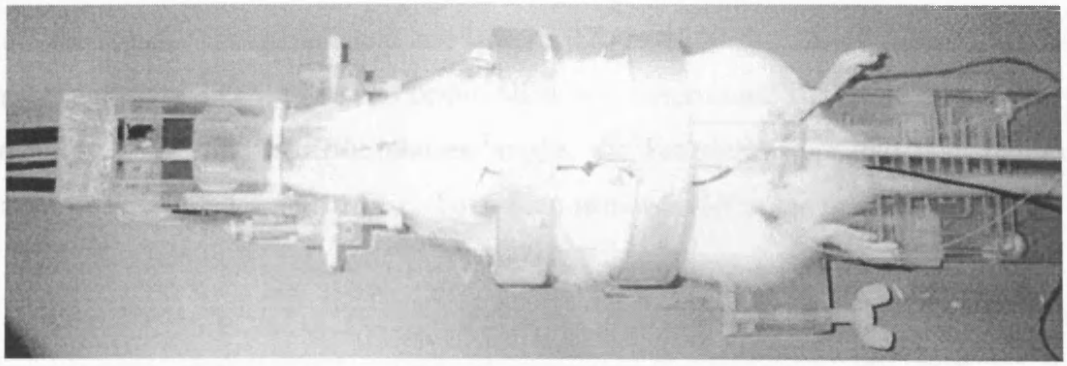

Figure 5.2. Animal in preparation for an MRI experiment. The head is secured by ear and bite bars and anaesthetics are delivered via the nose cone.

Images were acquired using a volume transmitter coil and a separate decoupled surface receiver coil. All sequences were run on a single 2-mm-thick coronal slice located in the MCA territory (0.5mm from bregma). The matrix size was 128x64 and the field of view was 40x20mm. The imaging protocol included two echo planar imaging (EPI) sequences, T_1 measurement and continuous arterial spin labelling (CASL), and a T_2-weighted spin echo (SE) sequence. The T_1 and CASL scans were used to determine CBF whereas the T_2-weighted SE was run to determine the lesion volume. The T_1 sequence parameters were 2000ms repetition time (TR), 18ms echo time (TE), an inversion time (TI) array of 284ms, 434ms, 634ms, 834ms, 1234ms, 1734ms, 2734ms, 3734ms and the number of averages was 16. For CASL, the TR was 1000ms, the TE was 18ms, and the number of averages was 44. The inversion slice was positioned approximately 13mm from the back of the cerebellum and labelling and reference scans were obtained with a 500ms delay time (Alsop & Detre, 1996). The multislice T_2-weighted SE sequence consisted of 9 slices with a 1-mm thickness. The parameters used were TR = 1500ms, TE = 120ms, and the number of averages was 8. The centre slice was determined by visual inspection of anatomical landmarks. In the chosen image, the ventricles appeared y-shaped and bright due to the presence of CSF. Total scan time was 35 minutes.

5.2.6 Image processing and data analysis

All images were reconstructed with IDL Software Version 5.2 (Research Systems Inc., USA) in order to obtain quantitative maps. Labelled and reference CASL images were subtracted and T_1 values used to calculate CBF maps. Lesions and regions of interest were delineated on all processed images and analyzed with SMIS Image Display Version 3.7 and Scion Image software. Lesion size was then expressed as a percentage of total pixel number in the brain slice. It is important to clarify that the term "lesion" will be used throughout the thesis in reference to the lesion seen on T_2-weighted images. Data analysis was performed by an observer blinded to the groups and resulting lesion areas per slice were used to determine lesion volume across the whole brain. An analysis of the group differences in lesion spread from front to back of the brain was performed using a random coefficients

model, as required to deal with the expected spatial correlation in the data. A comparison based on Akaike's Information Criterion indicated that a parallel response model provided an adequate description of the lesion data over slices 3 to 9 inclusive, covering the MCA territory. These calculations were performed using SAS PROC MIXED (SAS Institute, 1999). Student's t-test assuming unequal variances and Mann-Whitney tests were used to compare all other measurements. Data were presented as mean ± standard error and considered significant at $p < 0.05$.

5.2.7 Western blots

5.2.7.1 General reagents and solutions

Phosphate buffered saline (PBS), stock concentration (x10): 104mM sodium, 1.8mM potassium chloride, 5.4mM disodium orthophosphate dihydrate, 1.25mM potassium dihydrogen orthophosphate (pH7) in ddH_2O.

Protein extraction buffer: 50 mM Tris HCl, 150 mM NaCl, 1 mM EDTA (ethylenediaminetetraacetic acid), 0.1% Tween 20 (polyoxyethylene sorbitan monolaurate), 10% glycerol, containing protease inhibitors (complete, mini protease inhibitor cocktail, Roche, Germany).

Resolving Gel (10%): 20ml of mix prepared as: 7.9ml dH_2O; 6.7ml 30% acrylamide mix (30% (w/v) acrylamide, 0.8% (w/v) bisacrylamide); 5ml 1.5M Tris (pH 8.8); 0.2ml 10% sodium dodecyl sulfate (SDS); 0.2ml 10% APS (ammonium persulfate, prepared fresh and added last); 0.008ml TEMED (NNNN-tetraethylethalinediamine).

Stacking gel (5%): 10ml of gel mix as: 6.8ml H_2O; 1.7ml 30% acrylamide mix; 1.25ml 1.0M Tris (pH 6.8); 0.1ml 10% SDS; 0.1ml 10% ammonium persulfate; 0.01ml TEMED.

Electrophoresis running buffer: 25mM Tris HCl; 250mM Glycine (pH 8.3); 0.1% SDS in ddH_2O.

Transfer buffer: 1x running buffer; 20% methanol.

Blocking buffer: 5% Marvel skimmed milk powder dissolved in 0.1% PBST (PBS-Tween 20).

Wash buffer: 1x PBS; 0.01% Tween 20.

Protein loading buffer (6 x): 300 mM TrisHCl (pH 6.8), 600 mM DTT, 10% SDS, 30% glycerol, 0.1% bromophenol blue.

5.2.7.2 Protein extraction and analysis

Fresh brain tissue of all animals in study C was quickly isolated and flash-frozen in liquid nitrogen. Basal ganglia and cortical regions were dissected and placed in sterile culture tubes. Vials were then flash frozen in liquid nitrogen and either used immediately or stored at -80°C. Total tissue weight was calculated by individually weighing the tubes and subtracting their weight from the weight of an empty vial. Protein extraction buffer was added as 3 volumes of buffer to 1 volume of tissue. The tissues were then homogenized with a Polytron PT 1600 E homogenizer (Kinematica AG, UK) on ice as 3 pulses at 30000rpm for 10 seconds cooling on ice in between. Samples were allowed to rest for at least 30 minutes on ice before being aliquoted into eppendorf tubes. The vials were then centrifuged at 1300g for 30 minutes at 4°C and the resulting supernatant was collected and frozen at -80°C.

5.2.7.3 Protein quantification

The Bradford Assay (Perbio Science, UK) was used to quantify total protein levels from homogenised samples. Briefly, bovine serum albumin (BSA) standards

were diluted to 1mg/ml in water. Solutions A and B were mixed as 50 to 1, loading 200µl per well (e.g. 10 samples, 2mls A + B = 1960µl A + 40µl B). Standards were then loaded onto the first row of a 96 well plate on an increasing protein concentration gradient as follows:

1st well: 195µl of A+B solution + 5µl of water

2nd well: 195µl of A+B + 5µl BSA standard

3rd well: 190µl of A+B + 10µl BSA standard

4th well: 185µl of A+B + 15µl BSA standard

.....etc

One of the wells was loaded with a tween extraction buffer (5µl tween buffer + 195µl A+B solution) as a control. All tissue samples were loaded as 5µl of sample + 195µl A+B solution. The plate was then incubated at 37°C for 30 minutes in an incubator in the dark, and then placed into a spectrophotometer in order to measure optical densities (ODs) with a 560nm filter (GS-800 calibrated densitometer, BIO-RAD, UK). The ODs obtained for the standards were used to plot a standard protein concentration curve, which in turn allowed the determination of the appropriate µg/µl protein values of the samples. Moreover, the standard curve was constructed by subtracting the first OD value (water+A+B) to all other ODs. As the values were given for µg protein/ 5µl sample volume, all final values were divided by 5 to obtain their concentration as µg/µl. All sample ODs were inserted into the formula for standard curve regression [eg y = (25.723xOD-1.0226)/5µl of sample]. Once all protein concentration values were obtained for all samples, the volume of sample required for 30µg of protein per well was calculated for Western blotting (see section 5.2.7.5).

5.2.7.4 Polyacrylamide gel electrophoresis

The mini-gel casting apparatus consisted of 0.1mm space glass plates and a 10 well comb. The resolving gel was prepared as detailed in Section 5.2.7.1 and poured in between the plates. Approximately 1cm space was calculated when

pouring the resolving gel to allow for the stacking gel and the comb. This space was covered with isopropanol in order to avoid air bubbles and seal the gel off from air to accelerate polymerization. The gel was then allowed to set for 30 minutes at room temperature (RT), isopropanol was poured out and rinsed with ddH_2O. Meanwhile, the stacking gel was prepared as stated in section 5.2.7.1. and generously poured over the resolving gel. The comb was immediately inserted and the gel was allowed to set at RT.

5.2.7.5 Protein loading

Values obtained with the Bradford assay were used to determine the amount of sample required for a final protein concentration of 30µg/µl. Protein samples were prepared as equal amounts of loading SDS buffer and cell lysate aliquots and a maximum total volume of 15µl per well was loaded. After mixing, all samples were placed in a hot plate for 1 minute, then on ice immediately and spun down at 14000rpm for 5 minutes. A rainbow ladder (Amersham Biotechnologies, UK) was used as a molecular weight marker and was prepared as 6µl of marker mixed with 6µl of SDS loading buffer. The comb was removed and the wells were flushed with running buffer. All samples were loaded in duplicate and run at 120 V for 1.5-2 hours.

5.2.7.6 Protein transfer to nitrocellulose membranes

Blotting paper, sponges, and hybond C membranes (Hybond C, Amersham Biotechnologies, UK) cut to fit the gel were pre-moistened in a tray with transfer buffer (see section 5.2.7.1). Once the run was finished, the plates were separated and the sacking gel removed. The gel was gently peeled off the plate and the transfer "sandwich" assembled as: sponge 1, blotting paper 1, hybond membrane, gel, blotting paper 2 and sponge 2. The "sandwich" was closed and tightened, making sure there were no air bubbles by rolling a falcon over it. After placing it in its holder, the tank was filled up completely with transfer buffer and run at room

temperature at 100 V for 1 hour. An ice block was placed in one of the compartments of the tank to cool down the buffer during the run.

5.2.7.7 Immunodetection of proteins on western blot

Once the transfer was over, the membranes were incubated in blocking buffer for 30-60 minutes. After rinsing 3 times in PBS, membranes were incubated with rabbit polyclonal anti-HSP27 (1:1000, product # SPA-801, Stressgen Biotechnologies, UK) and monoclonal anti-human HSP70 (1:1000, product # SPA-810, Stressgen Biotechnologies, UK) overnight at 4°C or at RT for 1.5 hours. Negative controls were incubated with blocking solution only. Membranes were washed 3 times for 5 minutes in 0.1% PBST before being incubated with the appropriate secondary antibody at RT for 1 hour. A secondary anti-rabbit HRP (1:2000, DAKO, Denmark) and anti-mouse HRP (1:2000, DAKO, Denmark) antibodies were used against HSP70 and HSP27 respectively. Once again, membranes were washed 3 times in 0.1% PBST for 5 minutes before developing with the enhanced chemoluminescence kit (ECL, Amersham Biotechnologies, UK). The solution was left on the membranes for 1 minute only and immediately exposed to X-ray film (Hyperfilm^{TM}-MP from Amersham International, UK) in the dark until the desired exposure was obtained, typically ranging from 10 seconds to a maximum of 1 minute. Band densities were measured in a GS-800 calibrated densitometer using QuantityOne Version 4.2.1 software (BIO-RAD, UK).

5.2.7.8 Re-probing membranes

All blots were re-probed with GAPDH antibody at room temperature for 1 hour (1:3000, Chemicon International, UK) followed by anti-mouse secondary to confirm equal protein loading. Membranes were rinsed 3 times for 5 minutes in PBST in order to remove any traces of the developing solution. After incubating in blocking solution for 30-60 minutes at room temperature, the primary GAPDH antibody (1:3000) and secondary anti-mouse HRP (1:2000) antibody were added at

RT for 1 hour as described the previous in section. If the original antibody could interfere with the new antibody, the membrane was stripped by washing 3 times for 5 minutes in 0.2M NaOH and a further 3 times in PBS before blocking and re-probing.

5.2.8 Immunohistochemistry

5.2.8.1 Tissue embedding for cryosections

Animals in study B were deeply anaesthetized with 5% halothane in 100% N_2O for decapitation, their brains extracted and lightly covered with Cryo-embed medium (Bright Instruments Co., UK). The tissue was snap frozen in isopentane (2-methyl-butane, BDH, UK) cooled in liquid nitrogen. Then, the brains were blot dried and quickly retuned to in liquid nitrogen before transfer to -80°C for storage. Alternatively, they were placed directly into the cryostat for 1 hour in order to equilibrate their temperature to -20°C before slicing. 10µm-thick sections were cut in a cryostat (Bright Instruments Ltd., UK), placed on polysine coated slides (BDH, UK) and allowed to air dry thoroughly before storing at -20°C.

5.2.8.2 Immunohistochemistry on cryosections

Brain sections taken from HSP treated animals were stained with HSP27 and HSP70 antibodies to verify expression levels of microinjected proteins in the brain. The slides were thoroughly thawed, fixed in 4% PFA for 10 minutes and rinsed 3 times for 5 minutes in PBS. Incubation in 0.3% H_2O_2-methanol for 10 minutes was used to quench endogenous peroxidase activity. Samples were rinsed 3 times for 5 minutes in PBS and incubated for 10 minutes in 0.1% Triton-X-PBS for membrane permeabilization followed by two 5 minute washes in water. Samples were then blocked in 3% goat serum-PBS for 30 minutes at room temperature. Rabbit anti-HSP27 (1:200, Stressgen Biotechnologies, UK) and mouse anti-HSP70 (1:500, Stressgen Biotechnologies, UK) primary antibodies were applied on the sections overnight at 4°C. Slides were then rinsed in TBS and incubated with secondary

antibody (StreptABC Complex/HRP Duet Mouse/Rabbit, DAKO, Denmark) according to manufacturer's instructions. Signal was amplified with DAB (3,3-Diaminobenzidine tetrahydrochloride, Sigma, UK) in the dark and rinsed in water several times. Haematoxylin and acid alcohol were used to counterstain the brain sections. Slices were dehydrated through gradient alcohols (50, 70, 100%), washed twice for 5 minutes in xylene and coverslips were mounted with DPX mounting media (BDH). All slides were viewed under an Axioskop 2 Plus microscope (Carl Zeiss Ltd., UK) and pictures captured with an AxioCam HRc camera and viewed with Axiovision 3.0.6 SP2 software.

5.2.9 X-gal staining

Three out of six brains extracted from animals in study A injected with the control HSV-LacZ vector were processed for X-gal staining to detect enzymatic activity as described in section 4.2.5. Briefly, 24 hours after MCAO, rats were deeply anaesthetized with 3-5% halothane in O_2 and transcardially exanguinated with 0.9% saline followed by 4% paraformaldehyde at 4°C. Brains were embedded in 3% agarose and sliced into 250μm thick slices. Sections were stained with X-gal solution (5mM potassium ferricyanide, 5mM potassium ferrocyanide, 1mM $MgCl_2$, 0.2% Igepal in PBS and 4 mg/ml X-gal, 5'bromo-4chloro-3indolyl-B-Dgalactopyranoside, in DMSO, di-methyl-sulfonamide) at 37°C for approximately 6 hours in the dark.

5.3 Results

5.3.1 MRI measurement of lesion size

Figure 5.3 shows multislice T_2-weighted-spin echo MR images obtained 24 hours after MCA occlusion. The three groups of six animals had been microinjected with HSV-HSP27, HSV-HSP70 or HSV-LacZ as a control, three days prior to occlusion (study A). The reason for this delay is that viral expression was shown to peak at three days post inoculation in rats that had not undergone MCAO (Chapter 4, section 4.3). Averaged total lesion volumes measured from the images were: 223.5 ± 5.2mm^3 for HSV-LacZ controls, 218.3 ± 4.6mm^3 for HSV-HSP70 injected rats and 100.1 ± 3.7mm^3 for HSV-HSP27 injected rats. A marked lesion volume reduction of 44.9 % [CI (26.4 %, 76.0 %)] was seen in HSP27 injected animals compared to LacZ injected rats ($p = 0.019$). HSP70 treated animals showed no significant difference in lesion size from controls ($p = 0.88$).

Figure 5.4 shows lesion volume per slice from front to back of the brain in HSV-HSP27, HSV-HSP70 and HSV-LacZ injected rats. Results yielded by the parallel response statistical model indicated that there was a constant volume difference between the HSP27 treated group and the other two groups in slices 3 to 9 of the multislice dataset [$p<0.003$, difference = 14.35mm^3, CI (5.08, 23.62)]. No lesion volume differences were found between HSP70 treated and control animals.

5.3.2 MRI measurement of CBF

Cerebral blood flow (CBF) was measured 24 hours after occlusion-reperfusion. Values in the ischaemic hemisphere were expressed as a percentage of flow in the contralateral hemisphere: 82.3% ± 5.3 for HSV-HSP27, 77.1% ± 1.4 for HSV-HSP70 and 78.2% ± 5.0 for control animals. Complete recovery of CBF was not achieved but all values were above the ischaemic threshold (Kohno *et al.*, 1995;

figure 5.5). Statistical analysis showed there were no significant differences between animals in each group (Controls vs. HSV-HSP27 $p>0.2$; Controls vs. HSV-HSP70 $p>0.7$) at 24 hours after reperfusion.

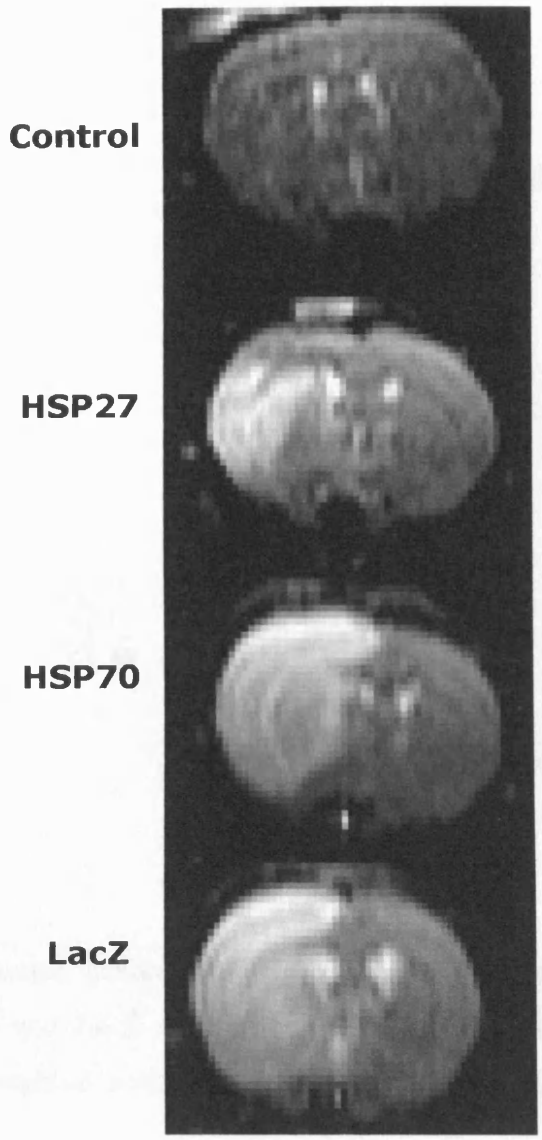

Figure 5.3. Representative centre slice T_2-weighted images of treated and control animals obtained 24 hrs after occlusion of the MCA. Intracerebral microinjections into the rat striatum with HSV-HSP27, HSV-HSP70 and HSV-LacZ were performed three days before ischaemia. Lesion area appears as bright signal on these T_2-weighted images. The first image was obtained from an un-operated, intact animal for anatomical comparison.

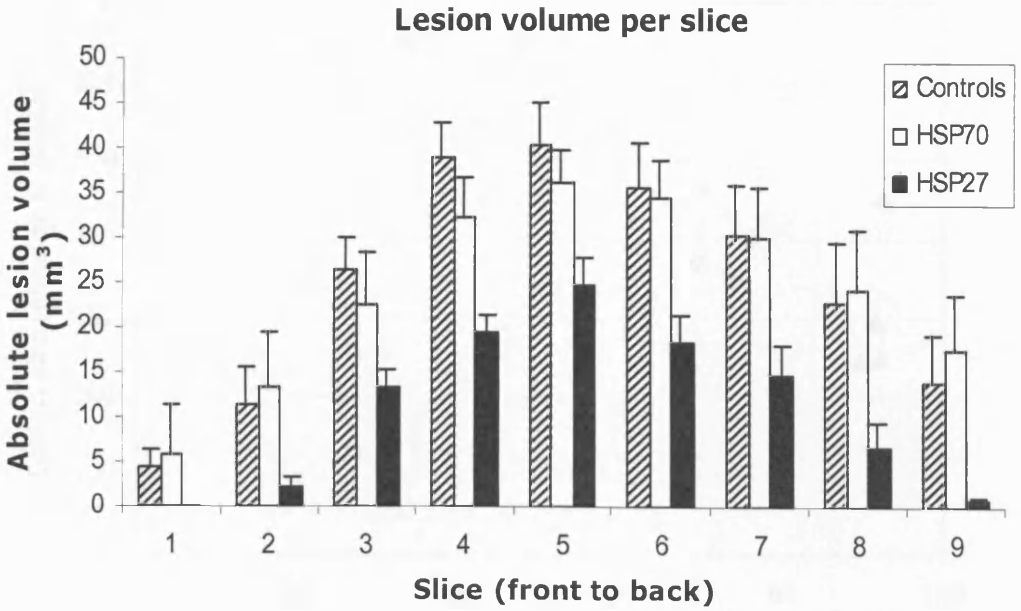

Figure 5.4. Absolute lesion volume per slice from front to back of the brain in HSP27, HSP70 and LacZ control groups. Total lesion size was calculated from multislice T_2-weighted scans at 24 hrs after ischaemia and expressed as volume (mm^3) ± s.e.m.

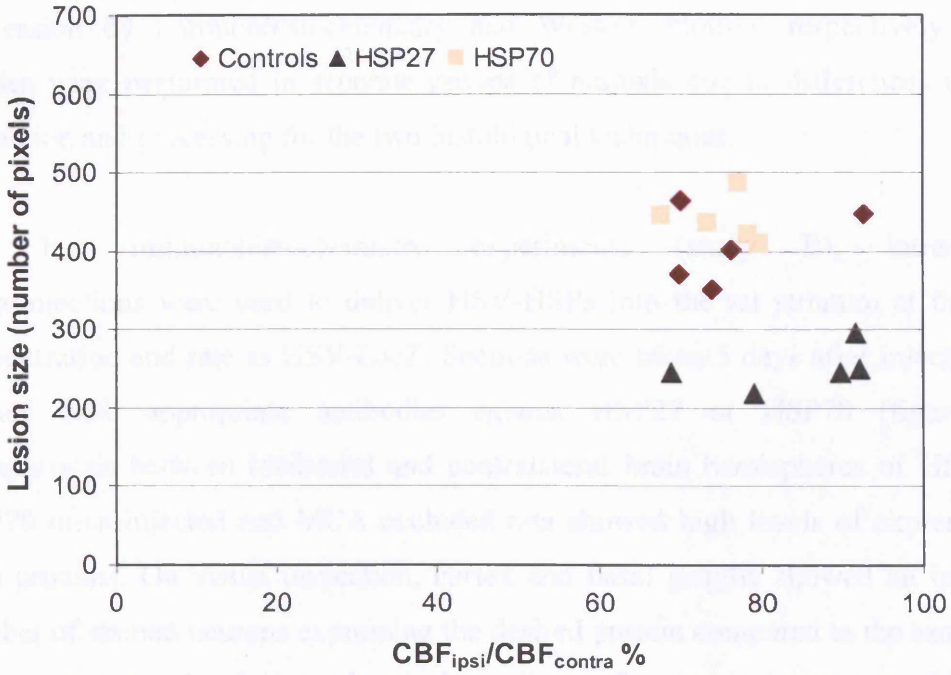

Figure 5.5. Cerebral blood flow (CBF) values and lesion size in HSP treated and control rats. CASL maps obtained 24 hours after MCAO were used to determine levels of reperfusion in the ischaemic hemisphere.

5.3.3 Histological detection of HSP27, HSP70 and LacZ expression

Studies B and C assessed the spatial distribution and levels of HSP expression by immunohistochemistry and Western blotting respectively. These studies were performed in separate groups of animals due to differences in brain extraction and processing for the two histological techniques.

For immunohistochemistry experiments (study B), intracerebral microinjections were used to deliver HSV-HSPs into the rat striatum at the same concentration and rate as HSV-LacZ. Sections were taken 5 days after injection and stained with appropriate antibodies against HSP27 or HSP70 (figure 5.6). Comparisons between ipsilateral and contralateral brain hemispheres of HSP27 or HSP70 microinjected and MCA occluded rats showed high levels of expression of both proteins. On visual inspection, cortex and basal ganglia showed an increased number of stained neurons expressing the desired protein compared to the same areas in the contralateral uninjected hemisphere. Figure 5.6 shows expression of HSPs in representative brain sections of the ipsilateral cortex and basal ganglia of HSP27, HSP70 and LacZ injected animals. However, these differences were very difficult to quantify. Therefore, the experiments were repeated (study C) and a different biochemical technique was used.

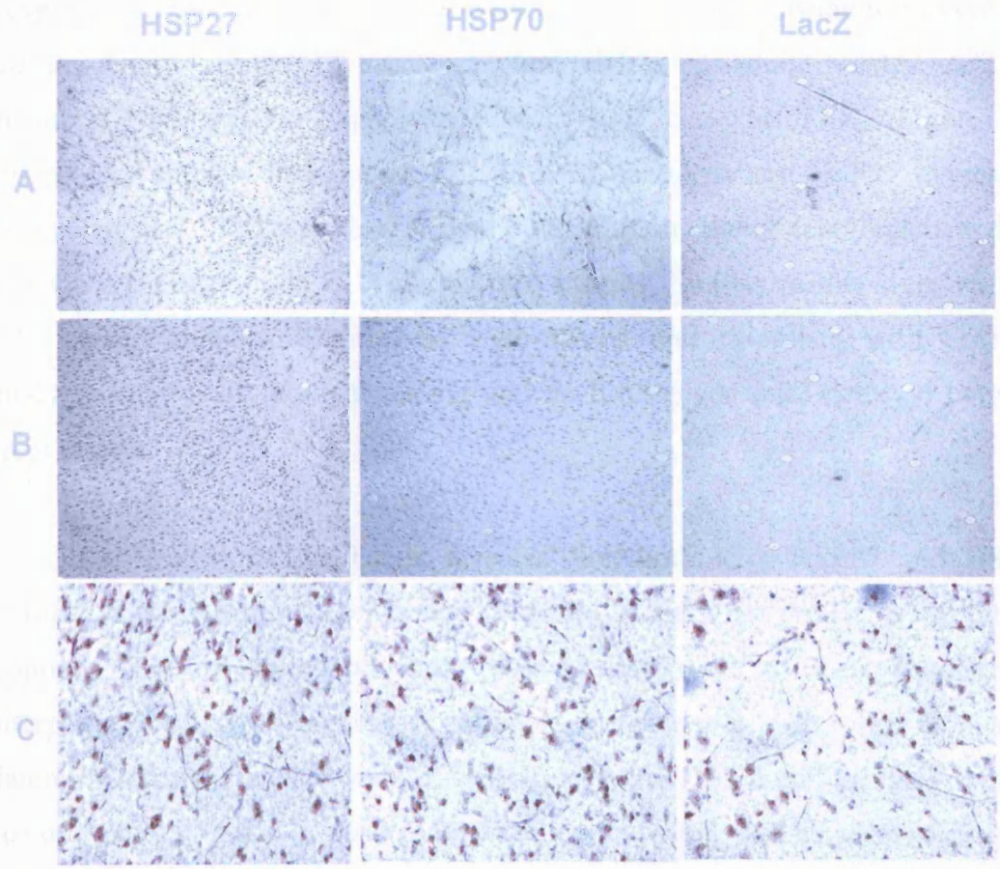

Figure 5.6. HSP27 and HSP70 protein expression in the rat brain. Immunohistochemistry on 10-μm cryo-sections taken 3 days after ischaemia induction shows both HSPs are overexpressed in the ipsilateral basal ganglia and cortex of microinjected and MCA-occluded rats. HSV-HSP27 and HSV-HSP70 injected rat brain sections were stained for HSP27 or HSP70 respectively. HSV-LacZ injected controls shown were stained with HSP27 antibody for comparison. (A) Coronal sections of the basal ganglia (magnification 4X); (B) Coronal sections of the cortex (4X); (C) High magnification pictures (40X) showing expression of HSP27 or HSP70 in HSP injected or LacZ injected rat brains.

Western blots were carried out for all animals in study C (n=12) in order to verify that total HSP levels were elevated due to both ischaemic insult and viral overexpression. Four different regions were dissected from each microinjected and ischaemic brain: ipsilateral basal ganglia (BGI), ipsilateral cortex (CTXI), contralateral basal ganglia (BGC) and contralateral cortex (CTXC). Figure 5.7a shows protein extracts from an HSP27 injected animal where HSP27 expression levels in BGI and CTXI were higher than both its contralateral counterparts and the equivalent brain regions in a LacZ injected control. Similar results were seen in HSP70 treated animals. Membranes were rinsed and re-probed with GAPDH antibody to control for protein loading and no differences were detected between samples (figure5.7b).

Quantification of the bands revealed that both HSV-HSP27 and HSP70 microinjected rats had an approximate four-fold increase in protein levels of the appropriate HSP in ipsilateral brain regions compared to their contralateral counterparts. Similarly, a significant four-fold increase was seen when comparing ipsilateral basal ganglia and cortex of HSP treated and HSV-LacZ injected animals. Ratios of protein increase in basal ganglia and cortex within and between animals are summarized in Table 5.1. These results indicated that the injected vectors were successfully expressing HSPs and raising the total levels of expression of the appropriate HSP after ischaemic insult. Moreover, this is consistent with immunohistochemistry findings, indicating that total HSP levels were higher in HSP injected hemispheres than in LacZ injected controls.

Finally, an X-gal assay was used to visualize LacZ expression in 3 of the 6 rats used as controls and the results confirmed that, as for previously described experiments, protein expression overlapped with the ischaemic lesion area in the basal ganglia but not in the cortex (see chapter 4).

HSP27 expression levels

	HSP27 treated	LacZ treated	p
BG	5.08	1.24	0.029
CTX	4.31	1.37	0.029

HSP70 expression levels

	HSP70 treated	LacZ treated	p
BG	5.27	1.12	0.029
CTX	9.19	1.92	0.057

Table 5.1. HSP protein levels in basal ganglia (BG) and cortex (CTX), expressed as ratios ipsilateral/contralateral. Values represent the average of Westerns run in duplicate for each sample (ipsilateral and contralateral basal ganglia and cortex) for each of the 12 animals in this study. The p values refer to the comparison between HSP treated and LacZ treated animals (Mann-Whitney test).

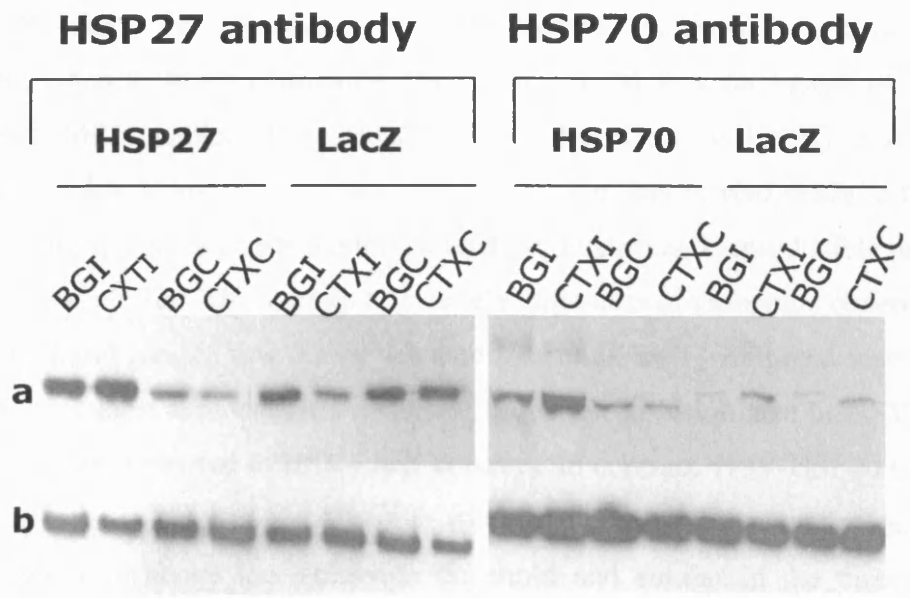

Figure 5.7. Western blots showing HSP27, HSP70 protein expression levels in three repersentative microinjected and MCA occluded rats. Four brain regions were dissected from each rat brain: ipsilateral basal ganglia (BGI), ipsilateral cortex (CTXI), contralateral basal ganglia (BGC) and contralateral cortex (CTXC).

(a) Protein levels in the ipsilateral basal ganglia and cortex in HSP injected rats and in LacZ injected controls.

(b) GAPDH loading controls for all samples.

5.4 Discussion

The aim of the study was to investigate neuroprotection *in vivo* after delivery of an HSV-based vector expressing HSP27 or HSP70 in a rat model of cerebral ischaemia. MRI enabled the measurement of the effect of HSP27 and HSP70 treatment on lesion size at 24 hours after stroke. For this *in vivo* study, a transient occlusion of the middle cerebral artery, a well established and reproducible rat model of stroke, was chosen. This creates a relatively large area of vasogenic oedema in the cortex and basal ganglia that can be detected by multislice T_2-weighted scans (figure 5.3). These images demonstrated a marked reduction in lesion size in HSV-HSP27 treated animals compared to HSV-LacZ controls. In contrast, HSV-HSP70 treatment had no effect on lesion size. All CBF values obtained 24 hours after occlusion-reperfusion were above the ischaemic threshold and similar in the three groups. Immunohistochemistry and Western blotting were used to examine the expression profile of the HSP27 and HSP70 vectors in brain tissue. It was not possible to establish whether the virus was infecting neurons, glial cells or both due to the absence of a specific neuronal marker in the sections. Thus, histology revealed widespread staining for both proteins in ipsi- and contralateral brain hemispheres of injected and MCA occluded rats. Western blots, however, demonstrated a significant increase in HSP27 and HSP70 expression in the ipsilateral cortex and basal ganglia of treated animals compared to LacZ injected and MCA occluded controls.

5.4.1 *HSP expression*

Interestingly, T_2-weighted images showed that reduction in lesion size was not only localized to the basal ganglia where the virus was injected but extended to the cortex. Based on HSV-LacZ profiles of spatial distribution and expression timecourse described in chapter 4, HSPs were expected to be present only within the basal ganglia. The reason for this increase in the cortex is unclear and needs to be further investigated. Several studies have shown that HSPs can either be locally produced in axonal compartments away from the neuronal cell body (Willis *et al.*,

2005) or transferred from glia to neuronal axons (Tytell *et al.*, 1986; Sheller & Bittner, 1992; Guzhova *et al.*, 2001). Moreover, *in vitro* studies in neurons suggest that uptake of exogenous HSPs added to the culture medium can protect these cells from stress (Tidwell *et al.*, 2004; Guzhova *et al.*, 2001). In the context of this study, increased HSP expression in the cortex could therefore reflect the secretion of proteins from virally transfected cells and their recruitment to the injured cortex.

5.4.2 *HSP27 effect on lesion size*

HSP27 treatment caused a significant 44% reduction in lesion size. This protein is naturally expressed in glial cells and not in neurons, and some have suggested it could not therefore directly contribute to neuroprotection (Kato *et al.*, 1994). However, glial cells appear to be crucial for structural and metabolic support of neurons, maintaining synapse homeostasis and regulating the rate of neuronal repair (Wagstaff *et al.*, 1996; Jessen, 2004). Thus, their ability to secrete HSPs upon stress might be a crucial mechanism to protect neurons, although this has not yet been investigated for HSP27. Regardless of the function of the endogenous protein, it was observed that viral microinjections successfully induce expression of exogenous HSP27 across the brain, thus raising total HSP levels and possibly enhancing the neuroprotective effect.

A "preconditioning" or "tolerance" effect in the brain has been reported in *in vitro* and *in vivo* studies showing that exposure to an initial mild stress can render cells more resistant by enhancing protection against a second more severe insult (Chen & Simon, 1997; Kirino, 2002; Dirnagl *et al.*, 2003). In experimental models, brief periods of global ischaemia have been shown to reduce lesion size after induction of permanent MCA occlusion (Simon *et al.*, 1993). Interestingly, the protection conferred was not limited to neurones but extended to glial and endothelial cells (Chen *et al.*, 1996). Experiments in global ischaemia in gerbils have suggested that tolerance develops 24 to 48 hours after the mild insult and lasts for approximately one week (Kitagawa *et al.*, 1990; Kirino *et al.*, 1991; Schaller *et al.*, 2003).

Heat shock proteins were originally described in thermotolerance *in vitro* experiments and their overexpression prior to insult was shown to confer protection. The protective role of these chaperones in the brain is supported by evidence of their expression pattern (Nishi *et al.*, 1993; Chen *et al.*, 1996). HSP70 mRNA increases 2 hours after ischaemia in affected regions and its temporal profile of expression mirrors the degree of vulnerability of the different cell populations, being present first in CA1 and then CA3 hippocampal neurones, then cortical and thalamic regions and finally in dentate granule cells (Simon *et al.*, 1991; Welsh *et al.*, 1992; Nishino & Nowak, 2004). Upregulation of heat shock proteins is therefore likely to be one of the mechanisms involved in ischaemic tolerance. The protection observed in this study may therefore be due to a pre-ischaemic induced tolerance following microinjection combined with the effect of the endogenous HSPs.

This could be relevant in a clinical context, since analogous situations have been described for stroke patients presenting multiple transient ischaemic attacks (TIAs). TIAs have long been identified as risk factors for subsequent ischaemic stroke but more recently they have been thought to improve outcome after stroke by triggering neuroprotective mechanisms (Schaller, 2005). In fact these have been described as a "naturally occurring analog to experimental ischaemic tolerance strategies" (Dirnagl *et al.*, 2003). Several studies now support the hypothesis that TIAs before stroke can decrease tissue vulnerability and therefore reduce infarct size in the human brain (Weih *et al.*, 1999; Moncayo *et al.*, 2000; Wegener *et al.*, 2004; Schaller, 2005).

HSP27 has been shown to protect cells *in vitro* by interfering with the stress-triggered apoptotic caspase-dependent and caspase-independent cascades (Melhen *et al.*, 1996; Paul *et al.*, 2002; Benn *et al.*, 2002; Akbar *et al.*, 2003; Latchman, 2004; Zourlidou *et al.*, 2004). Several experiments have shown that this protein is able to sequester cytochome *c* after release from the mitochondria, prevent formation of the apoptosome, block caspase-3 activation and decrease the amount of AIF (apoptosis inducing factor) released by mitochondria after ischaemia (Garrido *et al.*, 1997 & 1999; Pandey *et al.*, 2000; Bruey *et al.*, 2000; Rashmi *et al.*, 2003; Whitlock *et al.*, 2005). Chapter 1 has already described these functions in detail together with the

cytoskeletal involvement of this chaperone in attempting to explain how HSP27 can accelerate cell recovery (Carper *et al.*, 1997; Costigan *et al.*, 1998; Paul *et al.*, 2002; Williams *et al.*, 2005). Perhaps one of the unique features of this chaperone is its ability to bind denatured proteins in an ATP independent fashion, which is advantageous in an energetically compromised ischaemic brain (Rogalla *et al.*, 1999; Garrido, 2002).

5.4.3 *HSP70 effect on lesion size*

MRI scans suggest that pre-ischaemic injections with HSP70 had no effect on lesion size in this model. Most of the literature concentrates on HSP70 as the major constitutive and inducible HSP in the brain (Yenari, 1999; Kelly & Yenari, 2002). It is widely accepted that HSP70 protects cells from apoptosis but it is important to note that many *in vitro* experiments use toxic substances to induce apoptosis without causing protein denaturation, misfolding and/or aggregation. This might therefore mask the chaperone functions of HSP70 and emphasize how it can interfere with the apoptotic cascade. In fact, at least one study has shown that neuronal cells virally transfected with HSP70 were protected against ischaemic and thermal stress but not against apoptosis (Wagstaff *et al.*, 1999). HSP70's ability to accelerate cell survival by repairing the protein machinery is more related to necrotic forms of death. Several studies have shown that binding of this chaperone to denatured proteins prevents their aberrant aggregation and restores their functional conformation, thus increasing stabilization and reactivation of protein machinery after stress (Kabakov *et al.*, 2002; Beaucamp *et al.*, 1998).

The evidence of HSP70's involvement in apoptosis indicates that it might regulate both upstream and downstream events, such as inhibiting the formation of the apoptosome, binding to cytochrome *c* or blocking the effector caspases like capsase 9 or 3 (Saleh *et al.*, 2000; Mosser *et al.*, 2000; Creagh *et al.*, 2000; Beere *et al.*, 2000; Tsuchiya *et al.*, 2003; Steel *et al.*, 2004). However, a different line of research suggests that overexpression of HSP70 can have damaging effects on cells. It is suggested that in the presence of TNF, the chaperone binds to survival elements

and prevents them from blocking apoptosis (Ran *et al.*, 2004). This may explain why HSP70 treatment fails to reduce lesion size since viral injections might induce activation of cytokines such as TNF. It is important to note that HSP27 can protect cells from TNF-induced apoptosis, which might account for the differences in protection observed in this study (Mehlen *et al.*, 1997).

In vitro and *in vivo* evidence of protection with HSP70 remains extremely dependent on the type and severity of insult and the susceptibility to different environmental insults of the cell population affected (Amin *et al.*, 1996; Jaattela *et al.*, 1998; Lee *et al.*, 2001*a*; Ran *et al.*, 2004; Latchman, 2004). Although morphological improvement of the cells is observed after viral delivery of HSP70, there is no indication of reduction in lesion size (Yenari *et al.*, 1998; Kelly *et al.*, 2002). It could be argued that, when using viral microinjections as a delivery method, the virus itself might render infected cells more or less responsive to HSP treatment. Previous studies however, suggest that microinjection of the vector used in this study does not cause any obvious damage to hippocampal cells *in vivo* and other neuronal cell types *in vitro* (Wagstaff *et al.*, 1999; Kalwy *et al.*, 2003; Zourlidou *et al.*, 2004). Literature on transgenic animals overexpressing HSP70 should help circumvent the problem of unwanted effects of virally delivered proteins. Some studies show reduction in lesion size both in stroke and epilepsy mouse models (Rajdev *et al.*, 2000; Tsuchiya *et al.*, 2003; van der Weerd *et al.*, 2005), while others show improved neuronal survival with no effect on the lesion size (Plumier *et al.*, 1997; Lee *et al.*, 2001a; Kelly *et al.*, 2001). The variability of protection against ischaemia reported in these HSP70 transgenic mice studies has been partially attributed to differential levels of expression. In the present experiments, the levels of endogenous and virally delivered HSP70 expression could have simply not reached a required threshold for lesion size to be reduced. However, histological analysis of the HSP70-injected and MCA-occluded animals showed widespread staining across the brain suggesting high levels of expression following ischaemia. Moreover, *in vitro* experiments have shown that the viral vector used yields the same levels of expression of both HSP27 and HSP70 (Wagstaff *et al.*, 1998), although only the former protein has a potent protective effect in this experimental model. It is also possible that although HSP70 can be protective, the lack of ATP in the ischaemic

lesion limits the chaperone's ability to bind and release denatured proteins and therefore the amount of repair this chaperone can exert.

5.4.4 *Summary*

This study is the first to show that viral delivery of HSP27 has a significant effect in reducing lesion volume after focal cerebral ischaemia in rats. The fact that HSP70 treatment was unable to decrease lesion size might reflect different protective activities of the two chaperones. In this particular model, HSP27 might be more efficient due to its links with cytoskeletal stability and its ability to bind proteins in an ATP-independent fashion in conjunction with its anti-apoptotic functions. The high expression levels of both HSPs detected in the cortex suggested these proteins could either be transported to or secreted in lesion areas. There could also be signaling events leading to cooperation between endogenous and exogenous HSPs that enhanced the brain's natural response to stress.

In conclusion, these findings provide evidence supporting the role of HSP27 as a major protective protein in the brain and highlight the need for further investigation of the mechanisms underlying its neuroprotective effect. The difficulty in elucidating a precise cascade of events might simply be due to the variability of experimental systems, cell lines and species employed, or the complexity and specificity of the cell repair machinery in response to stress.

POST-ISCHAEMIC THERAPY

Chapter 6 *Post-ischaemic viral delivery of heat shock proteins in vivo*

6.1 Introduction

In view of the pre-ischaemic evidence of protection described in Chapter 5, the effect of post-ischaemic viral delivery of HSPs on lesion size was investigated in the same rat MCAO model of stroke. MRI techniques were once again used to measure lesion size and CBF at 6 different timepoints after induction of ischaemia. Moreover, behavioural tests were used to assess whether gene therapy could improve the functional deficits caused by the stroke in treated animals compared to controls.

6.1.1 Post-ischaemic gene therapy: general considerations

Animal models have made important contributions to elucidate the pathophysiology of stroke and this has in turn helped to develop treatment strategies. The middle cerebral artery occlusion model of stroke in rats has been extensively used because it reproduces the most common type of stroke occurring in humans (Hunter *et al.*, 1995). The focal lesion produced has a core with severe decrease in blood flow and a peri-infarct or penumbral region with moderate reductions in CBF (see chapter 2). The duration of the ischaemic period is an essential factor in determining final lesion size. Aronowski and colleagues generated a computerized graded bioassay in order to correlate these two variables. No infarct was observed after 5 minutes of transient MCA occlusion, whereas small lesions were apparent after 10 minutes of ischaemia. Occlusion times of 20 to 50 minutes triggered a dramatic increase in brain damage and this was maximal at 1 hour and remained constant up to 2.5 hours of ischaemia (Aronowski *et al.*, 1994). Similarly, these experiments showed that treatment was most effective if administrated at 50 minutes

of occlusion time or less. A 30 minute occlusion followed by reperfusion was used in the present study because it has been estimated to be the minimum time required to produce a reproducible lesion encompassing basal ganglia and cortex (van Lookeren Campagne *et al.*, 1999). Thus, the extent of damage caused is expected to be less than with longer occlusion times and should provide more potentially salvageable tissue to target by gene therapy.

The interval between onset of stroke and therapeutic intervention is another crucial factor to consider. While the effect of HSP27 treatment has not been previously investigated, the only post-ischaemic HSP neuroprotection study to date demonstrated that viral delivery of HSP70 at 0.5 and 2 hours after transient ischaemia in rats results in lesion size reduction (Hoehn *et al.*, 2001). Interestingly, delivering a virus expressing HSP70 5 hours after reperfusion had no effect on lesion size or neuronal morphology as assessed at 48 hours. This suggests a narrow window of therapeutic intervention of ~3-6 hours after stroke that is consistent with clinical scenarios. In fact, patients show a significant improvement in neurological outcome when thrombolytic therapy is applied within 3 hours after the ischaemic event (NINDS Stroke Study Group, 1995). In general terms, the outcome of the patient is expected to improve the earlier the therapy is applied (Aronowski *et al.*, 1994). Neuroprotective drugs delivered within the first few hours after stroke are likely to reduce final lesion size by preventing the growth of the lesion at this critical stage (see Ward *et al.*, 1997). In the present study, gene therapy was applied at 30 minutes after the start of reperfusion, the earlier timepoint of the established therapeutic window, to allow for maximal efficacy of the treatment.

The route of administration of the treatment is also important. Pharmacological drugs are easier to administrate immediately after stroke. In the present study, however, the use of a vector implied a delay between administration and active therapeutic intervention, as the virus requires some time to express the transgene. An early delivery timepoint was therefore chosen in order to allow enough time for the viral vector to infect cells and guarantee expression the HSP genes by 3 hours after stroke induction (Hoehn *et al.*, 2001). Moreover, since intracerebral microinjections were used to deliver the viral vector, the area of infarction was directly targeted. The high infectivity and spatio-temporal distribution of the virus in

the basal ganglia and its overlap with the area affected by MCA occlusion has already been discussed (chapter 4) and is assumed to be similar in this study.

It should be noted that experimental evidence of protection with a variety of drugs in rats often cannot be directly translated to effective clinical trials in stroke patients (reviewed in Hunter *et al.*, 1995, 1998; de Keyser *et al.*, 1999; Modo *et al.*, 2000). One of the limitations of animal neuroprotective experiments is that long-term functional recovery in motor and cognitive tasks is not always assessed. Although reduction in the size of the infarct is an important predictor of outcome, equal attention should be given to the ability of these treatments to resolve sensorimotor deficits. The next section will review the literature on the relevant behavioural studies that have been carried out in animal models of stroke.

6.1.2 Behavioural studies

Neurological score scales have been more widely used than sensorimotor tests in animal models and give an adequate but crude estimation of functional impairment due to stroke. Moreover, many studies have reported spontaneous recovery when using these tests at acute or short timepoints after ischaemia (Modo *et al.*, 2000). More comprehensive scales include limb placement, beam or grid walking, rotarod, sticky label and staircase tests alongside the global neurological score tests such as postural/righting reflex, spontaneous exploration, circling behaviour, visual placement, inclined platform and horizontal bar (reviewed in Hunter *et al.*, 1998). A more sophisticated analysis of impairment requires a more complex battery of tests to probe for spatial memory and cognitive function, such as the radial or water maze tests (Yamamoto *et al.*, 1991; Wahl *et al.*, 1992; Markgraf *et al.*, 1992; Okada *et al.*, 1995).

In this study, long-lasting behavioural impairment was assessed via the bilateral asymmetry or "sticky tape" and the grid walking or foot-fault tests. Animals were not tested until 72 hours after ischaemia since it has been shown that 48 hours are required for animals to recover from MCA occlusion and this delay could

therefore minimize the measurement of acute deficits due to the surgical procedure (van der Staay *et al.*, 1996*b*). The rational behind the bilateral asymmetry test is that animals suffering from unilateral damage will experience sensory neglect of the contralateral limbs (Schallert *et al.*, 1982). This task mimics the contralateral neglect syndrome caused by damage to the parietal cortex and the tactile extinction observed in patients with unilateral stroke (Heilman *et al.*, 1985; Rose *et al.*, 1994). A variety of parameters can be measured with this test such as time to contact each paw and order of contact, however time to removal has been previously suggested to be the most reliable measure (Corbett & Nurse, 1998; Modo *et al.*, 2000). No tests were performed in pre-ischaemic animals in this study because no differences have been previously found in baseline testing between operated and control animals (Hunter *et al.*, 2000).

The foot-fault test measures spontaneous locomotor activity, motor coordination, and sensorimotor integration (Hunter *et al.*, 1998). The total number of steps taken in 1 minute is counted together with the number of left paw misplacements on the grid. No pre-ischaemic testing was performed because previous studies have established that the number of foot faults are typically zero or near zero in intact animals (Rogers *et al.*, 1997; Modo *et al.*, 2000). This test has been shown to give a good indication of motor impairment due to unilateral MCA occlusion up to 3 weeks after stroke (Markgraf *et al.*, 1992; Aronowski *et al.*, 1996). Interestingly, a study in spontaneously hypertensive rats suggests that the behavioural recovery observed in the foot-fault test at 1 month after stroke is related to functional plasticity, to the ability of neurones to integrate to other regions in the cortex. This was shown by correlating the resolution of the motor deficit of the affected forelimb only at 30 days after stroke with elevated GAP-43 and synaptophysin expression in the ipsilateral neocortex. These two proteins are involved in neurite growth and in the increase in number of synapses and are often used as markers of neuroanatomical remodelling and neural development (Stroemer *et al.*, 1995).

6.1.3 Neurological score and experimental stroke

Differences in the evolution of pathology between permanent and transient occlusion models used in the literature could explain some of the variability observed in the rate of recovery of these animals (Hunter *et al.*, 1998). Many permanent and transient stroke models in rats have demonstrated varying degrees of behavioural deficit compared to sham operated controls (Benderson *et al.*, 1986; Persson *et al.*, 1989; Belayev *et al.*, 1995). Early experiments established a direct correlation between the extent of neurological deficit and histological determination of lesion size at 24 hours after MCAO in rats (Benderson *et al.*, 1986). Similarly, neurological tests were used to predict the degree of injury after stroke. A strong correlation was found between the number of necrotic neurones due to ischaemia and the mean neurological score with increasing times of transient occlusion (30 and 60 minutes respectively) and permanent occlusion in rats measured 1 week after stroke (Garcia *et al.*, 1995). Subsequent experiments in cats subjected to permanent or 0.5, 4 and 8 hours of transient MCA occlusion further supported these findings (de Courten Myers *et al.*, 1998).

Permanent MCA occlusion in rats caused deficits in postural reflex, visual placement, grasping, motor coordination and bilateral asymmetry tests that were restored to pre-operative standards only 30 days after stroke induction. This was correlated with histology, where severe neuronal loss was observed in the striatum and the parietal, temporal and frontolateral cortex (Markgraf *et al.*, 1992, 1994). In transient rat models, 90 minutes of MCA occlusion cause a decrease in the number of rearing in locomotor tests at 1 and 30 days after stroke (Sakai *et al.*, 1996). Wood and colleagues showed that photothrombotic lesions in the cortex cause sensorimotor deficits, impairing rats in beam walk tests and grid walk tests (Wood *et al.*, 1996). Hunter and colleagues used rotarod and bilateral asymmetry tests to assess functional deficit at 24 hours and 1 week in rats subjected to 90 minutes of MCA occlusion. Their results indicate that the performance on the rotarod is significantly impaired at 1 but not at 7 days after stroke, whereas deficits in the bilateral asymmetry test were maintained at 1 week. The same laboratory has used MRI to correlate how specific pathological changes in different regions of the ischaemic brain contributed to

functional impairment in the sticky tape task over 1 month after 90 minutes of MCAO (Virley *et al.*, 2000).

6.1.4 Neurobehaviour and lesion size

Fewer studies have, however, attempted to correlate functional impairments as well as neurological score with lesion size. One study used a pathological scale to measure lesion size in combination with a neurological scale to validate the stroke model itself. Thus, infarct size could be predicted from the results of the neurological evaluation in 83% of the 82 MCA occluded animals tested (Menzies *et al.*, 1992). Rogers and colleagues have shown that there is a correlation between motor impairment and extent and severity of infarct by varying the duration of the ischaemic period from 0 to 120 minutes in transient models and comparing these with permanent occlusion. The volume of infarction was seen to increase with occlusion time as expected and correlated with severity of neuronal and pancellular necrosis on histological sections. Moreover, permanently occluded rats showed more foot-fault errors than sham operated or rats occluded for 30 minutes and a linear relationship between the duration of ischaemia and number of errors was observed (Rogers *et al.*, 1997). Similarly, MCA occlusion by endothelin-1 injection had a significant effect on sensorimotor function even if the infarct size was heterogeneous. Rats preferentially contacted the ipsilateral paw first and took longer to contact the contralateral paw as measured at 2 and 3 weeks after stroke induction (Ward *et al.*, 1997).

These findings are further validated by neuroprotection studies that have shown reductions in lesion size and improved neurological outcome in focal models of ischaemia in rats (Belayev *et al.*, 1995; Mackay *et al.*, 1996; Minematsu & Fisher, 1993). Infarct volume was significantly reduced in rats undergoing 2 hours of MCA occlusion and treated with neutrophil inhibitory factor upon reperfusion and at 4 and 6 hours after insult. This was in turn correlated with a reduction in brain swelling and an improved neurological outcome as measured at 24 hours after stroke (Mackay *et al.*, 1996). Post-ischaemic delivery of a different drug, HU-211, caused significant

reductions in lesion volume, brain swelling, improved neurological score and forelimb placing after 90 minutes of occlusion in rats (Belayev *et al.*, 1995).

Some studies, however, suggest that infarct size does not necessarily correlate to improvement in behavioural outcome. Experiments in hypertensive rats have shown that varying the duration of ischaemia from 45 to 60, 90 and 120 minutes correlated directly with an increase in lesion size and in sensorimotor impairment measured at 21 days by forearm flex and foot-fault tests (Aronowski *et al.*, 1994, 1996). Interestingly, post-ischaemic treatment with CNS-1102 caused a significant improvement in all behavioural tasks but no reduction in maximal lesion size (at maximum occlusion time) compared to untreated MCA occluded controls (Aronowski *et al.*, 1996). A similar lack of correlation between infarct size and neurological impairment was reported in focal cerebral ischaemia in rats (Wahl *et al.*, 1992; van der Staay *et al.*, 1996*a*). Nevertheless, most studies support such correlation allowing for variations in the size and location of the lesion, strain of rat and sensitivity of the scoring systems used (Benderson *et al.*, 1986; Markgraf *et al.*, 1992; Grabowski *et al.*, 1993; Belayev *et al.*, 1995; van der Staay et al., 1996*b*).

6.1.5 Summary

As described in chapter 1, HSPs are naturally upregulated after a range of stresses both *in vitro* and *in vivo*. The experiments presented in this chapter investigate the effect of enhancing the levels of HSP overexpression after a transient ischaemic insult by delivering an HSV-1 viral vector engineered to express HSP27 or HSP70 30 minutes after tissue reperfusion. Although MRI scans indicated that *pre-ischaemic* overexpression of HSP27 caused a significant reduction in lesion size (chapter 5), it was necessary to test the efficacy of such treatment *after* stroke induction in order to relate these findings to clinical scenarios. Finally, neurobehavioural improvement was assessed by two sensorimotor tests in an attempt to correlate changes in lesion size with functional recovery over time.

6.2 Methods

6.2.1 Experimental design

Three groups (n=6) of adult male Sprague-Dawley rats (220-280gr) were subjected to 30 minutes MCA occlusion and microinjected with either HSV-HSP27, HSV-HSP70, or HSV-LacZ as a control. Rats were allowed to recover for 24 hours before scanning. All animals were then scanned at multiple timepoints and subjected to behavioural tests up to 1 month after stroke as schematically shown in the diagram below (figure 6.1).

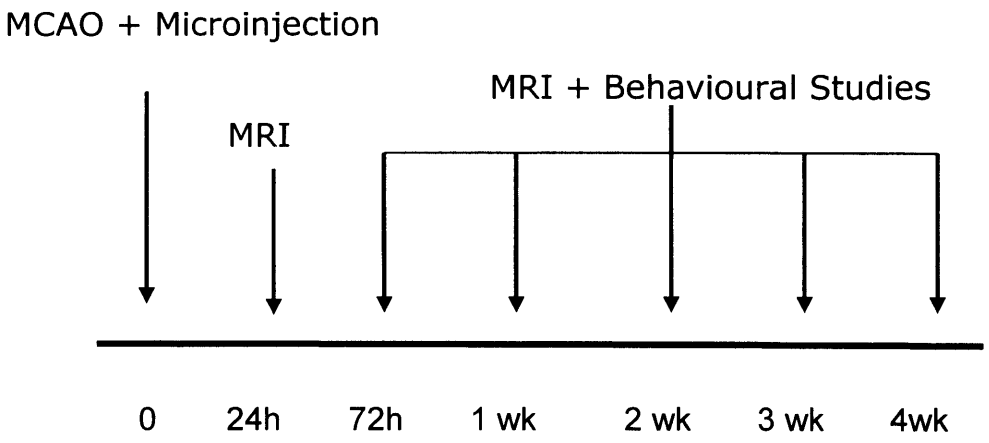

Figure 6.1. Schematic representation of the experimental design for the post-ischaemic gene therapy study. Three groups of animals (n=6) were subjected to MCA occlusion and microinjected on day zero and subsequently scanned and tested for behavioural recovery up to 1 month after stroke.

6.2.2 Virus growth

Viral growth methods have been thoroughly described in section 4.2.2 and microinjection procedures have been detailed in section 4.2.4. Briefly, a herpes simplex virus type 1 strain deleted for ICP27 and engineered to express either HSP27, HSP70, or LacZ was grown in B130/2 BHK complementing cells. The viral suspensions were harvested, filtered and concentrated and the virus pellets were resuspended in sterile PBS. Titration assays confirmed the viruses had a high titre of $1\text{-}2x10^{10}$ plaque forming units (pfu).

6.2.3 Intracerebral microinjections and middle cerebral artery occlusion

Rats were anaesthetized with 2% isoflurane in 70:30 N_2O:O_2 placed in a stereotaxic frame (Korf, Germany). A midline incision was made on the head and the skin was carefully retracted. A burr hole was made on the skull at the appropriate coordinates for the striatum (Bregma coordinates: AP= +0.10cm; L = -0.35cm; V= -0.50cm) on the right hemisphere. The skin was then temporarily closed with masking tape and the animals were transferred to the microscope for MCA occlusion. The common, internal and external carotid arteries were exposed and a 290μm Monocryl suture (Ethicon, UK) with an araldite-coated tip was introduced into the lumen of the right common carotid artery up to the origin of the MCA. The animals remained occluded for a total of 30 minutes after which they the embolus was carefully retracted and the tissue reperfused. The cutaneous wound was then sutured and cleaned and the animals were placed in the stereotaxic frame once more. The rats were kept under anaesthetics and the intracerebral microinjections were performed 30 minutes after the start of reperfusion for all three groups. Viral suspensions were diluted to $1x10^6$ pfu/μl and a microsyringe pump (WPI, UK) was used to deliver 2.5μl of HSV-LacZ, HSV-HSP70 and HSV-HSP27 to the right striatum at a constant rate of 0.25μl/min. Throughout the surgery, rectal temperature was maintained at 37±1°C via a heating blanket controlled by a thermocouple. The whole procedure

took 2 hours and the animals were left to recover for 24 hours before scanning with free access to food and water.

6.2.4 Magnetic Resonance Imaging

Scans were performed on a 2.35 Tesla horizontal bore magnet (Oxford Instruments, UK) interfaced to a SMIS console (Guilford, UK). All animals were anaesthetized with 2% halothane in a 70:30 N_2O:O_2 mix delivered via nose cone and placed on a probe with bite and ear bars securing the head to minimize movement artefacts. Physiological parameters monitored included electrocardiography (ECG) recordings and rectal temperature, which was maintained at 37±1°C using an air warming system.

The imaging protocol included two echo planar imaging (EPI) sequences, T_1 and continuous arterial spin labelling (CASL), for the determination of CBF and a multislice T_2-weighted spin echo (SE) sequence for the determination of lesion size. The sequence parameters were identical to the ones described in section 5.2.5 and total scan time was 35 minutes. As stated in the previous chapter, the centre slice of the multislice dataset was determined via anatomical landmarks on visual inspection of pilot coronal scans and not by the maximal lesion area.

6.2.5 Image processing and data analysis

Quantitative maps were obtained by reconstructing all images with IDL Software Version 5.2 (Research Systems Inc., USA). T_1 values and subtracted labelled and reference CASL images were used to calculate CBF maps. Lesion area and regions of interest were delineated on all processed images and analyzed with SMIS Image Display Version 3.7. The resulting lesion areas per slice were used to determine lesion volume across the whole brain. Moreover, a regional analysis was performed on the T_2-weighted multislice dataset based on knowledge of the vascular territories in the rat brain (Paxinos, 2004). Slices were grouped into three regions: the

frontal region (slices 1, 2), the mid MCA territory region (slices 3, 4, 5, 6) and the posterior region (slices 7, 8, 9). A restricted maximum likelihood (REML) analysis of the longitudinal lesion volume data was performed using a full random coefficients model, assuming a linear dependence on time. The probability values were obtained using the F test and considered significant at $p < 0.05$. These calculations were performed using SAS PROC MIXED (SAS Institute, 1999).

The CBF and behavioural test results were analyzed using repeated measures ANOVA (SPSS 12.0.1, SPSS Inc., USA) with groups as the between-subjects factor and assessment timepoints as the within-subjects factor. The Bonferroni correction was used post hoc to compare groups. Standard *t* tests were used for end point comparisons.All data is presented as mean ± standard error.

6.2.6 Behavioural tests

6.2.6.1 Bilateral asymmetry test

The bilateral asymmetry or sticky label test gives a measure of sensory neglect and tactile extinction (Schallert *et al.*, 1982). Two identical strips of brown packing tape of approximately 6cm in length and 0.5-0.8cm in width were wrapped around the hairless part of the forepaws of the animal. Care was taken in order to apply the tape with equal pressure and the order of the application (i.e., left or right paw first) was reversed for each consecutive trial. The time to removal from each paw was measured and each trial lasted a maximum of 180 seconds. Tests were not considered or repeated if the animal was unable to remove the tape from both the affected and the unaffected paw. Similarly, if the tape was not removed from one paw, the test was assigned the maximum value of 180 seconds for that paw. Two trials were performed and averaged per timepoint, starting at three days and up to one month after stroke.

6.2.6.2 Foot-fault test

The foot-fault test was used to assess the animal's motor-coordination deficit over time. To this end, a homebuilt frame of 40cm in width, 1m in length and 30cm in height was used. The frame was covered with a 7-cm-whole mesh wire and the animals were placed at one end and encouraged to walk on this surface. The total number of steps and the correct or incorrect placement of the left affected forelimb (contralateral to the infarction) were recorded. Precise grip and placement of the limbs is required to successfully complete the test (Hernandez & Schallert, 1988). Each trial lasted 60 seconds and, as for the bilateral asymmetry test, two trials per timepoint were averaged. The test was discarded and not repeated if the animal took less than 10 steps.

6.3 Results

6.3.1 Effect of HSP expression on lesion size

Figure 6.2 shows the centre slice of a multislice T_2-weighted-spin echo image dataset obtained 24 hours, 1 week and 3 weeks after transient MCA occlusion. The three groups of six animals had been microinjected with HSV-HSP27, HSV-HSP70 or HSV-LacZ as a control 30 minutes after suture retraction and tissue reperfusion. Averaged total lesion volumes measured from the images at all timepoints are presented in table 6.1, and figure 6.3 shows lesion volume per slice from front to back of the brain for all rats at all 6 timepoints.

A regression analysis was carried out to assess the evolution of the lesion over time. *t* tests on the individual regression slopes indicated a significant change in the mean lesion volume in HSP27 treated animals over time (-0.59 ± 0.2 mm^3/day; p = 0.01) (figure 6.4). The regression slopes for the two other groups were -0.08 ± 0.2 mm^3/day for HSP70 and -0.07 ± 0.2 mm^3/day for LacZ injected animals respectively and did not achieve statistical significance (p_{HSP70}= 0.72; p_{LacZ}= 0.75).

The mean absolute lesion volume estimates at 28 days were 48.5 ± 8.3mm^3 for HSP27 injected rats, 68.9 ± 8.3mm^3 for HSP70 injected rats and 71.5 ± 8.3mm^3 for LacZ injected animals. The difference in mean lesion volume between HSP27 treated and LacZ injected controls was statistically significant (difference = 23 ± 11.8mm^3; p = 0.05), whereas no significant difference was found between HSP70 treated animals and controls (difference = 2.6 ± 11.8mm^3; p = 0.8).

A regional analysis was performed on the multislice data by grouping frontal slices (1, 2), mid MCA territory slices (3, 4, 5, 6) and posterior slices (7, 8, 9) (figure 6.5). Results indicated that the three groups differed in their regional dependence in lesion volume (p = 0.02). The regional population mean volume estimates at 28 days suggested that HSP27 treatment was more effective in the posterior region than in the frontal and mid regions (table 6.2). In fact, the differences in mean absolute lesion volumes in regions 1 and 2 between HSP27 treated rats and controls were 1.8 ±

$4.4mm^3$ ($p = 0.4$) and $5.05 \pm 4.4mm^3$ ($p = 0.2$), while region 3 presented a significant $16.1 \pm 4.4mm^3$ difference in lesion volume ($p = 0.0003$). No differences were found when comparing mean absolute lesion volume estimates over time in regions 1, 2 and 3 in HSP70 treated rats and controls ($difference_{region1} = 2.6 \pm 4.4mm^3$, $p = 0.6$; $difference_{region2} = 2.3 \pm 4.4mm^3$, $p = 0.6$; $difference_{region3} = 2.9 \pm 4.4mm^3$, $p = 0.5$).

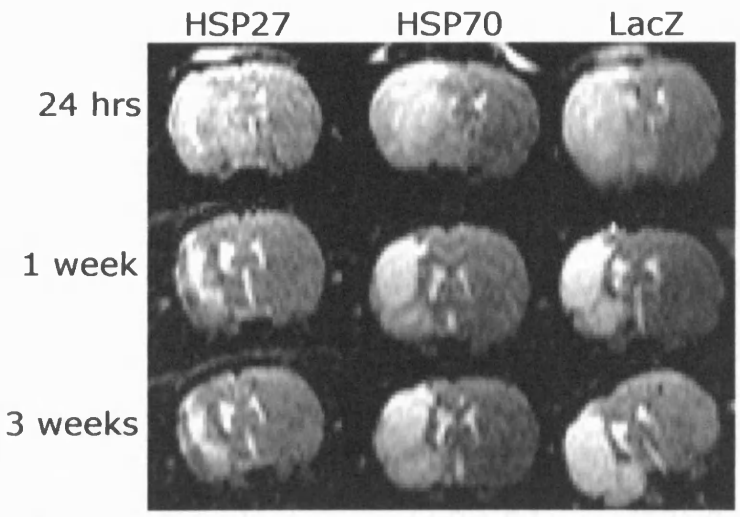

Figure 6.2. Representative centre slices of multislice T_2-weighted spin echo datasets. The scans show the lesion area (bright) in HSP27, HSP70 and LacZ injected rats at 24 hours, 1 week and 3 weeks after MCA occlusion.

Timepoint	Lesion Size (mm^3)		
	HSV-HSP27	HSV-HSP70	HSV-LacZ
24 hours	60 ± 12.4	68.6 ± 7	71.5 ± 7.5
72 hours	60 ± 8.5	69.9 ± 5.2	73.3 ± 4.6
1 week	59.6 ± 9.9	65.2 ± 4.1	73.3 ± 4.9
2 weeks	44.5 ± 9.2	71.4 ± 3.6	74.7 ± 6
3 weeks	44.8 ± 10.7	57.5 ± 4.4	69.6 ± 4.4
4 weeks	41.4 ± 10.4	64.9 ± 5.1	71.9 ± 3.8

Table 6.1. Mean lesion size at each timepoint for HSP-treated and LacZ injected control animals (n = 6). Values represent absolute lesion volume (mm^3) determined on multislice T_2-weighted spin echo scans ± s.e.m.

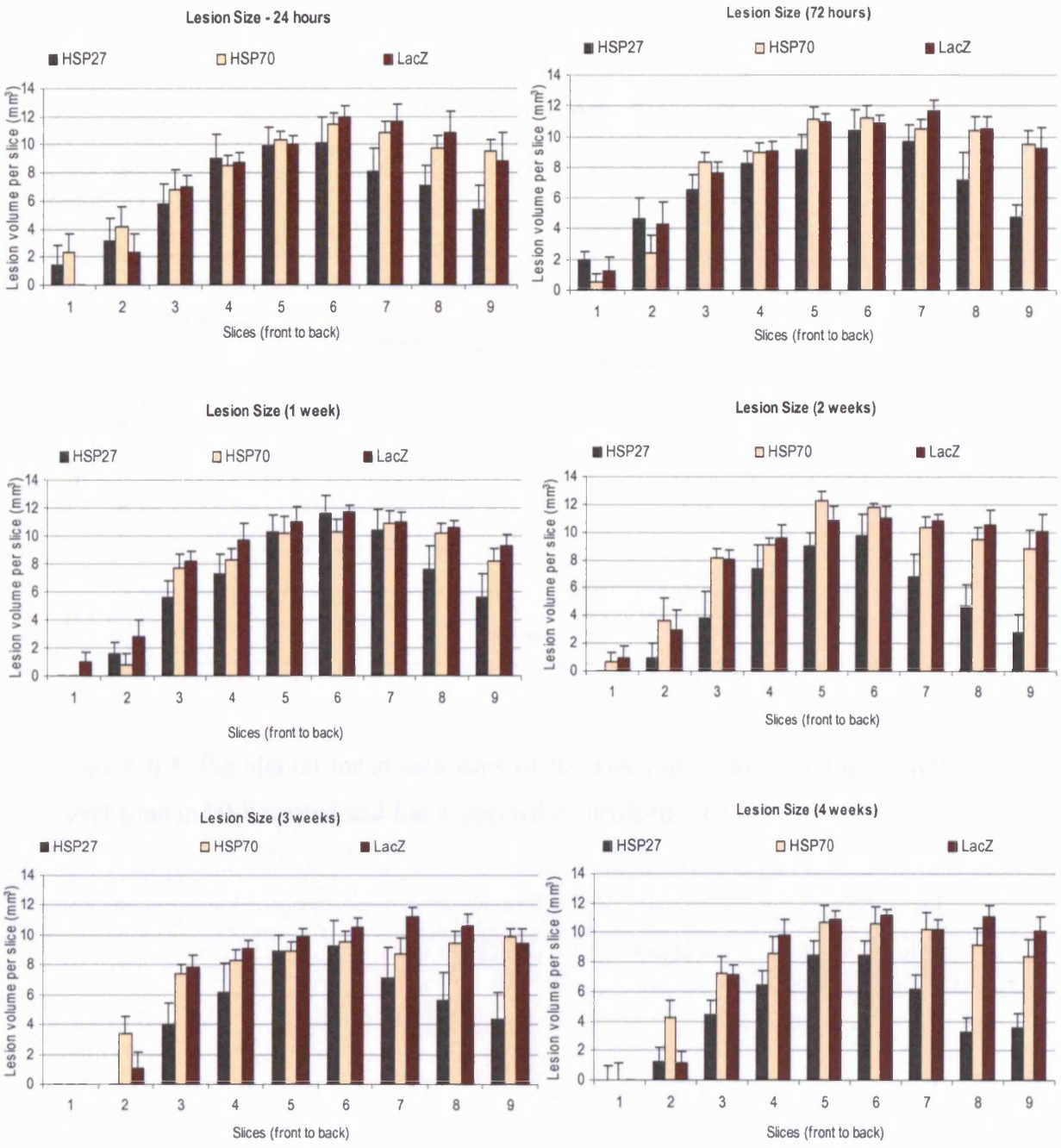

Figure 6.3. Mean lesion size calculated from multislice T_2-weighted spin echo images for HSP27, HSP70 and LacZ injected animals at 6 different timepoints (n = 6). Bars represent absolute lesion volume (mm^3) in 9 slices from front to back of the brain ± s.e.m.

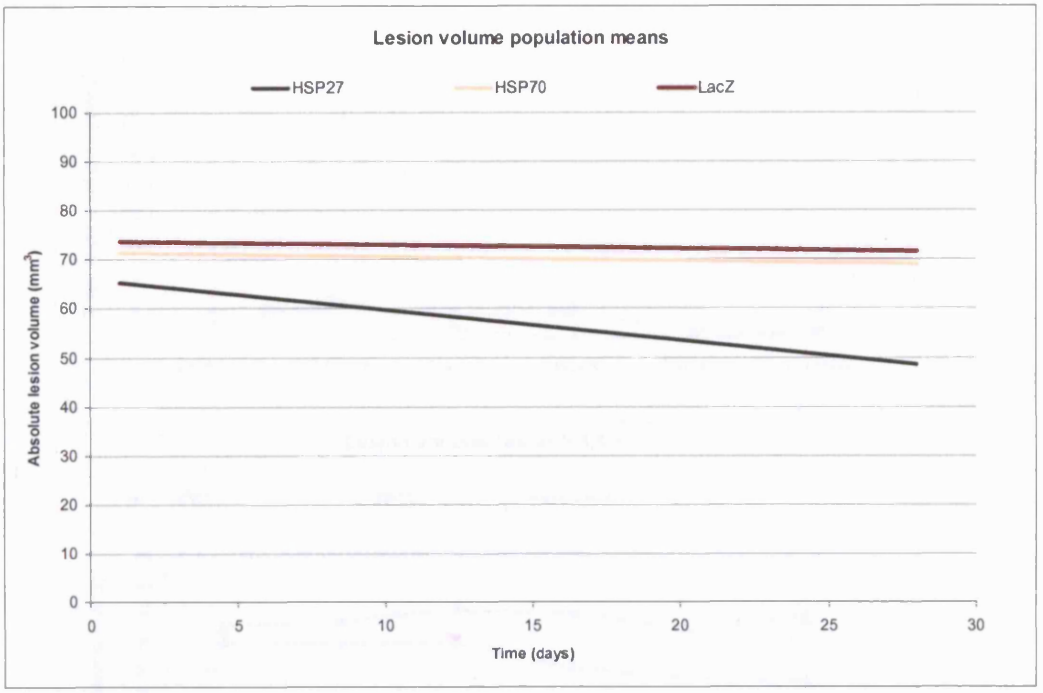

Figure 6.4. Population mean estimates of the absolute lesion volume evolution over time in HSP treated and LacZ injected controls (n = 6).

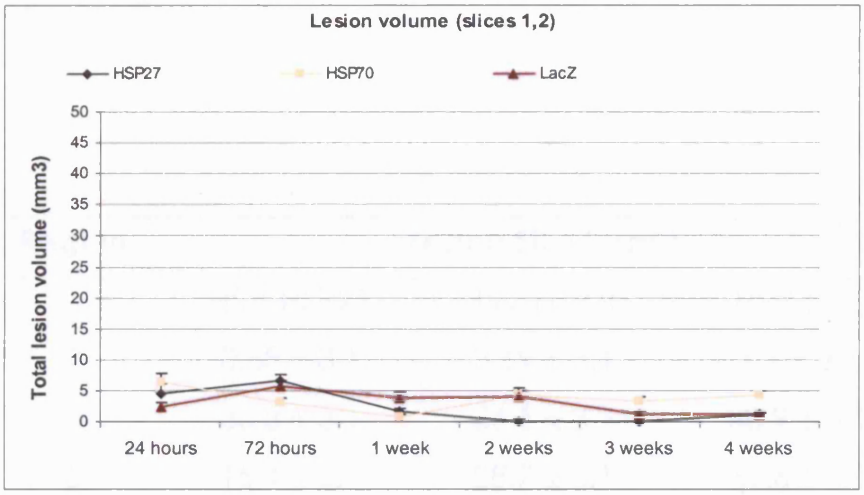

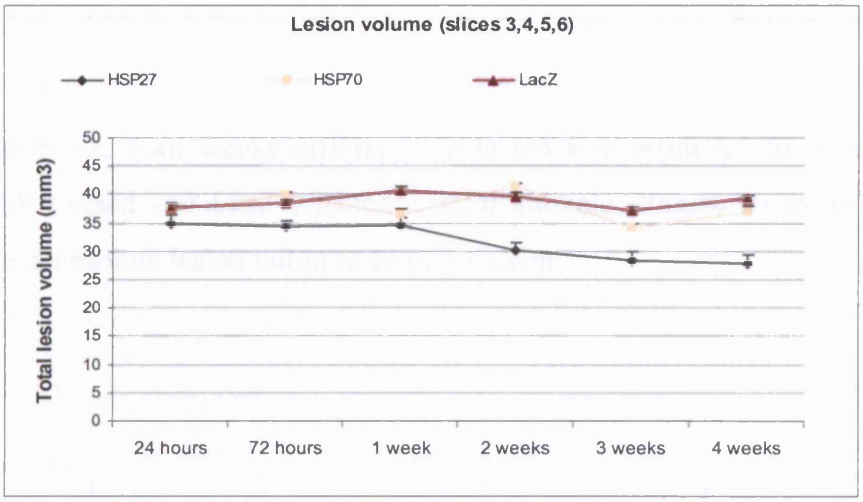

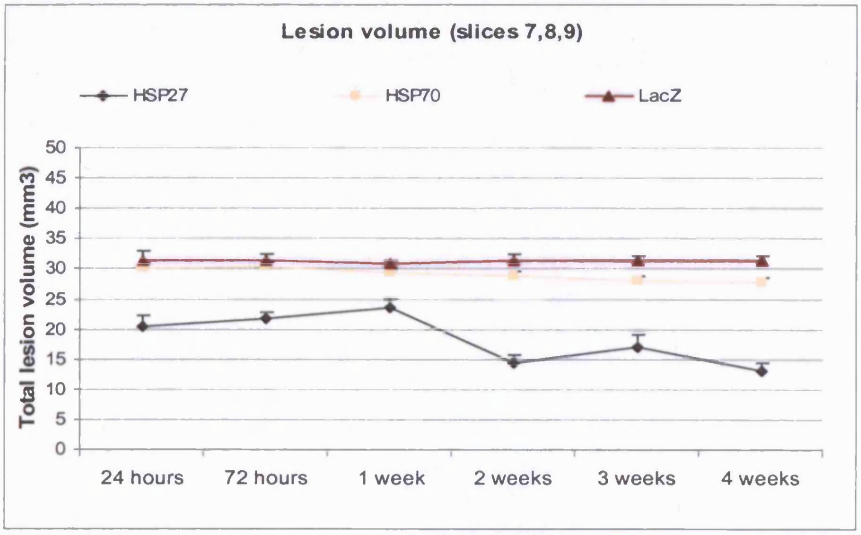

Figure 6.5. Regional analysis of mean absolute lesion volume estimates in frontal (1, 2), mid (3, 4, 5, 6), and posterior (7, 8, 9) slices calculated form multislice T_2-weighted spin echo images at 6 different timepoints in HSP treated and control animals.

Region	Lesion Size (mm^3)		
	HSV-HSP27	HSV-HSP70	HSV-LacZ
1	0.68 ± 3.1	3.69 ± 3.1	1.1 ± 3.1
2	33.8 ± 3.1	36.5 ± 3.1	38.9 ± 3.1
3	15.4 ± 3.1	28.7 ± 3.1	31.6 ± 3.1

Table 6.2. Four weeks difference in lesion size estimates for each region in HSP treated and LacZ injected control animals. Values represent population mean absolute lesion volumes (mm^3) ± s.e.m.

6.3.2 CBF

Cerebral blood flow (CBF) was measured at 24 hours, 72 hours, 1 week, 2, weeks, 3 weeks, and 4 weeks after occlusion-reperfusion. Values in the ischaemic hemisphere for treated and control animals are presented in table 6.3, expressed as a percentage of flow in the contralateral hemisphere. Complete recovery of CBF was not achieved acutely but all values were above the ischaemic threshold (Kohno *et al.*, 1995). Statistical analysis showed no significant differences between the groups (Controls vs. HSV-HSP27 [$F(2;15) = 1.9$, $p > 0.2$]; Controls vs. HSV-HSP70 ($p > 0.9$) at all timepoints after reperfusion.

Timepoint	% $CBF_{ipsi/contra}$		
	HSV-HSP27	HSV-HSP70	HSV-LacZ
24 hours	85.5 ± 5	90.6 ± 8.7	76.1 ± 7.8
72 hours	85.9 ± 2.8	86.6 ± 5.6	84.3 ± 5.1
1 week	96.3 ± 3.4	90.25 ± 1.5	93.1 ± 4.5
2 weeks	97.51 ± 4.5	92.8 ± 1.7	89.7 ± 4.4
3 weeks	89.9 ± 2.5	88.5 ± 4.2	86.7 ± 3.5
4 weeks	96.8 ± 2.3	87 ± 4.8	87.5 ± 4.1

Table 6.3. CBF measurements obtained at 6 timepoints after 30 minutes of MCA occlusion in HSV-HSP27, HSV-HSP70 and control animals (n = 6). Values represent averaged CBF in the ipsilateral hemisphere as a percentage of the contralateral flow values (% $CBF_{ipsi/contra}$) ± s.e.m.

6.3.3 Effect of gene therapy on functional recovery

6.3.3.1 Bilateral asymmetry test

The sensorimotor asymmetry test showed that all animals subjected to transient MCA occlusion preferentially removed the tape from the forelimb ipsilateral to the ischaemic hemisphere first. The time to removal of the tape from left (affected) and right (unaffected) paws was recorded at 5 different timepoints: 72 hours, 1 week, 2 weeks, 3 weeks, 4 weeks. All animals performed the task twice per timepoint and the average of the two trials was used to calculate the mean removal time per paw for each group presented in table 6.4 below. The values demonstrate a marked difference in removal time from the left and right paw for all three groups and such sensory neglect persisted throughout the period tested. Figure 6.6 shows the plots for removal time with the affected and the unaffected paw for all three groups.

A significant difference was found in the difference between left and right paw removal times in HSP27 and LacZ controls at all post-ischaemic timepoints [$F(2;10) = 4.656$, $p < 0.05$], while no differences were found between HSP70 and controls ($p < 1.00$) (figure 6.7).

The total removal time from left and right paws was not different across groups at most timepoints. However, a significant improvement was observed in HSP27 treated animals at 3 ($p < 0.03$) and 4 weeks ($p < 0.02$). Interestingly, HSP70 treated animals took slightly longer than controls to remove the sticky tape from the left paw at most timepoints although this difference did not reach statistical significance (table 6.4; figure 6.8).

Timepoint	Removal time (secs)					
	HSV-HSP27		HSV-HSP70		HSV-LacZ	
	Left	Right	Left	Right	Left	Right
72 hours	146.6 ± 26.5	42.2 ± 6.2	171.5 ± 6.7	72.9 ± 12.4	154 ± 20.3	71.2 ± 23.7
1 weeks	124.3 ± 21.6	47 ± 11.2	180 ± 0.0	52.6 ± 6.8	167.1 ± 3.5	42.1 ± 7.4
2 weeks	114.2 ± 24.2	55.7 ± 25.8	159.3 ± 15.5	60.2 ± 22.2	114.6 ± 22.9	47.6 ± 10.9
3 weeks	72.6 ± 20.5	32 ± 8.9	122.6 ± 16.8	67.7 ± 18.8	100.5 ± 23.7	44.7 ± 13.4
4 weeks	83.7 ± 21.8	43.7 ± 14.6	131.7 ± 25.3	61.3 ± 26.1	133.9 ±16.6	56.9 ± 17.3

Table 6.4. Bilateral asymmetry test. Mean removal times from affected (left) and unaffected (right) forelimbs at 72 hours, 1 week, 2 weeks, 3 weeks and 4 weeks after MCA occlusion for HSP treated and LacZ injected controls.

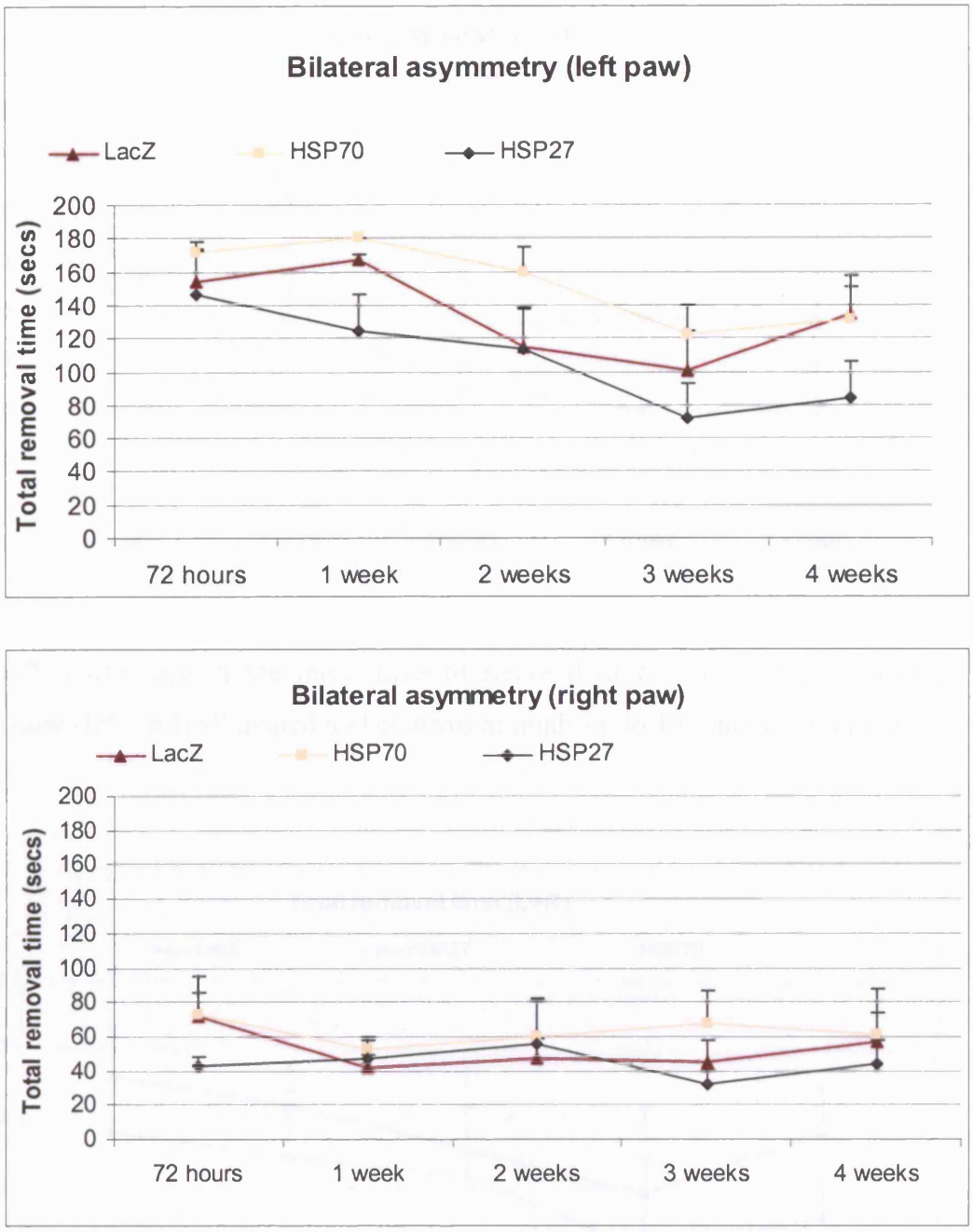

Figure 6.6. Total removal time of the sticky tape from left and right forepaws in HSP27, HSP70 and LacZ injected animals over time.

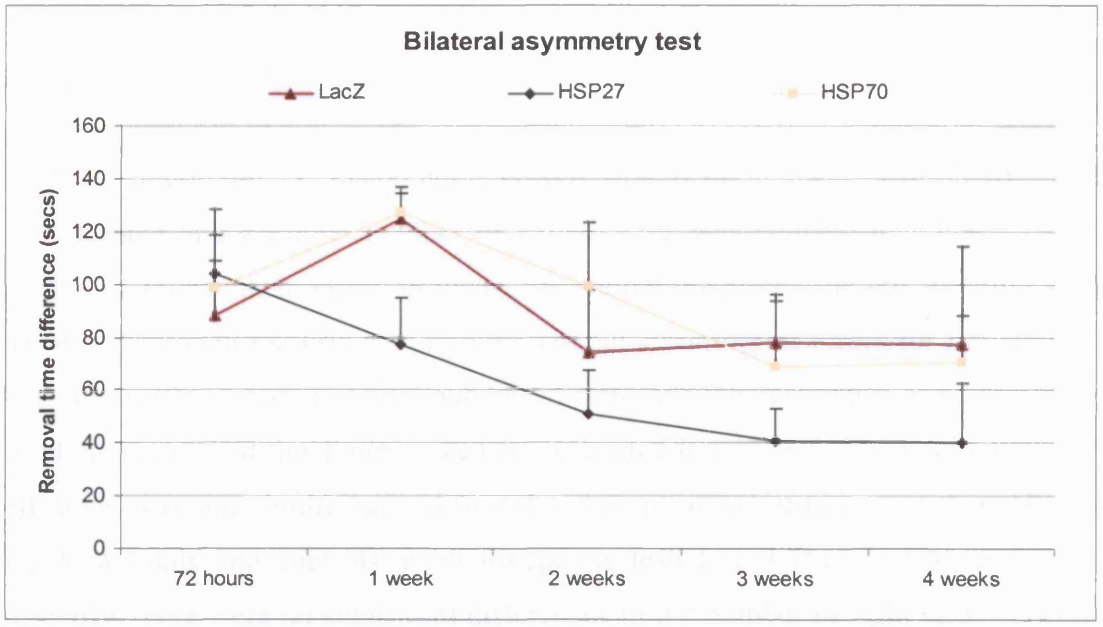

Figure 6.7. Difference in the mean time to removal of the sticky tape from the affected paw (left) in HSP treated and controls animals up to 1 month after stroke.

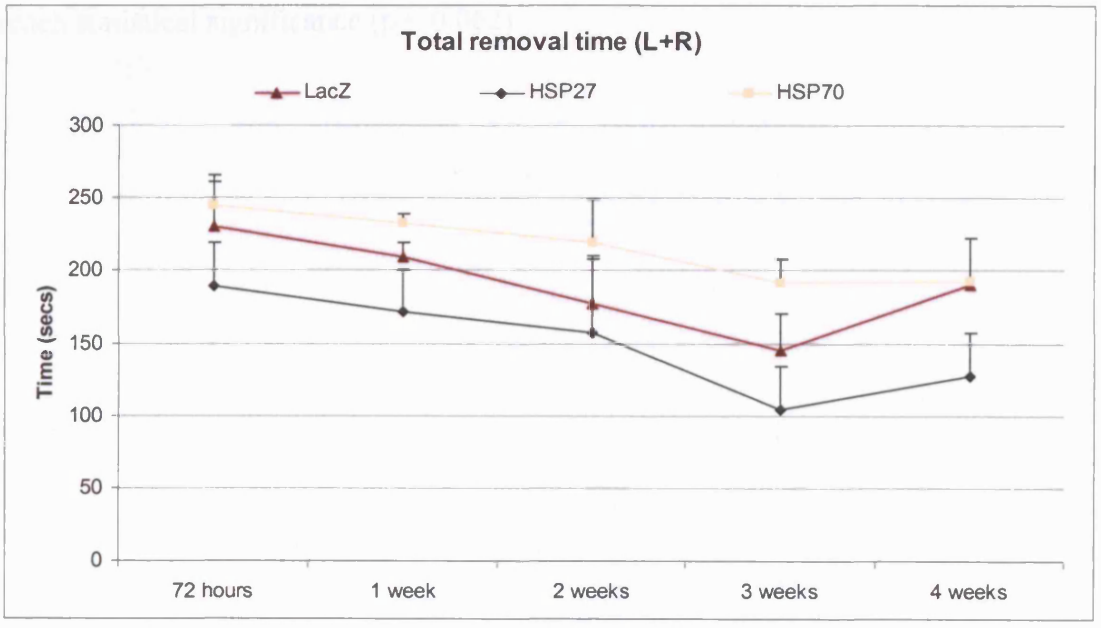

Figure 6.8. Total removal time from left and right paws in HSP27, HSP70 and LacZ injected rats over time. Values represent the addition of removal times for both paws (L+R) in seconds.

6.3.3.2 Foot-fault test

At 72 hours after occlusion animals were placed in an elevated mesh wire grid for 1 minute and the total number of paired steps was counted together with the number of foot-fault or errors in which the animal misplaced the left forelimb such that it fell through the grid (figure 6.9). The total number of errors for the affected forelimb was recorded. The total number of steps and the percentage of correct steps for all animals at all timepoints tested are presented in table 6.5. The total number of left steps was not significantly different between either HSP27 treated or HSP70 treated animals and controls at all timepoints tested [$F(2;75) = 3.520$, $p <$ n.s.]. Similarly, there were no significant differences in the number of right steps between the three groups over time [$F(2;75) = 4.637$, $p <$ n.s.]. All animals showed some degree of impairment in this task on the first few weeks after MCA occlusion (figure 6.10). HSP27 treated animals, however, showed a higher percentage of correct steps compared to controls [$F(2;15) = 29.878$, $p < 0.0001$]. HSP70 treated animals, on the other hand, performed worse than controls in this task but this difference did not reach statistical significance ($p < 0.062$).

Timepoint	HSV-HSP27		HSV-HSP70		HSV-LacZ	
	Total	% correct L	Total	% correct L	Total	% correct L
72 hours	32.5	73.4	26.7	53.5	27.33	57.2
1 weeks	24.7	74.4	23.5	45.1	25.08	51.5
2 weeks	25	87.3	19.8	48.4	26.83	60.5
3 weeks	29.5	85	21.5	50.1	22.5	59.7
4 weeks	22.4	82.8	20.3	53.1	22.59	68.8

Table 6.5. Total mean number of steps and percentage of correct steps with the affected paw (L, left) in HSV-HSP27, HSV-HSP70 and HSV-LacZ injected rats at all timepoints.

Figure 6.9. Foot-fault test. The picture illustrates a foot-fault with the left forepaw in a rat performing the grid walking test.

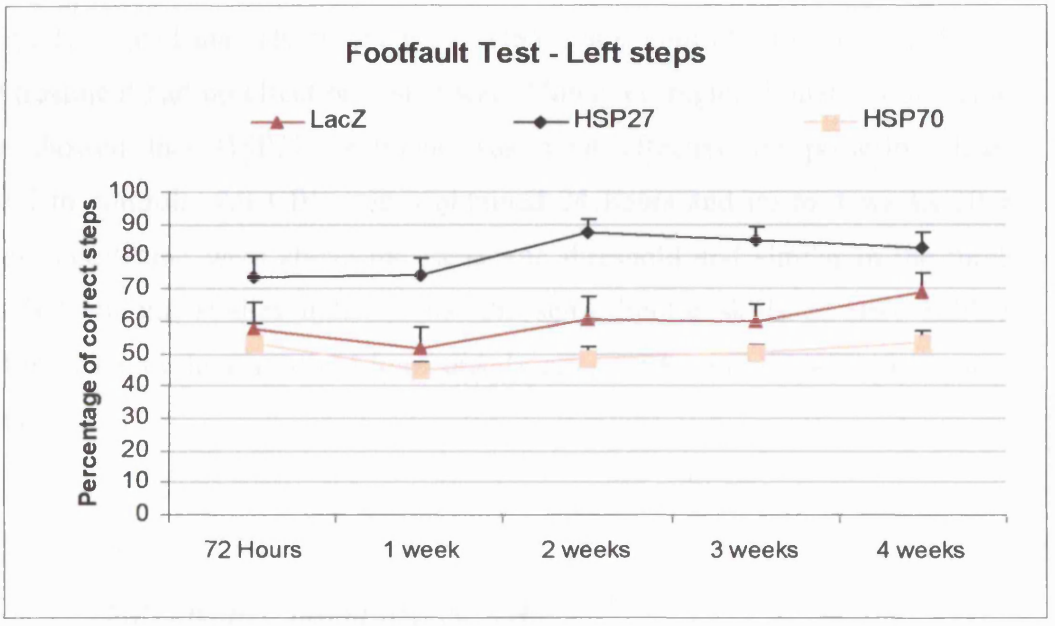

Figure 6.10. Foot-fault test in HSP27, HSP70 and LacZ control animals. The percentage of correct left steps was calculated from the total mean number of left steps at 5 different timepoints after MCA occlusion in treated and untreated rats.

6.4 Discussion

The aim of the study was to investigate neuroprotection *in vivo* after post-ischaemic delivery of an HSV-based vector expressing HSP27 or HSP70 in a rat focal model of transient cerebral ischaemia. Longitudinal MRI measurements enabled the assessment of the effect of HSP27 and HSP70 treatment on lesion size at 1, 3, 7, 14, 21 and 28 days after stroke. Behavioural tests were performed at the same scanning timepoints in order to get an indication of sensorimotor impairment and recovery over time. The model of stroke chosen for this *in vivo* study has been previously reported to produce a reproducible lesion encompassing the right cortex and basal ganglia. Similarly, direct intrastriatal microinjection of viral vectors was previously observed to yield high levels of protein expression in the ipsilateral hemisphere of HSP treated and LacZ injected control animals (chapters 4 and 5). Multislice T_2-weighted scans provide an indirect measure of the area of vasogenic oedema in the cortex and basal ganglia, and were used to determine lesion size (figure 6.2). These images demonstrated a marked reduction in lesion volume in HSV-HSP27 treated animals compared to HSV-LacZ controls. In contrast, HSV-HSP70 treatment had no effect on lesion size. Moreover, regional analysis of lesion volume showed that HSP27 treatment was most effective on posterior slices compared to controls. All CBF values obtained 24 hours and up to 4 weeks after occlusion-reperfusion were above the ischaemic threshold and similar in the three groups. Behavioural studies indicate that the sensorimotor skills of HSV-HSP27 injected animals are less impaired immediately after stroke and show improvement over time.

6.4.1 *MRI findings: lesion size and CBF*

The changes in lesion volume over time were different among the three groups tested here. Multislice T_2-weighted images acquired at 24, 72 hours, and weekly for one month after transient occlusion of the MCA indicate that overall lesion volume at 4 weeks was 25% smaller in HSP27 treated animals while LacZ injected controls

showed no reduction over time. HSP70 treatment caused a 3% reduction in lesion size at 4 weeks and the lesion volume values were not significantly different from those obtained for LacZ controls at the same timepoint. MRI techniques also confirmed that the tissue was highly although not fully reperfused in all three groups and that CBF levels were above ischaemic levels at all timepoints measured. This rules out the possibility that the changes in lesion size were caused by incomplete tissue reperfusion over time. These results are in line with findings described in chapter 5, where pre-ischaemic microinjections of HSV-HSP27 and not HSV-HSP70 caused a significant 44% reduction in lesion size. Contrary to the present experiments, the only other post-ischaemic study to date using an HSV viral vector to deliver HSP70 to the ischaemic brain showed protection (Hoehn *et al.*, 2001). Gene therapy applied at 0.5 and 2 hours but not 5 hours after transient MCA occlusion improved survival of striatal neurones but had no effect on lesion size. This discrepancy could be due to differences between the two studies, such as the animal model, the delivery method chosen, the HSP expression levels and the lesion size assessment and time. Hoehn and colleagues induced 60 minutes of MCA occlusion followed by reperfusion (as opposed to 30 minutes in this study), used an amplicon HSV vector and gave two injections in the ipsilateral and contralateral striatum respectively, assessed damage at 48 hours only and used a semiquantitative histological scale to determine lesion size. Such differences in study design and methodology have been thought to underlie the variable results obtained for HSP70 transgenic mouse models of stroke and also the rat studies using viral vectors to deliver HSP70 before and after stroke. This has been reviewed in detail in section 5.4.3.

The fact that the two *in vivo* studies presented here are consistent indicates that, at least in this model, HSP27 has an obvious neuroprotective effect and HSP70 does not. This in turn might reflect a difference in the mechanisms of action of HSP27 and HSP70 after an ischaemic insult. The roles of these two chaperones in cerebral ischaemia have been detailed in chapter 1: they are both potentially involved in improving cell survival by refolding denatured proteins and/or interfering with apoptotic pathways (Melhen *et al.*, 1996; Garrido *et al.*, 1997; Garrido *et al.*, 1999; Pandey *et al.*, 2000; Bruey *et al.*, 2000; Saleh *et al.*, 2000; Mosser *et al.*, 2000; Creagh *et al.*, 2000; Beere *et al.*, 2000; Paul *et al.*, 2002; Benn *et al.*, 2002; Akbar *et*

al., 2003; Garrido & Solari, 2003; Rashmi *et al.*, 2003; Tsuchiya *et al.*, 2003; Takayama *et al.*, 2003; Steel *et al.*, 2004; Latchman, 2004; Zourlidou *et al.*, 2004; Whitlock *et al.*, 2005). However, there is currently not enough evidence to distinguish specific functions that might make one chaperone more suitable than the other. Section 5.4 has, however, attempted to enumerate a series of "advantages" that HSP27 might have over HSP70 in an ischaemic environment, ATP dependence being the most salient one (Rogalla *et al.*, 1999; Garrido *et al.*, 2002; Riordan *et al.*, 2005). Moreover, this chaperone has been implicated in antioxidant mechanisms by causing a decrease in intracellular ROS and thus protecting against cell death due to oxidative stress (Melhen *et al.*, 1996, 1997; Orrenius *et al.*, 1998). Cytoskeletal stabilization by capping and decapping of actin filaments could protect such microfilaments from degradation and depolymerization due to stress (Guay *et al.*, 1997). *In vitro* experiments in astroglia have shown that HSP27 interacts with GFAP and vimentin and prevents stress-induced aggregation of these proteins, thus promoting cell stabilization and survival (Perng *et al.*, 1999). Moreover, as previously suggested (section 5.4.3), the protective effect of increasing the levels of HSP70 could be limited by the low levels of ATP at early timepoints after ischaemia onset (Mallouk *et al.*, 1999). Alternatively, the inefficacy of HSP70 could be explained by the pro-apoptotic role of this chaperone observed in the presence of TNF, which could be triggered by the viral microinjection (Ran *et al.*, 2004).

6.4.2 *Lesion size and behaviour*

Regional analysis suggests that posterior slices are more protected against stroke progression in HSP27 treated animals only. In fact, the lesion seems to be larger in the posterior brain region in untreated MCA occluded controls. Moreover, this progression becomes more obvious at 2, 3 and 4 weeks after stroke induction (figure 6.5).

The peri-infarct region or penumbra corresponds to moderately ischaemic tissue peripheral to the core of the infarct. Viable neurones can be found in this region and it is thought that suitable therapeutic intervention can salvage this tissue

(Astrup *et al.*, 1981; Hossman, 1994). This region is, however, metabolically demanding and if the energetic requirement is not met due to hypoperfusion, the lesion can expand into the penumbral zone (reviewed in van der Weerd *et al.*, 2004). Post-ischaemic neuroprotective strategies attempt to prevent such compromised tissue to progress to infarction. The posterior region (slices 7, 8, 9), could correspond to a penumbral zone that proceeds to infarction over time without intervention as seen in HSV-LacZ injected controls.

It is interesting to note that differences in lesion size in the posterior region became more apparent at 2 weeks after MCA occlusion in HSP27 treated animals. Differences in behavioural improvement between treated and untreated animals were more obvious at this timepoint in the total removal time (figure 6.8) and in the percentage of correct steps (figure 6.10) in particular, and this correlates to other experimental evidence. Stroke patients exhibit functional recovery over time and this has been associated with functional reorganization and plasticity in the brain. Animal studies using MRI to investigate functional activation after stroke in combination with behavioural tests have shown correlations between contralateral limb impairment and activation impairment in the lesioned cortex (Dijkhuizen *et al.*, 2001). An increase in activation in the contralateral hemisphere was observed at 3 days after stroke but was significantly reduced at 14 days after stroke, and this was accompanied by an increase in activation of the ipsilateral cortex. This and other studies support the idea that the activation shifts correspond to the contralateral hemisphere compensating for the sensorimotor deficit at early timepoints after stroke. The activation balance is then restored once the ipsilateral hemisphere recovers and reorganizes. Furthermore, a different study by the same group later established that the degree of injury determines the extent of activation shift to the contralateral hemisphere at early timepoints and that the extent of functional recovery over time is related to the preservation or restoration of activation in the lesioned hemisphere (Dijkhuizen *et al.*, 2003). In this context, the reduction in lesion size found in HSP27 treated animals in the present study could be associated with an increased preservation of function in the ipsilateral hemisphere and explain why these animals exhibit a behavioural improvement compared to untreated controls.

The mechanisms by which HSP27 could prevent cellular damage and therefore lesion size from expanding have been described in the previous section. However, certain experiments investigating the role of endogenous HSP27 highlight its involvement in plasticity. Astroglial expression of HSP27 has been observed in the immature and mature rat brain *in vivo* after different insults including ischaemia, excitotoxicity, axonal degeneration and photothrombotic injury, suggesting that this is a common defence mechanism in the brain (reviewed in Acarin *et al.*, 2002). Moreover, there is evidence supporting the role of HSP27 in protecting not only the cells where it is expressed (i.e. astroglia), but also the surrounding damaged tissue. Acarin and colleagues found HSP27 expression in the subthalamic nuclei secondarily damaged after excitotoxic cortical injury. This and other studies looking at HSP27 in epilepsy rat models, suggest there is a relationship between HSP27 expression and areas undergoing anatomical reorganization and axonal sprouting (Kato *et al.*, 1999). Such evidence, in conjunction with a reduction in lesion size, could explain the behavioural improvement observed in this study in HSP27 treated animals compared to untreated controls.

6.4.3 *Behavioural studies*

Physical and cognitive impairments ranging from mobility to communication deficits have been described in stroke patients (reviewed in Rose *et al.*, 1994; Hunter *et al.*, 1998). Hemineglect has been extensively investigated, as it is one of the most commonly reported sensorimotor impairments resulting from MCA occlusion in rats and humans (Andersen *et al.*, 1991; Markgraf *et al.*, 1992, 1994; Nudo *et al.*, 1999). Patients can in fact present tactile extinction and partial or total hemiparesis on the contralateral side of stroke. This impairment was detected by simultaneously stimulating both sides of the body and showing that the brain can process information from the ipsilateral side more efficiently (Heilman *et al.*, 1985; Rose *et al.*, 1994).

The bilateral asymmetry or "sticky label" test in rats detects the delay in removing the tape from the contralateral forepaw due to stroke-induced damage and

can be useful in relating experimental and clinical findings after MCA occlusion. This test was used together with the foot-fault test, which measures motor coordination, in order to evaluate the effects of HSP treatment on functional outcome up to one month after transient focal ischaemia. The results of the bilateral asymmetry test show that HSP27 treated animals become faster at removing the sticky tape from their left paw over time than LacZ injected controls, while HSP70 treated animals behave similarly to controls (figures 6.6, 6.7). Since the initial deficit was similar for all groups, this suggests that the HSP27 treated animals are able to change the tape removal strategy over time in order to solve the test more effectively. The foot-fault test indicates that HSP27 treated animals present a higher number of correct steps than controls at all timepoints assessed. In this case, the initial deficit was already reduced in HSP27 treated animals compared to HSP70 treated and LacZ injected controls (figure 6.10).

Several studies have found strong correlations between infarct size and neurobehaviour. Menzies and colleagues showed that neurological score scales could be reliably used to predict lesion size (Menzies *et al.*, 1992). Other studies found a linear relationship between the severity of the lesion with varying occlusion times and the degree of functional impairment in the foot-fault test (Rogers *et al.*, 1997). Neuroprotective experiments using a variety of drugs have further supported the correlation between reduction in lesion volume and improved sensorimotor function (Belayev *et al.*, 1995; Mackay *et al.*, 1996; Minematsu & Fisher, 1993). The behavioural work presented in this chapter is in agreement with the literature since improvements in sensorimotor tasks were accompanied by reduction in lesion size in HSP27 treated animals. Conversely, no improvement in deficit recovery or significant reduction in lesion size was observed control animals.

As mentioned in the introduction, some neuroprotection studies have suggested that behavioural outcome is not necessarily related to a decrease in lesion volume (Wahl *et al.*, 1992; Aronowski *et al.*, 1996; van der Staay *et al.*, 1996*a*). In this context, the lack of effect on lesion size observed in HSP70 treated animals did not rule out the possibility that the therapeutic intervention could have some effect on sensorimotor deficit recovery. HSP70 injected rats, however, presented similar

behaviour to LacZ injected controls, suggesting that this chaperone has no beneficial effect in this animal model of stroke.

6.4.6 *Conclusion*

In spite of the many experimental studies on the MCA occlusion model, efficient therapy for stroke is still lacking. Moreover, the increasing number of therapies attempting repair and regeneration has enhanced the need for investigation of functional outcome in clinical and experimental stroke. The study presented here addresses both these issues by evaluating the effects of HSP treatment on stroke on the basis of longitudinal non-invasive MRI measurements of lesion size and long term sensorimotor testing.

Consistent to the pre-ischaemic findings described in chapter 5, post-ischaemic viral delivery of HSP27 causes a reduction in lesion size that persists up to one month after transient focal cerebral ischaemia. Moreover, the foot-fault and bilateral asymmetry tests demonstrated that these animals present an increased ability to integrate sensory and motor responses over time compared to controls. No reduction in lesion size was observed in HSP70 treated animals and their performance on the behavioural tests over time was similar to that of untreated MCA occluded controls.

These results are in agreement with most of the literature on neurobehaviour and further support a correlation between reductions in functional impairment and in lesion size. The mechanisms underlying the protective effect of HSP27 *in vivo* have not been elucidated yet. A possible explanation is that the tissue that was salvaged by early therapeutic intervention with HSP27 undergoes some degree of functional reorganization that is absent in controls. The improvement in behavioural deficit observed might therefore reflect an enhancement in remodelling or connectivity in HSP27 treated animals compared to MCA occluded controls.

DISCUSSION

Chapter 7 *The neuroprotective effect of HSPs in vivo*

The work presented in this thesis investigates the hypothesis that gene therapy with heat shock proteins is protective in an experimental model of transient focal cerebral ischaemia. Moreover, it evaluates the relevance of combining MRI techniques, histology and behavioural tests to assess the effect of therapy *in vivo*.

The experiments described in chapter 4 deal with the spatio-temporal expression profile of the disabled HSV viral vector used. Expression of the LacZ transgene after intrastriatal microinjection was assessed in intact rats at six different timepoints ranging from 3 days to 1 month. The results confirmed that the virus was able to infect neurones *in vivo* and that it was expressed at high levels in the basal ganglia at all timepoints tested. Previous work had shown that the viral construct carrying HSP27 was able to express the protein *in vivo* after direct microinjection to the brain (Kalwy *et al.*, 2003). HSP70 expression was not tested and was assumed to be similar since the same backbone and promoter were used.

Chapter 5 details the effect of pre-ischaemic viral gene delivery in a transient middle cerebral artery occlusion model of stroke. While the neuroprotective effect of pre-ischaemic HSP70 expression had previously been investigated (Yenari *et al.*, 1998), the study here described was the first to report a significant reduction in lesion size after HSP27 treatment using MRI techniques. A four-fold increase in HSP27 and HSP70 expression was detected via histology in the ipsilateral hemisphere. However, in the present study, HSP70 treatment appeared to have no effect on lesion size as assessed by MRI at 24 hours. One previous study had found HSP27 to enhance hippocampal neurone survival in a kainic acid model of epilepsy in rats (Kalwy *et al.*, 2003) and one later experiment found HSP27 transgenic animals to be protected from permanent middle cerebral artery occlusion (van der Weerd, personal communication).

The effects of post-ischaemic HSP gene therapy in the same MCAO animal model were described in chapter 6. Once more, MRI images demonstrated that viral delivery of HSP27 at 30 minutes after reperfusion caused a reduction in lesion size, and that this persisted up to 1 month after stroke induction. The implication of such reduction was further evaluated via behavioural studies which confirmed that the degree of functional deficit in HSP27 treated animals was significantly less than in LacZ injected and MCA occluded controls. HSP70 treatment appeared to have no positive effect on lesion size or on sensorimotor tests.

It is biologically feasible that the number of denatured proteins upon stress exceeds the ability or rate at which the cell can repair such damage, thus leading to the formation of protein aggregates (Cohen *et al.*, 1999). Aggregates have been found to be associated with a number of conditions and attempts to use chaperones for the treatment of protein aggregation and misfolding have been made in neurodegenerative diseases, cancer and ischaemia (Hu *et al.*, 2000, 2001; Bonini *et al.*, 2002; Scott & Frydman 2003). The studies described in this thesis are consistent with previous *in vivo* work supporting HSP27 as a strong candidate for therapy in the rat brain (Kalwy *et al.*, 2003; van der Weerd *et al.*, personal communication).

Heat shock proteins act as inducible molecular chaperones, preventing changes in protein conformation, facilitating cell repair and mediating the delivery of proteins to their appropriate intracellular domain. Both of the HSPs used in this study have been extensively investigated *in vitro* and to a lesser extent *in vivo* in the brain and have been shown to be involved in a variety of protective mechanisms such as:

- mitochondrial membrane stabilization
- inhibition of apoptosis
- reduction of protein aggregation
- protein refolding
- alteration of protein kinase activity
- maintenance of normal cellular homeostasis
- cytoskeletal repair and reorganization

Chapter 1 has given a detailed account of the literature that has described these functions. Overall, experiments have focussed on either the upregulation of endogenous HSPs as a mechanism of cell defence after an insult, or on pre-insult expression of exogenous HSPs conferring protection against a subsequent insult. Consistent with the previous work, the purpose of the present study was to exploit and enhance an endogenous mechanism of cell survival upon ischaemic stress. The results are partially in agreement with the literature described, although current knowledge is insufficient to explain the differential protective effects observed.

HSP27 has been shown to have a potent anti-apoptotic effect *in vitro* and to significantly reduce cell death in stroke and epilepsy animal models *in vivo*. Similarly, the protective role of HSP70 has been long established in neuronal cell lines *in vitro* and to some extent in transgenics and virally transfected neurones *in vivo*. However, the results for HSP70 in the rat brain *in vivo* show more variability on the extent of protection, mostly improving neuronal morphology and/ or survival but only sometimes causing reductions in lesion size.

Although HSP27 has been associated with tissue remodelling more than HSP70 (Kato *et al.*, 1999; Acarin *et al.*, 2002), most of the functions listed above are shared by both chaperones. The most salient difference that could be relevant to this animal model is the dependence on ATP to exert chaperoning functions. As mentioned in previous chapters, ATP binds to the N terminus of HSP70 and induces a conformational change, locking the unfolded proteins. It is only through ATP hydrolysis that bound proteins can be released after being refolded. HSP27, on the other hand, does not require ATP to perform its chaperoning functions. The HSP70 refolding complex also recruits other co-chaperones, like HSP40, that help increase and stabilize the ATPase activity of HSP70. It is therefore plausible that overexpressing HSP70 on its own is not sufficient to enhance its protective function while other co-factors are not simultaneously available at the same levels, and this could explain the lack of protection observed in this study. However, previous experiments carried out *in vitro* in this laboratory have attempted co-transfection with viruses expressing HSP40 and HSP70 and did not observe an increase in protection in ND7 and B130/2 BHK cell lines subjected to a range of stresses such as

ischaemia and serum removal (Zourlidou *et al.* 2004, 2005). Moreover, the fact that some studies have identified the pro-apoptotic role of HSP70 suggest that this chaperone can have a detrimental role in the presence of specific molecules such as TNF (Ran *et al.*, 2004).

The importance and novelty of the work here described relies not only on the results of the individual studies but also on the experimental design. In fact, each of the individual techniques described has been previously used and it is the combinatorial approach taken that makes these findings more interesting.

MRI has been extensively used to investigate stroke both in research and clinical settings. MRI techniques can identify physiological and pathological changes in the brain that are reflected by alterations in the physical micro-environment of water in tissue (Knight *et al.*,1991; Gadian, 1995; Hoehn-Berlage *et al.*, 1995; van der Weerd *et al.*, 2004). Thus, MRI can detect changes occurring in the brain after ischaemia and evaluate the effect of therapeutic agents on structure and on metabolic and haemodynamic responses (chapter 2). Moreover, histological determination of lesion size by either tetrazolium chloride (TTC) or cresyl violet stains has been extensively correlated to imaging findings, implying that MRI techniques can be reliably used to determine lesion size non-invasively. Similarly, behavioural tests have been correlated to lesion size and widely used to evaluate recovery after stroke and the effect of neuroprotective drugs (see section 6.1.4).

The bimodal approach described in chapter 5, combining non-invasive MRI with histology, is certainly beneficial in the investigation of the pathophysiology and evolution of the ischaemic lesion after therapy. However, there is a limitation in trying to fully capture the complexity of damaging and repairing the brain by delineating a lesion area on a tissue section or scan, or by quantifying the number of necrotic neurones. This is why it is increasingly important to complement histological or MRI analysis with behavioural assessment in order to predict outcome or to evaluate the effect of stroke therapies. Impairment of behaviour detected by sensorimotor tests might reflect changes at a subcellular level, not only in morphology but also in synaptic function or electrophysiology of neurones.

This issue was directly addressed by the work described in chapter 6, where longitudinal MRI measurements of lesion size were related to functional recovery to evaluate the effects of post-ischaemic therapy. Many parameters had to be considered in these set of experiments, such as the model of stroke used, the route of delivery and dose of therapeutic agent applied, the sensitivity of the tests and methods used to evaluate the effect of therapy, and the timing of such assessment. This and other studies have highlighted the importance of choosing a battery of tests and scoring systems that can detect specific damage and be sensitive to differences according to the duration and areas affected by the stroke (see section 6.1.2). It has been suggested that long periods of ischaemia can damage the brain to such an extent that treatment appears ineffective, and this could explain why other studies with shorter times of occlusion find the same treatment to be protective (Aronowski *et al.*, 1994). Moreover, the timepoints of post-ischaemic assessment are also crucial since some reflexes and motor deficits have been shown to recover spontaneously. Some studies, for example, have observed recovery in the asymmetry test at 3 or 4 weeks after stroke, suggesting that the initial impairment might be related to the extent of cerebral oedema and that oedema reduction over time underlies the sensorimotor improvement detected (Aronowski *et al.*, 1996; Corbett & Nurse, 1998; Szentirmai & Carter, 2004).

The relevance of using gene therapy in experimental ischaemia is that it relates better to clinical scenarios. Other *in vivo* experiments in HSP27 and HSP70 transgenic animals have shown neuroprotection, but the therapeutic proteins were expressed before and after the insult and the possibility of a preconditioning phenomenon cannot be ruled out. The advantage of using gene therapy in this study is that it allowed to separately test whether pre-ischaemic and post-ischaemic HSP delivery had an effect on lesion size. Moreover, the work reported in this thesis benefits from the use of non-invasive neuroimaging techniques to determine cerebral blood flow and lesion size *in vivo*. This approach yields multiparametric data while significantly reducing the number of animals required if histological measurements were performed instead. This becomes more obvious when the data is acquired at several timepoints as described in chapter 6. Furthermore, the correlation with repeated neurological assessment on the same animals over time would have been technically demanding without non-invasive lesion size determination. Finally, a

further strength of the present study is the evaluation of behavioural deficits after stroke and therapy, an approach that is becoming increasingly important in relating pre-clinical and clinical neuroprotection studies.

Overall, these results significantly contribute to the ongoing stroke research by providing further support to the role of HSP27 as a major protective protein in the rat brain. However, this also highlights the need for further investigation of the mechanisms underlying such neuroprotection. Since the contribution of endogenous and exogenous HSP27 cannot be determined with current antibodies, it would be useful to engineer the viral vector further by inserting a marker gene such as LacZ in the same cassette as HSP27 in order to determine exact expression site. If the expression was more glial than neuronal it would in turn clarify the supportive role that is increasingly attributed to glial cells. Similarly, it would be interesting to investigate the lack of neuroprotection observed after HSP70 treatment. Following the line of research that identified the pro-apoptotic role of this chaperone, immunohistochemistry with apoptotic markers could be performed and compared to both HSP27 treated animals and controls. Moreover, only one post-ischaemic timepoint has been attempted in this study with encouraging results. A therapeutic window could be investigated by viral delivery of HSP genes at intermediate (2 hours) and long (5 hours) timepoints after ischaemia onset in order to establish the feasibility of this therapeutic approach in the clinical setting. Finally, once this window was defined, other strategies should be devised to circumvent the limitations of this therapeutic approach, mainly the duration of HSP overexpression and the route of administration.

References

Abe K, Kawagoe J, Araki T, Aoki M, Kogure K (1992) Differential expression of heat shock protein 70 gene between the cortex and caudate after transient focal cerebral ischaemia in rats. *Neurol Res* **14**:381-385

Acarin L, Paris J, Gonzalez B, Castellano B (2002) Glial expression of small heat shock proteins following an excitotoxic lesion in the immature rat brain. *Glia* **38**:1-14

Akbar MT, Lundberg AMC, Liu K, Vidyadaran S, Wells KE, Dolatshad H, *et al.* (2003) The neuroprotective effects of heat shock protein 27 overexpression in transgenic animals against kainate-induced seizures and hippocampal cell death. *J Biol Chem* **278**:19956-19965

Allegrini PR, Sauer D (1992) Application of magnetic resonance imaging to the measurement of neurodegeneration in rat brain: MRI data correlate strongly with histology and enzymatic analysis. *Magn Reson Imaging* **10**:773-778

Allen KL, Busza AL, Proctor E, King MD, Williams SR, *et al.* (1993) Controllable graded cerebral ischaemia in the gerbil: studies of cerebral blood flow and energy metabolism by hydrogen clearance and 31P NMR spectroscopy. *NMR Biomed* **6**:181-186

Alsop DC, Detre JA (1996) Reduced transit-time sensitivity in noninvasive magnetic resonance imaging of human cerebral blood flow. *J Cereb Blood Flow Metab* **16**:1236-1249

Amin V, Cumming DV, Latchman DS (1996) Overexpression of heat shock protein 70 protects neuronal cells against both thermal and ischemic stress but with different efficiencies. *Neurosci Lett* **206**:45-48

Andersen CS, Andersen AB, Finger S (1991) Neurological correlates of unilateral and bilateral "strokes" of the middle cerebral artery in the rat. *Physiol Behav* **50**:263-269

Aronowski J, Samways E, Strong R, Grotta JC (1994) A graded bioassay for demonstration of brain rescue from experimental acute ischaemia. *Stroke* **25**:2235-2240

Aronowski J, Samways E, Strong R, Rhoades HM, Grotta JC (1996) An alternative method for the quantitation of neurological damage after experimental middle cerebral artery occlusion in rats: analysis of behavioural deficit. *J Cereb Blood Flow Metab* **16**:705-713

Arrigo AP (1998) Small stress proteins: chaperones that act as regulators of intracellular redox state and programmed cell death. *Biol Chem* **379**:19-26

Arrigo AP, Virot S, Chaufour S, Firdaus W, Kretz-Remy C, *et al.* (2005) Hsp27 consolidates intracellular redox homeostasis by upholding glutathione in its reduced form and by decreasing iron intracellular levels. *Antiox Redox Signal* **7**:414-422

Aspey BS, Cohen S, Patel Y, Terruli M, Harrison MJG (1998) Middle cerebral artery occlusion in the rat: consistent protocol for a model of stroke. *Neuropath Appl Neurobiol* **24**:487-497

Astrup J, Siesjo BK, Symon L (1981) Thresholds in cerebral ischemia: the ischemic penumbra. *Stroke* **12**:723-725

Beaucamp N, Harding TC, Geddes BJ, Williams J, Uney J (1998) Overexpression of hsp70i facilitates reactivation of intracellular proteins in neurons and protects them from denaturing stress. *FEBS Letters* **441**:215-219

Beere HM, Wolf BB, Cain K, Mosser DD, Mahboubi A, Kuwana T, *et al.* (2000) Heat-shock protein 70 inhibits apoptosis by preventing recruitment of procaspase-9 to the Apaf-1 apoptosome. *Nat Cell Biol* **2**:469-475

Belayev L, Busto R, Zhao W, Ginsberg MD (1995) HU-211, a novel non-competitive N-methyl-d-aspartate antagonist, improves neurological deficit and reduces infarct volume after reversible focal ischaemia in the rat. *Stroke* **26**:2313-2320

Benderson JB, Pitts LH, Tsuji M, Nishimura MC, Davis RL, Bartkowski H (1986) Rat middle cerebral artery occlusion: evaluation of the model and development of a neurologic examination. *Stroke* **17**:472-476

Benn SC, Perrelet D, Kato AC, Scholz J, Decosterd I, Mannion RJ, *et al.* (2002) Hsp27 upregulation and phosphorylation is required for injured sensory and motor neuron survival. *Neuron* **36**:45-56

Ben-Zvi A, De Los Rios P, Dietler G, and Goloubinoff P (2004) Active solubilization and refolding of stable protein aggregates by cooperative unfolding action of individual HSP70 chaperones. *J Biol Chem* **279**:37298-37303

Bett AJ, Haddara W, Prevec L, Graham FL (1994) An efficient and flexible system for construction of adenovirus vectors with insertions or deletions in early regions 1 and 3. *Proc Natl Acad Sci* **91**:8802-8806

Blomer U, Naldini L, Kafri T, Trono D, Verma IM, Gage FH (1997) Highly efficient and sustained gene transfer in adult neurons with a lentivirus vector. *J Virol* **71**:6641-6649

Bonini NM (2002) Chaperoning brain degeneration. *Proc Natl Acad Sci USA* **99**:16407-16411

Bova MP, McHaourab HS, Han Y, Fung BK (2000) Subunit exchange of small heat shock proteins. Analysis of oligomer formation of alphaA-crystallin and Hsp27 by fluorescence resonance energy transfer and site-directed truncations. *J Biol Chem* **275**:1035-1042

Brint S, Jacewicz M, Kiessling M, Tanabe J, Pulsinelli W (1988) Focal brain ischemia in the rat: methods for reproducible neocortical infarction using tandem occlusion of the distal middle cerebral and ipsilateral common carotid arteries. *J Cereb Blood Flow Metab* **8**:474-85

Bruey JM, Ducasse C, Bonniaud P, Ravagnan L, Susin SA, Diaz-Latoud C *et al.* (2000) Hsp27 negatively regulates cell death by interacting with cytochrome *c*. *Nat Cell Biol* **2**:645-652

Burton EA, Bai Q, Goins WF, Glorioso JC (2002) Replication-defective genomic herpes simplex vector: design and production. *Curr Opin Biotechnol* **13**:424-428

Busch E, Kruger K, Hossmann KA (1997) Improved model of thromboembolic stroke and rt-PA induced reperfusion in the rat. *Brain Res* **778**:16-24

Busch E, Kruger K, Allegrini PR, Kerskens CM, Gyngell ML, *et al.* (1998) Reperfusion after thrombolytic therapy of embolic stroke in the rat: magnetic resonance and biochemical imaging. *J Cereb Blood Flow Metab* **18**:407-418

Busza AL, Allen KL, King MD, van Bruggen N, Williams SR, Gadian DG (1992) Diffusion-weighted imaging studies of cerebral ischemia in gerbils. Potential relevance to energy failure. *Stroke* **23**:1602-1612

Calamante F, Lythgoe MF, Pell GS, Thomas DL, King MD, Busza AL, *et al.* (1999*a*) Early changes in water diffusion, perfusion, T_1, and T_2 during focal cerebral ischaemia in the rat studied at 8.5 T. *Magn Reson Med* **41**:479-485

Calamante F, Thomas DL, Pell GS, Wiersma J, Turner R (1999*b*) Measuring cerebral blood flow using magnetic resonance imaging techniques. *J Cereb Blood Flow Metab* **19**:701-735

Carper SW, Rocheleau TA, Comino D, Storm FK (1997) Heat shock protein 27 stimulates recovery of RNA and protein synthesis following a heat shock. *J Cell Biochem* **66**:153-164

Charette SJ, Lavoie JN, Lambert H & Landry J (2000) Inhibition of Daxx-mediated apoptosis by heat shock protein 27. *Mol Cell Biol* **20**:7602-7612

Chen ST, Hsu CY, Hogan EL, Maricq H, Balentine JD (1986) A model of focal ischemic stroke in the rat: reproducible extensive cortical infarction. *Stroke* **17**:738-743

Chen J, Graham SH, Zhu RL, Simon RP (1996) Stress proteins and tolerance to focal cerebral ischemia. *J Cereb Blood Flow Metab* **16**:566-577

Chen J, Simon R (1997) Ischemic tolerance in the brain. *Neurology* **48**:306-311

Chiocca EA, Choi BB, Cai WZ, DeLuca NA, Schaffer PA, DiFiglia M, *et al.* (1990) Transfer and expression of the lacZ gene in rat brain neurons mediated by herpes simplex virus mutants. *New Biol* **2**:739-746

Choi-Lundberg DL, Lin Q, Chang YN, Chiang YL, Hay CM, Mohajeri H, *et al.* (1997) Dopaminergic neurons protected from degeneration by GDNF gene therapy. *Science* **275**:838-841

Coffin RS, Maclean AR, Latchman DS, Brown SM (1996) Gene delivery to the central and peripheral nervous systems of mice using HSV1 ICP34.5 deletion mutant vectors. *Gene Ther* **3**:886-891

Cohen FE (1999) Protein misfolding and prion diseases. *J Mol Biol* **293**:313-320

Concannon CG, Orrenius S, Samali A (2001) HSP27 inhibits cytochrome c-mediated caspase activation by sequestering both pro-caspase-3 and cytochrome c. *Gene Expr* **9**:195-201

Corbett D & Nurse S (1998) The problem of assessing effective neuroprotection in experimental cerebral ischemia. *Prog Neurobiol* **54**:531-548

Costigan M, Mannion RJ, Kendall G, Lewis SE, Campagna JA, Coggeshall RE, *et al.* (1998) Heat shock protein 27: developmental regulation and expression after peripheral nerve injury. *J Neurosci* **18**:5891-5900

Creagh EM, Carmody RJ, Cotter TG (2000) Heat shock protein 70 inhibits caspase-dependent and -independent apoptosis in Jurkat T cells. *Exp Cell Res* **257**:58-66

Davidson BL, Breakefield XO (2003) Viral vectors for gene delivery to the nervous system. *Nat Rev* **4**:353-364

de Courten Myers GM, Kleinholz M, Wagner KR, Myers RE (1998) Stroke assessment: morphometric infarct size versus neurologic deficit. *J Neurosci Meth* **83**:151-157

de Keyser J, Sulter G, Luiten PG (1999) Clinical trials with neuroprotective drugs in acute ischaemic stroke: are we doing the right thing? *Trends Neurosci* **22**:535-540

Detre JA, Leigh JS, Williams DS, Koretsky AP (1992) Perfusion imaging. *Magn Reson Med* **23**:37-45

Diaz-Latoud C, Buache E, Javouhey E, Arrigo AP (2005) Substitution of the unique cysteine residue of murine HSP27 interferes with the protective activity of this stress protein through inhibition of dimer formation. *Antiox Redox Signal* **7**:436-445

Dijkhuizen RM, Ren J, Mandeville JB, Wu O, Ozdag FM, *et al.* (2001) Functional magnetic resonance imaging of reorganization in rat brain after stroke. *Proc Nat Acad Sci USA* **98**:12766-12771

Dijkhuizen RM, Singhal AB, Mandeville JB, Wu O, Halpern EF, *et al.* (2003) Correlation between brain reorganization, ischaemic damage, and neurologic status after transient focal cerebral ischaemia in rats: a functional magnetic resonance imaging study. *J Neurosci* **23**:510-517

Dirnagl U, Iadecola C, Moskowitz (1999) Pathobiology of ischaemic stroke: an integrated view. *Trends Neurosci* **22**:391-397

Dirnagl U, Simon RP, Hallenbeck JM (2003) Ischemic tolerance and endogenous neuroprotection. *Trends Neurosci* **26**:248-254

Dobson AT, Margolis TP, Sederati F, Stevens JG, Feldman LT (1990) A latent, non-pathogenic HSV-1-derived vector stably expresses beta-galactosidase in mouse neurons. *Neuron* **5**:353-360

Doppler H, Storz P, Li J, Comb MJ & Toker A (2005) A phosphorylation state-specific antibody recognizes Hsp27, a novel substrate of protein kinase D. *J Biol Chem* **280**:15013-15019

Ecob-Prince MS, Hassan K, Denheen MT, Preston CM (1995) Expression of beta-galactosidase in neurons of dorsal root ganglia which are latently infected with herpes simplex virus type 1. *J Gen Virol* **76**:1527-1532

Edwards DP, Estes PA, Fadok VA, Bona BJ, Onate S, *et al.* (1992) Heat shock alters the composition of heterometric steroid receptor complexes and enhances receptor activity *in vivo*. *Biochemistry* **31**:2482-2491

Ehrnsperger M, Gräber S, Gaestel M, Buchner J (1997) Binding of non-native protein to Hsp25 during heat shock creates a reservoir of folding intermediates for reactivation. *EMBO J* **16**:221-229

Ehrnsperger M, Hergersberg C, Wienhues U, Nichtl A, Buchner J (1998) Stabilization of proteins and peptides in diagnostic immunological assays by the molecular chaperone Hsp25. *Anal Biochem* **259**:218-225

Ehrnsperger M, Gräber S, Gaestel M, Buchner J (2000) Analysis of chaperone properties of small Hsps. *Methods Mol Biol* **99**:421-429

Feder ME, Hofmann GE (1999) Heat Shock proteins, molecular chaperones and the stress response. *Ann Rev Physiol* **61**:243-282

Fink DJ, De Luca NA, Goins WF, Glorioso JC (1996) Gene transfer to neurons using herpes simplex virus-based vectors. *Ann Rev* **19**:265-287

Fink S, Chang L, Ho D, Sapolsky R (1997) Defective herpes simplex virus vectors expressing the rat brain stress-inducible heat shock protein 72 protect cultured neurons from severe heat shock. *J Neurochem* **68**:961-969

Fisher LJ, Jinnah HA, Kale LC, Higgins GA, Gage FH (1991) Survival and function of intrastriatally grafted primary fibroblasts genetically modified to produce L-dopa. *Neuron* **6**:371-80

Foster JA, Brown IR (1997) Differential induction of heat shock mRNA in oligodendrocytes, microglia, and astrocytes following hyperthermia. Brain Res Mol *Brain Res* **45**:207-218

Frampton AR, Goins WF, Nakano K, Burton EA, Glorioso JC (2005) HSV trafficking and development of gene therapy vectors with applications in the nervous system. *Gene Ther* **12**:891-901

Freeman BC, Myers MP, Schumacher R, Morimoto RI (1995) Identification of a regulatory motif in Hsp70 that affects ATPase activity, substrate binding and interaction with HDJ-1. *EMBO J* **14**:2281-2292

Freese A, Stern M, Kaplitt MG, O'Connor WM, Abbey MV, O'Connor MJ, *et al.* (1996) Prospects for gene therapy in Parkinson's disease. *Mov Disord* **11**:469-488

Gabai VL, Meriin AB, Mosser DD, Caron AW, Rits S, Shifrin VI, *et al.* (1997) Hsp70 prevents activation of stress kinases. A novel pathway of cellular thermotolerance. *J Biol Chem* **272**:18033-18037

Gadian DG (1995) *NMR and Its Applications to Living Systems*. Oxford University Press, Oxford

Garcia JH, Yoshida Y, Chen H, Li Y, Zhang ZG, *et al.* (1993) Progression form ischaemic injury to infarct following middle cerebral artery occlusion in the rat. *Am J Pathol* **142**:623-635

Garcia JH, Liu KF, Ho KL (1995) Neuronal necrosis after middle cerebral artery occlusion in Wistar rats progresses at different time intervals in the caudoputamen and the cortex. *Stroke* **26**:636-643

Garrido C, Ottavi P, Fromentin A, Hammann A, Arrigo AP, *et al.* (1997) HSP27 as a mediator of confluence-dependent resistance to cell death induced by anticancer drugs. *Cancer Res* **57**:2661-2667

Garrido C, Bruey JM, Fromentin A, Hammann A, Arrigo AP, Solary E (1999) HSP27 inhibits cytochrome *c*-dependent activation of procaspase-9. *FASEB J* **13**:2061-2070

Garrido C (2002) Size matters: of the small HSP27 and its large oligomers. *Cell Death Differentiation* **9**:483-485

Garrido C, Solari E (2003) A role of HSPs in apoptosis through "protein triage"? *Cell Death Diff* **10**:619-620

Giffard RG, Xu L, Zhao H, Carrico W, Ouyang Y *et al.* (2004) Chaperones, protein aggregation, and brain protection from hypoxic/ischemic injury. *J Experim Biol* **207**:3213-3220

Giffard RG, Yenari MA (2004) Many mechanisms for Hsp70 protection from cerebral ischaemia. *J Neurosurg Anesthesiol* **16**:53-61

Goins WF, Sternberg LR, Croen KD, Krause PR, Hendricks RL, Fink DJ, *et al.* (1994) A novel latency-active promoter is contained within the herpes simplex virus type 1 UL flanking repeats. *J Virol* **68**:2239-2252

Grabowski M, Brundin P, Johansson BB (1993) Paw-reaching, sensorimotor, and rotational behavior after brain infarction in rats. *Stroke* **24**:889-895

Guay J, Lambert H, Gingras-Breton G, Lavoie JN, Huot J, Landry J (1997) Regulation of actin filament dynamics by p38 map kinase-mediated phosphorylation of heat shock protein 27. *J Cell Sci* **110**:357-368

Guzhova I, Kislyakova K, Moskaliova O, Fridlanskaya I, Tytell M, Cheetham M, *et al.* (2001) *In vitro* studies show that Hsp70 can be released by glia and that exogenous Hsp70 can enhance neuronal stress tolerance. *Brain Res* **914**:66-73

Haase G, Kennel P, Pettmann B, Vigne E, Akli A, Revah F, *et al.* (1997) Gene therapy of murine motor neuron disease using adenoviral vectors for neurotrophic factors. *Nat Med* **3**:429-436

Hansen AJ (1985) Effect of anoxia on ion distribution in the brain. *Physiol Rev* **65**:101-48

Hansen RK, Parra I, Lemieux P, Oesterreich S, Hilsenbeck SG & Fuqua SA (1999) Hsp27 overexpression inhibits doxorubicin-induced apoptosis in human breast cancer cells. *Breast Cancer Res Treat* **56:**187–196

Hartl FU, Hayer-Hartl M (2002) Molecular chaperones in the cytosol: from nascent chain to folded protein. *Science* **295**:1852-1858

He B, Gross M, Roizman B (1997) The $\gamma_1$34.5 protein of herpes simplex virus 1 complexes with protein phosphatase 1α to dephosphorylate the α subunit of the eukaryotic translation initiation factor 2 and preclude the shutoff of protein synthesis by double-stranded RNA-activated protein kinase. *Proc Nat Acad Sci USA* **94**:843-848

Heilman KM, Watson RT, Valenstein E (1985) Neglect and related disorders. In: *Clinical neuropsychology*, pp. 243-294 (Eds KM Heilman and E Valenstein). Oxford University Press, New York, London

Herscovitch P, Raichle ME (1985) What is the correct value for the blood-brain partition coefficient for water? *J Cereb Blood Flow Metab* **5**:65-69

Hershko A, Ciechanover A (1998) The ubiquitin system. *Annu Rev Biochem* **67**:425-479

Higashi T, Takechi H, Uemura Y, Kikuchi H, Nagata K (1994) Differential induction of mRNA species encoding several classes of stress proteins following focal cerebral ischemia in rats. *Brain Res* **650**:239-248

Ho DY, Mocarski ES (1989) Herpes simplex virus latent RNA (LAT) is not required for latent infection in the mouse. Proc Natl Acad Sci USA 86:7596-7600

Hoehn B, Ringer TM, Xu L, Giffard RG, Sapolsky RM, Steinberg GK, *et al.* (2001) Overexpression of HSP72 after induction of experimental stroke protects neurons from ischemic damage. *J Cereb Blood Flow Metab* **21**:1303-1309

Hoehn-Berlage M, Eis M, Back T, Kohno K, Yamashita K (1995) Changes in relaxation times (T_1, T_2) and apparent diffusion coefficient after permanent middle cerebral artery occlusion in the rat: temporal evolution, regional extent and comparison with histology. *Magn Reson Med* **34**:824-834

Hossmann KA, Fischer M, Bockhorst K, Hoehn-Berlage M (1994) NMR imaging of the apparent diffusion coefficient (ADC) for the evaluation of metabolic suppression and recovery after prolonged cerebral ischemia. *J Cereb Blood Flow Metab* **14**:723-31

Hossmann KA (1998) Experimental models for the investigation of brain ischemia. *Cardiovasc Res* **39**:106-20

Howard MK, Kershaw T, Gibb B, Storey N, MacLean AR, Zeng B-Y, *et al.* (1998) High efficiency transfer to the central nervous system of rodents and primates using herpes virus vectors lacking functional ICP27 and ICP34.5. *Gene Ther* **5**:1137-1147

Hu BR, Janelidze S, Ginsberg MD, Busto R, Perez-Pinzon M, *et al.* (2001) Protein aggregation after focal brain ischemia and reperfusion. *J Cereb Blood Flow Metab* **21**:865-875

Hu BR, Martone ME, Jones YZ, Liu CL (2000). Protein aggregation after transient cerebral ischemia. *J Neurosci* **20**:3191-3199

Huang P, Gautschi M, Walter W, Rospert S, Craig EA (2005) The Hsp70 Ssz1 modulates the function of the ribosome-associated J-protein Zuo1. *Nat Struct Mol Biol* **12**:497-504

Hundley H, Walter W, Bairstow S, Craig EA (2005) Human Mpp11 J protein: ribosome-tethered molecular chaperones are ubiquitous. *Science* **308**:1032-1034

Hunter AJ, Green AR, Cross AJ (1995) Animal models of acute ischaemic stroke: can they predict clinically successful neuroprotective drugs? *Trends Pharmacol Sci* **16**:123-1128

Hunter AJ, Mackay KB, Rogers DC (1998) To what extent have functional studies of ischaemia in animals been useful in the assessment of potential neuroprotective agents? *Trends Pharmacol Sci* **19**:59-66

Hunter AJ Hatcher J, Virley D, Nelson P, Irving E, *et al.* (2000) Functional Assessments in mice and rats after focal stroke. *Neuropharmacology* **39**:806-816

Imaoka T, Date I, Miyoshi Y, Ono T, Furuta T, Asari S, *et al.* (1995) Preliminary results of gene transfer to central nervous system by continuous injection of DNA-liposome complex. *Cell Transplant* **4**:S23-26

Jaattela M, Wissing D, Kokholm K, Kallunki T, Egeblad M (1998) Hsp70 exerts its anti-apoptotic function downstream of caspase-3-like proteases. *EMBO J* **17**:6124-6134

Jakob U, Gaestel M, Engel K, Buchner J (1993) Small heat shock proteins are molecular chaperones. *J Biol Chem* **268**:1517-1520

Jessen KR (2004) Glial Cells. *Int J Biochem Cell Biol* **36**:1861-1867

Jiang Q, Zhang RL, Zhang ZG, Ewing JR, Divine GW, Chopp M (1998) Diffusion-, T2-, and perfusion-weighted nuclear magnetic resonance imaging of middle cerebral artery embolic stroke and recombinant tissue plasminogen activator intervention in the rat. *J Cereb Blood Flow Metab* **18**:758-767

Kabakov AE, Budagova KR, Latchman DS, Kampinga HH (2002) Stressful preconditioning and HSP70 overexpression attenuate proteotoxicity of cellular ATP depletion. *Am J Physiol Cell Physiol* **283**:C521-C534

Kalwy S, Akbar MT, Coffin RS, de Belleroche JS, Latchman DS (2003) Heat shock protein 27 delivered via a herpes simplex virus vector can protect neurones of the hippocampus against kainic-acid-induced cell loss. *Mol Brain Res* **111**:91-103

Kaplan B, Brint S, Tanabe J, Jacewicz M, Wang XJ, Pulsinelli W (1991) Temporal thresholds for neocortical infarction in rats subjected to reversible focal cerebral ischemia. *Stroke* **22**:1032-1039

Kato H, Liu Y, Kogure K, Kato K (1994) Induction of 27-kDa heat shock protein following cerebral ischemia in a rat model of ischemic tolerance. *Brain Res* **634**:235-244

Katschinski DM (2004) On heat and cells and proteins. *News Physiol Sci* **19**:11-15

Kawagoe J, Abe K, Sato S, Nagano I, Nakamura S, Kogure K (1992*a*) Distributions of heat shock protein-70 mRNAs and heat shock cognate protein-70 mRNAs after transient global ischemia in gerbil brain. *J Cereb Blood Flow Metab* **12**:794-801

Kawagoe J, Abe K, Kogure K (1992*b*) Different thresholds of HSP70 and HSC70 heat shock mRNA induction in post-ischemic gerbil brain. *Brain Res* **599**:197-203

Kawagoe J, Abe K, Kogure K (1993) Regional differences of HSP70 and HSC70 heat shock mRNA inductions in rat hippocampus after transient global ischemia. *Neurosci Lett* **153**:165-168

Kelly S, Bieneman A, Horsburgh K, Hughes D, Sofroniew MV, McCulloch J, *et al.* (2001*a*) Targeting expression of hsp70i to discrete neuronal populations using the *Lmo-1* promoter: assessment of the neuroprotective effects of hsp70i *in vivo* and *in vitro*. *J Cereb Blood Flow Metab* **21**:972-981

Kelly S, Uney JB, McCulloch J (2001*b*) Adenovirus HSP70 gene transfer ameliorates neuronal damage following ischemia. *J Cereb Blood Flow Metab* **21**:s22

Kelly S, Zhang ZJ, Zhao H, Xu L, Giffard RG, Sapolsky RM, *et al.* (2002) Gene transfer of HSP72 protects cornu ammonis 1 region of the hippocampus neurons from global ischemia: influence of Bcl-2. *Ann Neurol* **52**:160-167

Kelly S, Yenari MA (2002) Neuroprotection: heat shock proteins. *Curr Med Res Op* **18**:55-60

Kiang JG, Tsokos GC (1998) Heat shock protein 70 kDa: molecular biology, biochemistry and physiology. *Pharmacol Ther* **80**:183-201

Kinouchi H, Sharp FR, Hill MP, Koistinaho J, Sagar SM, Chan PH (1993) Induction of 70-kDa heat shock protein and HSP70 mRNA following transient focal ischaemia in the rat. *J Cereb Blood Flow Metab* **13**:105-115

Kirino T (2002) Ischemic tolerance. *J Cereb Blood Flow Metab* **22**:1283-1296

Kirino T, Tsujita Y, Tamura A (1991) Induced tolerance to ischemia in gerbil hippocampal neurons. *J Cereb Blood Flow Metab* **11**:299-307

Kitagawa K, Matsumoto M, Tagaya M, Hata R, Ueda H, Niinobe M, *et al.* (1990) 'Ischemic tolerance' phenomenon found in the brain. *Brain Res* **528**:21-24

Klatzo I (1987) Pathophysiological aspects of brain edema. *Acta Neuropathol* **72**:236-239

Knight RA, Ordidge RJ, Helpern JA, Chopp M, Rodolosi LC, Peck D (1991) Temporal evolution of ischemic damage in the rat brain measured by proton nuclear magnetic resonance imaging. *Stroke* **22**:802-808

Kohno K, Hoehn-Berlage M, Mies G, Back T, Hossmann KA (1995) Relationship between diffusion-weighted MR images, cerebral blood flow, and energy state in experimental brain infarction. *Magn Res Imaging* **13**:73-80

Koizumi J, Yoshida Y, Nakaqawa T, Ooneda G (1986) Experimental studies of ischaemic brain edema, I: a new experimental model of cerebral embolism in rats in which recirculation can be introduced in the ischemic area. *Jpn J Stroke* **8**:1-8

Krisky DM, Wolfe D, Goins WF, Marconi PC, Ramakrishnan R, Mata M, *et al.* (1998) Deletion of multiple immediate-early genes from herpes simplex virus reduces cytotoxicity and permits long-term gene expression in neurons. *Gene Ther* **5**:1593-1603

Lambert H, Charette SJ, Bernier AF, Guimond A, Landry J (1999) HSP27 multimerization mediated by phosphorylation-sensitive intermolecular interactions at the amino terminus. *J Biol Chem* **274**:9378-9385

Latchman DS (1998) Stress proteins: an overview. In: *Stress Proteins* (Latchman DS, ed) Springer-Verlag, New York

Latchman DS, Coffin RS (2000) Viral vectors in the treatment of Parkinson's disease. *Mov Disord* **15**:9-17

Latchman DS (2001) Gene delivery and gene therapy with herpes simplex virus-based vectors. *Gene* **264**:1-9

Latchman DS (2002) Herpes simplex virus vectors for gene delivery to a variety of different cell types. *Curr Gene Ther* **2**:415-426

Latchman DS (2004) Protective effects of heat shock proteins in the nervous system. *Curr Neurovasc Res* **1**:21-27

Lavoie JN, Hickey E, Weber LA, Landry J (1993) Modulation of actin microfilament dynamics and fluid phase pinocytosis by phosphorylation of heat shock protein 27. *J Biol Chem* **268**:24210-24214

Lawrence MS, Ho DY, Sun GH, Steinberg GK, Sapolsky RM (1996) Overexpression of Bcl-2 with herpes simplex virus vectors protects CNS neurons against neurological insults *in vitro* and *in vivo*. *J Neurosci* **16**:486-496

Lawrence MS, McLaughlin JR, Sun GH, Ho DY, McIntosh L, Kunis DM, *et al.* (1997) Herpes simplex viral vectors expressing Bcl-2 are neuroprotective when delivered after a stroke. *J Cereb Blood Flow Metab* **17**:740-744

Lee J, Yenari MA, Sun GH, Xu L, Emond MR, Cheng D, *et al.* (2001*a*) Differential neuroprotection from human heat shock protein 70 overexpression in *in vitro* and *in vivo* models of ischemia and ischemia-like conditions. *Exp Neurol* **170**:129-139

Lee SH, Kim M, Yoon BW, Kim YJ, Ma SJ, Roh JK, *et al.* (2001*b*) Targeted *hsp70.1* disruption increases infarction volume after focal cerebral ischemia in mice. *Stroke* **32**:2905-2912

Lee SH, Kim M, Kim YJ, Kim YA, Chi JG, *et al.* (2002) Ischaemic intensity influences the distribution of delayed infarction and apoptotic cell death following transient focal cerebral ischaemia in rats. *Brain Res* **956**:14-23

Lee YJ, Lee DH, Cho CK, Chung HY, Bae S, *et al.* (2005) HSP25 inhibits radiation-induced apoptosis through reduction of PCKdelta-mediated ROS production. *Oncogene* **24**:3715-3725

Levine S, Payan H (1966) Effects of ischemia and other procedures on the brain and retina of the gerbil (Meriones unguiculatus). *Exp Neurol* **16**:255-262

Lewis SE, Mannion RJ, White FA, Coggeshall RE, Beggs S, *et al.* (1999) A role for HSP27 in sensory neuron survival. *J Neurosci* **19**:8945-8953

Li CY, Lee JS, Ko YG, Kim JI, Seo JS (2000*a*) Heat shock protein 70 inhibits apoptosis downstream of cytochrome *c* release and upstream of caspase-3 activation *J Biol Chem* **275**:25665-25671

Li F, Liu KF, Silva MD, Omae T, Sotak CH, *et al.* (2000*b*) Transient and permanent resolution of ischemic lesions on diffusion-weighted imaging after brief periods of focal ischaemia in rats. *Stroke* **31**:946-954

Liberek K, Marszalek J, Ang D, Georgopoulos C, Zylicz M (1991) Escherichia coli DnaJ and GrpE heat shock proteins jointly stimulate ATPase activity of DnaK. *Proc Natl Acad Sci USA* **88**:2874-8

Lilley CE, Groutsi F, Han Z, Palmer JA, Anderson PN, Latchman DS, *et al.* (2001) Multiple Immediate-early gene-deficient herpes simplex virus vectors allowing efficient gene delivery to neurons in culture and widespread gene delivery to the central nervous system *in vivo*. *J Virol* **75**:4343-4356

Lindquist S. (1986) The heat-shock response. *Annu Rev Biochem* **55**:1151-1191

Lindquist S, Craig EA (1988) The heat-shock proteins. *Ann Rev Gen* **22**:631-677

Lo EH, Dlakara T, Moskowitz MA (2003) Mechanisms, challenges and opportunities in stroke. *Nat Rev Neurosci* **4**:399-414

Longa EZ, Weinstein PR, Carlson S, Cummins R (1989) Reversible middle cerebral artery occlusion without craniectomy in rats. *Stroke* **20**:84-91

Lu P, Jones FE, Saffran HA, Smiley JR (2001) Herpes simplex virus virion host shutoff protein requires a mammalian factor for efficient in vitro endoribonuclease activity. *J Virol* **75**:1172-1185

Lythgoe MF, Gadian DG (2000) Animal models of stroke studied by MRI. In: *Methods in biological magnetic resonance imaging and spectroscopy*, vol 2, p 904-914. (Eds: Young IR, Grant DM, Harris RK). John Wiley & Sons Ltd., London

Lythgoe MF, Sibson NR, Harris NG (2003) Neuroimaging of animal models of brain disease. *Br Med Bull* **65**:235-257

Lythgoe MF, Thomas DL, King MD, Pell GS, van der Weerd L, Ordidge RJ, Gadian DG (2005) Gradual changes in the apparent diffusion coefficient of water in selectively vulnerable brain regions following brief ischemia in the gerbil. *Magn Reson Med* **53**:593-600

Mackay KB, Bailey SB, King PD, Patel S, Hamilton TC, Campbell CA (1996) Neuroprotective effect of recombinant neutrophil inhibitory factor in transient focal cerebral ischaemia in the rat. *Neurodegeneration* **5**:319-323

MacLean AR, Ul-Fareed M, Robertson L, Harland J, Brown SM (1991) Herpes simplex virus type 1 deletion variants 1714 and 1716 pinpoint neurovirulence-related sequences in Glasgow strain 17+ between immediate early gene 1 and the 'a' sequence. *J Gen Virol* **72**:631-639

Mailhos C, Howard MK, Latchman DS (1994) Heat shock proteins hsp90 and hsp70 protect neuronal cells from thermal stress but not from programmed cell death. *J Neurochem* **63**:1787-1795

Mallouk Y, Vayssier-Taussat M, Bonventre JV, Polla BS (1999) Heat shock protein 70 and ATP as partners in cell homeostasis. *Int J Mol Med* **4**:463-474

Markgraf CG, Green EJ, Hurwitz BE, Morikawa E, Dietrich WD, *et al.* (1992) Sensorimotor and cognitive consequences of middle cerebral artery occlusion in rats. *Brain Res* **575**:238-246

Mayer MP & Bukau B (2005) Hsp70 chaperones: cellular functions and molecular mechanism. *Cell Molec Life Sci* **62**:670-684

Mayzel-Oreg O, Omae T, Kazemi M, Li F, Fisher M, Cohen Y, Sotak CH (2004) Microsphere-induced embolic stroke: an MRI study. *Magn Reson Med* **51**:1232-8

Mehlen P, Schulze-Osthoff K & Arrigo AP (1996) Small stress proteins as novel regulators of apoptosis: heat shock protein 27 blocks Fas/APO-1- and staurosporine-induced cell death. *J Biol Chem* **271**:16510–16514

Mehlen P, Hickey E, Weber LA, Arrigo AP (1997) Large unphosphorylated aggregates as the active form of hsp27 which controls intracellular reactive oxygen species and glutathione levels and generates a protection against TNFalpha in NIH-3T3-ras cells. *Biochem Biophys Res Commun* **241**:187-192

Menzies SA, Hoff JT, Betz AL (1992) Middle cerebral artery occlusion in rats: a neurological and pathological evaluation of a reproducible model. *Neurosurgery* **31**:100-106

Meriin AB, Yaglom JA, Gabai VL, Zon L, Ganiatsas S, Mosser DD, *et al.* (1999) Protein-damaging stresses activate c-Jun N-terminal kinase via inhibition of its dephosphorylation: a novel pathway controlled by HSP72. *Mol Cell Biol* **19**:2547-2555

Mies G, Ishimaru S, Xie Y, Seo K, Hossmann KA (1991) Ischemic thresholds of cerebral protein synthesis and energy state following middle cerebral artery occlusion in rat. *J Cereb Blood Flow Metab* **11**:753-761

Minematsu K, Fisher M (1993) MK-801 reduces extensive infarction after suture middle cerebral artery occlusion in rats. *Cerebrovasc Dis* **3**:99-104

Mitani K, Graham FL, Thomas Caskey C, Kochanek S (1995) Rescue, propagation, and partial purification of a helper virus-dependent adenovirus vector. *Proc Nat Acad Sci* **92**:3854-3858

Modo M, Stroemer RP, Tang E Veizovic T, Sowniski P, Hodges H (2000) neurological sequelae and long-term behavioural assessment of rats with transient middle cerebral artery occlusion. *J Neurosci Meth* **194**:99-109

Moncayo J, de Freitas GR, Bogousslavsky J, Altieri M, van Melle G (2000) Do transient ischaemic attacks have a neuroprotective effect? *Neurology* **54**:2089-2094

Morrison EE, Stevenson AJ, Wang YF, Meredith DM (1998) Differences in the intracellular localization and fate of herpes simplex virus tegument proteins early in the infection of Vero cells. *J Gen Virol* **79**:2517-2528

Moseley ME, Kucharczyk J, Mintorovitch J, Cohen Y, Kurhanewicz J, Derugin N, Asgari H, Norman D (1990) Diffusion-weighted MR imaging of acute stroke: correlation with T2-weighted and magnetic susceptibility-enhanced MR imaging in cats. *AJNR Am J Neuroradiol* **11**:423-429

Mosser DD, Caron AW, Bourget L, Meriin AB, Sherman MY, Morimoto RI, *et al.* (2000) The chaperone function of hsp70 is required for protection against stress-induced apoptosis. *Mol Cell Biol* **20**:7146-59

Muchowski PJ, Bassuk JA, Lubsen NH, Clark JI (1997) Human alphaB-crystallin. Small heat shock protein and molecular chaperone. *J Biol Chem* **272**:2578-82

Neumann-Haefelin T, Kastrup A, de Crespigny A, Yenari MA, Ringer T, Sun GH, Moseley ME (2000) Serial MRI after transient focal cerebral ischemia in rats: dynamics of tissue injury, blood-brain barrier damage, and edema formation. *Stroke* **31**:1965-1972

NINDS (The National Institute of Neurological Disorders and Stroke) rt-PA Stroke Study Group (1995) Tissue plasminogen activator for acute ischaemic stroke. *N Engl J Med* **333**:1581-1587

Nishi S, Taki W, Uemura Y, Higashi T, Kikuchi H, Kudoh H, *et al.* (1993) Ischemic tolerance due to the induction of HSP70 in a rat ischemic recirculation model. *Brain Res* **615**:281-288

Nishino K, Nowak TS (2004) Time course and cellular distribution of hsp27 and hsp72 stress protein expression in a quantitative gerbil model of ischemic injury and tolerance: thresholds for hsp72 induction and hilar lesioning in the context of ischemic preconditioning. *J Cereb Blood Flow Metab* **24**:167-178

Nudo RJ (1999) Recovery after damage to motor cortical areas. *Curr Op Neurobiol* **9**:740-747

Nudo RJ, Nelson RJ (2003) Animal models of stroke and rehabilitation. *ILAR J* **44**:81-82

Obrenovitch TP, Garofalo O, Harris RJ, Bordi L, Ono M, Momma F, *et al.* (1988) Brain tissue concentration of ATP, phosphocreatine, lactate, and tissue pH in relation to reduced cerebral blood flow following experimental acute middle cerebral artery occlusion. *J Cereb Blood Flow Metab* **8**:866-874

Ogawa S, Lee TM, Nayak AS, Glynn P (1990) Oxygenation-sensitive contrast in magnetic resonance image of rodent brain at high magnetic fields. *Magn Reson Med* **14**:68-78

O'Hare P (1993) The virion transactivator of herpes simplex virus. *Sem Virol* **4**:145-155

Okada M, Nakanishi H, Tamura A, Urae A, Mine K, Yamamoto K, Fujiwara M (1995) Long-term spatial cognitive impairment after middle cerebral artery occlusion in rats: no involvement of the hippocampus. *J Cereb Blood Flow Metab* **15**:1012-1021

Ordidge RJ, Helpern JA, Knight RA, Quing ZX, Welch KMA (1991) Investigation of cerebral ischaemia using magnetization transfer contrast (MTC) MR imaging. *Magn Reson Imaging* **9**:895-902

Palmer JA, Branston RH, Lilley CE, Robinson MJ, Groutsi F, Smith J, *et al.* (2000) Development and optimization of herpes simplex virus vectors for multiple long-term gene delivery to the peripheral nervous system. *J Virol* **74**:5604-5618

Pandey P, Farber R, Nakazawa A, Kumar S, Bharti A, Nalin C, *et al.* (2000) Hsp27 functions as a negative regulator of cytochrome *c*-dependent activation of procaspase-3. *Oncogene* **19**:1975-1981

Papadopoulos MC, Sun XY, Cao J, Mivechi NF, Giffard RG (1996) Over-expression of HSP-70 protects astrocytes from combined oxygen-glucose deprivation. *Neuroreport* **7**:429-432

Patel YJK, Payne Smith MD, de Belleroche J, Latchman DS (2005) Hsp27 and Hsp70 administered in combination have a potent protective effect against FALS-associated SOD1-mutant-induced cell death in mammalian neuronal cells. *Molec Brain Res* **134**:256-274

Paul C, Manero F, Gonin S, Kretz-Remy C, Virot S, Arrigo AP (2002) Hsp27 as a negative regulator of cytochrome *c* release. *Mol Cell Biol* **22**:816-834

Pavlik A, Aneja IS, Lexa J, Al-Zoabi BA (2003) Identification of cerebral neurons and glial cell types inducing heat shock protein Hsp70 following heat stress in the rat. *Brain Res* **973**:179-189

Paxinos G (1995) *The rat nervous system* (2nd edition). Academic Press, London, San Diego

Perng MD, Muchowski PJ, van den IJssel P, Wu GJ, Hutcheson AM, Clark JI, Quinlan RA (1999) The cardiomyopathy and lens cataract mutation in alphaB-crystallin alters its protein structure, chaperone activity, and interaction with intermediate filaments *in vitro*. *J Biol Chem* **274**:33235-33243

Persson L, Hardemark HG, Bolander HG, Hillered L, Olsson Y (1989) Neurologic and neuropathologic outcome after middle cerebral artery occlusion in rats. *Stroke* **20**:641-645

Pierpaoli C, Righini A, Linfante I, Tao-Cheng JH, Alger JR, Di Chiro G (1993) Histopathologic correlates of abnormal water diffusion in cerebral ischemia: diffusion-weighted MR imaging and light and electron microscopic study. *Radiology* **189**:439-448

Pivovarova AV, Mikhailova VV, Chernik IS, Chebotareva NA, Levitsky DI, Gusev NB (2005) Effects of small heat shock proteins on the thermal denaturation and aggregation of F-actin. *Biochem Biophys Res Commun* **331**:1548-1553

Plumier JC, Krueger AM, Currie RW, Kontoyiannis D, Kollias G, Pagoulatos GN (1997) Transgenic mice expressing the human inducible Hsp70 have hippocampal neurones resistant to ischemic injury. *Cell Stress Chap* **2**:162-167

Post LE, Roizman B (1981) A generalized technique for deletion of specific genes in large genomes: alpha gene 22 of herpes simplex virus 1 is not essential for growth. *Cell* **25**:227-232

Powers WJ (1991) Cerebral hemodynamics in ischaemic cerebrovascular disease. *Ann Neurol* **29**: 231-240

Pulsinelli WA, Brireley JB (1979) A new model of bilateral hemispheric ischemia in the unanesthetized rat. *Stroke* **10**:267-272

Rajdev S, Hara K, Kokubo Y, Mestril R, Dillman Weinstein PR, Sharp FR (2000) Mice overexpressing rat heat shock protein 70 are protected against cerebral infarction. *Ann Neurol* **47**:782-791

Ran R, Lu A, Zhang L, Tang Y, Zhu H, Xu H, *et al.* (2004) Hsp70 promotes TNF-mediated apoptosis by binding IKKγ and impairing NF-κB survival signaling. *Genes Dev* **18**:1466-1481

Rashmi R, Santhosh Kumar TR, Karunagaran D (2003) Human colon cancer cells differ in their sensitivity to curcumin-induced apoptosis and heat shock protects them by inhibiting the release of apoptosis-inducing factor and caspases. *FEBS Lett* **538**:19-24

Ravagnan L, Gurbuxani S, Susin SA, Maisse C, Daugas E, Zamzami N, *et al.* (2001) Heat-shock protein 70 antagonizes apoptosis-inducing factor. *Nat Cell Biol* **3**:839-843

Rebel A, Koehler RC and Martin LJ (2005) In situ immunoradiographic method for quantification of specific proteins in normal and ischaemic brain regions. *J Neurosci Meth* **143**:227-235

Richter-Landsberg C, Goldbaum O (2003) Stress proteins in neural cells: functional roles in health and disease. *Cell Mol Life Sci* **60**:337-349

Riordan M, Sreedharan R, Wang S, Thulin G, Mann A, *et al.* (2005) HSP70 binding modulates detachment of Na-K-ATPase following energy deprivation in renal epithelial cells. *Am J Physiol Renal Physiol* **288**:F1236-F1242

Ritossa FA (1962) A new puffing pattern induced by temperature shock and DNP in Drosophila. *Experimentia* **18**:571-573

Robertson LM, MacLean AR, Brown SM (1992) Peripheral replication and latency reactivation kinetics of the non-neurovirulent herpes simplex virus type 1 variant 1716. *J Gen Virol* **73**:967-970

Roberts TPL, Vexler ZS, Vexler V, Derugin N, Kucharczyk J (1996) Sensitivity of high-speed "perfusion-sensitive" magnetic resonance imaging to mild cerebral ischemia. *Eur Radiol* **6**:645-649

Rogalla T, Ehrnsperger M, Preville J, Kotlyarov A, Lutsch G, Ducasse C, *et al.* (1999) Regulation of Hsp27 oligomerization, chaperone function, and protective activity against oxidative stress/tumor necrosis factor α by phosphorylation. *J Biol Chem* **274**:18947-18956

Rogers DC, Campbell CA, Stretton JL, Mackay KB (1997) Correlation between motor impairment and infarct volume after permanent and transient middle cerebral artery occlusion in the rat. *Stroke* **28**:2060-2066

Roizman B, Sears AE (1987) An inquiry into the mechanisms of herpes simplex virus latency. *Annu Rev Microbiol* **41**:543-571

Roizman B, Sears AE (1996) Herpes simplex viruses and their replication. In: *Fields Virology*, 3rd edition, pp. 2231-2295 (Eds: Fields NB, Knipe DM, Howley PM). Lippincott-Raven, Philadelphia

Rose L, Bakal DA, Fung TS, Farn P, Weaver LE (1994) Tactile extinction and functional status after stroke. A preliminary investigation. *Stroke* **25**:1973-1976

Sacks WR, Schaffer PA (1987) Deletion mutants in the gene encoding the herpes simplex virus type 1 immediate-early protein ICP0 exhibit impaired growth in cell culture. *J Virol* **61**:829-839

Sakai N, Yanai K, Ryu JH, Nagasawa H, Hasegawa T, Sasaki T, *et al.* (1996) Behavioral studies on rats with transient cerebral ischemia induced by occlusion of the middle cerebral artery. *Behav Brain Res* **77**:181-188

Saleh A, Srinivasula SM, Balkir L, Robbins PD, Alnemri ES (2000) Negative regulation of the Apaf-1 apoptosome by Hsp-70. *Nat Cell Biol* **2**:476-483

Samali A, Cotter TG (1996) Heat shock proteins increase resistance to apoptosis. *Exp Cell Res* **223**:163-170

Samali A, Zhivotovsky B, Jones D, Nagata S, Orrenius S (1999) Apoptosis: cell death defined by caspase activation. *Cell Death Differ* **6**:495-496

SAS Institute (1999) SAS/STAT user's guide, Version 8. SAS Institute, Cary, North Carolina

Sato K, Saito H, Matsuki N (1996) HSP70 is essential to the neuroprotective effect of heat-shock. *Brain Res* **740**:117-123

Schaller B, Graf R, Jacobs AH (2003) Ischaemic tolerance: a window to endogenous neuroprotection? *Lancet* **362**:1007-1008

Schaller B (2005) Ischaemic preconditioning as induction of ischaemic tolerance after transient ischaemic attacks in human brain: its clinical relevance. *Neurosci Lett* **377**:206-211

Schallert T, Upchurch M, Lobaugh N, Farrar SB (1982) Tactile extinction: distinguishing between sensorimotor and motor asymmetries in the rats with unilateral nigrostriatal damage. *Pharmacol Biochem Behav* **16**:455-462

Scott MD, Frydman J (2003). Aberrant protein folding as the molecular basis of cancer. *Methods Mol Biol* **232:**67-76

Sharp F, Massa SM, Swanson, RA (1999) Heat shock protein protection. *Trends Neurosci* **22**:97-99

Sheller RA, Bittner GD (1992) Maintenance and synthesis of proteins for an anucleate axon. *Brain Res* **580**:68-80

Shen Q, Fisher M, Sotak CH, Duong TQ (2004) Effects of reperfusion on ADC and CBF pixel-by-pixel dynamics in stroke: characterizing tissue fates using quantitative diffusion and perfusion imaging. *J Cereb Blood Flow Metab* **24**:280-290

Shigeno T, Teasdale GM, McCulloch J, Graham DI (1985) Recirculation model following MCA occlusion in rats. Cerebral blood flow, cerebrovascular permeability, and brain edema. *J Neurosurg* **63**:272-277

Simon RP, Cho H, Gwinn R, Lowenstein DH (1991) The temporal profile of 72-kDa heat-shock protein expression following global ischemia. *J Neurosci* **11**:881-889

Simon RP, Niiro M, Gwinn R (1993) Prior ischemic stress protects against experimental stroke. *Neurosci Lett* **163**:135-137

Small DL, Buchan AM (2000) Animal models. *Br Med Bull* **56**:307-317

Smith MD, Melton LA, Ensor EA, Packham G, Anderson P, Kinloch RA, *et al.* (2001) Brn-3a activates the expression of Bcl-x(L) and promotes neuronal survival *in vivo* as well as *in vitro*. *Mol Cell Neurosci* **17**:460-470

Steel R, Doherty JP, Buzzard K, Clemons N, Hawkins CJ, Anderson RL (2004) Hsp72 inhibits apoptosis upstream of the mitochondria and not through interactions with Apaf-1. *J Biol Chem* **279**:51490-51499

Stingley SW, Ramirez JJ, Aguilar SA, Simmen K, Sandri-Goldin RM, Ghazal P, *et al.* (2000) Global analysis of herpes simplex virus type 1 transcription using an oligonucleotide-based DNA microarray. *J Virol* **74**:9916-9927

Stroemer RP, Kent TA, Hulsebosch CE (1995) Neocortical neural sprouting, synaptogenesis, and behavioral recovery after neocortical infarction in rats. *Stroke* **26**:2135-2144

Szentirmai O, Carter BS (2004) Genetic and cellular therapies for cerebral infarction. *Neurosurgery* **55**:283-296

Takayama S, Reed JC, Homma S (2003) Heat shock proteins as regulators of apoptosis. *Oncogene* **22**:9041-9047

Tamura A, Graham DI, McCulloch J, Teasdale GM (1981) Focal cerebral ischaemia in the rat: 1. Description of technique and early neuropathological consequences following middle cerebral artery occlusion. *J Cereb Blood Flow Metab* **1**:53-60

Tandrup T, Woolf CJ, Coggeshall RE (2000) Delayed loss of small dorsal root ganglion cells after transection of the rat sciatic nerve. *J Comp Neurol* **422**:172-180

Taylor JP, Hardy J, Fischbeck KH (2002) Toxic proteins in neurodegenerative disease. *Science* **296**:1991-1995

Taylor RP & Benjamin IJ (2005) Small heat shock proteins: a new classification scheme in mammals. *J Molec Cell Card* **38**:433-444

Tissieres A, Mitchell HK, Tracy UM (1974) Protein synthesis in salivary glands of Drosophila melanogaster: relation to chromosome puffs. *J Mol Biol* **84**:389-398

Theriault JR, Lambert H, Chavez-Zobel AT, Charest G, Lavigne P, Landry J (2004) Essential role of the NH2-terminal WD/EPF motif in the phosphorylation-activated protective function of mammalian Hsp27. *J Biol Chem* **279**:23463-23471

Thomas SK, Lilley CE, Latchman DS, Coffin RS (1999) Equine herpesvirus 1 gene 12 can substitute for vmw65 in the growth of herpes simplex virus (HSV) type 1, allowing the generation of optimized cell lines for the propagation of HSV vectors with multiple immediate-early gene defects. *J Virol* **73**:7399-7409

Thomas DL, Lythgoe MF, Pell GS, Calamante F, Ordidge RJ (2000) The measurement of diffusion and perfusion in biological systems using magnetic resonance imaging. *Phy Med Biol* **45**:r97-138

Tidwell JL, Houenou LJ, Tytell M (2004) Administration of Hsp70 *in vivo* inhibits motor and sensory neuron degeneration. *Cell Stress Chap* **9**:88-98

Tsuchiya D, Hong S, Matsumori Y, Kayama T, Swanson RA, Dillman WH, *et al.* (2003) Overexpression of rat heat shock protein 70 reduces neuronal injury after transient focal ischemia, transient global ischemia, or kainic acid-induced seizures. *Neurosurgery* **53**:1179-1188

Tsuda M, Imaoka T (1996) Direct injection of plasmid DNA into the brain. In: *Genetic manipulation of the nervous system*, pp.235-248 (Ed. Latchman DS). Academic Press, London

Tytell M, Greenberg SG, Lasek RJ (1986) Heat shock-like protein is transferred from glia to axon. *Brain Res* **363**:161-164

Uney JB, Kew JN, Staley K, Tyers P, Sofroniew MV (1993) Transfection-mediated expression of human hsp70i protects rat dorsal root ganglia neurones and glia from severe heat stress. *FEBS Lett* **334**:313-316

Van Bruggen N, Cullen BM, King MD, Doran M, Williams SR, Gadian DG, Cremer JE (1992) T2- and diffusion-weighted magnetic resonance imaging of a focal ischemic lesion in rat brain. *Stroke* **23**:576-82

Van Bruggen N, Roberts TP, Cremer JE (1994) The application of magnetic resonance imaging to the study of experimental cerebral ischaemia. *Cerebrovasc Brain Metab Rev* **6**:180-210

Van der Staay FJ, Augstein KH, Horvath E (1996*a*) Sensorimotor impairments in rats with cerebral infarction, induced by unilateral occlusion of the left middle

cerebral artery: strain differences and effects of the occlusion site. *Brain Res* **735**:271-284

Van der Staay FJ, Augstein KH, Horvath E (1996*b*) Sensorimotor impairments in Wistar Kyoto rats with cerebral infarction, induced by unilateral occlusion of the middle cerebral artery: recovery of function. *Brain Res* **715**:180-188

Van der Toorn A, Dijkhuizen RM, Tulleken CA, Nicolay K (1996) Diffusion of metabolites in normal and ischemic rat brain measured by localized 1H MRS. *Magn Reson Med* **36**:914-22

Van der Weerd L, Thomas DL, Lythgoe MF, Thornton JS (2004) MRI models of brain disease. In: *Imaging in Biological Research.* Methods in Enzymology. Elsevier Academic Press, London

Van der Weerd L, Lythgoe MF, Aron Badin R, Valentim L, Akbar TM, de Belleroche JS, *et al.* (2005) Neuroprotective effects of HSP70 overexpression after cerebral ischemia – an MRI study. *Exp Neurol* **195**:257-266

Van Dorsten FA, Olah L, Schwindt W, Grune M, Uhlenkuken U, Pillekamp F, *et al.* (2002) Dynamic changes of ADC, perfusion, and NMR relaxation parameters in transient focal ischaemia of rat brain. *Magn Reson Med* **47**:97-104

Van Lookeren Campagne M, Thomas GR, Thibodeaux H, Palmer JT, Williams SP, *et al.* (1999) Secondary reduction in the apparent diffusion coefficient of water, increase in cerebral blood volume, and delayed neuronal death after middle cerebral artery occlusion and early reperfusion in the rat. *J Cereb Blood Flow Metab* **19**:1354-1364

Verma IM, MD Weitzman (2005) Gene Therapy: twenty-first century medicine. *Ann Rev Biochem* **74**: 711-738

Virley D, Beech JS, Smart SC, Williams SCR, Hodges H, Hunter AJ (2000) A temporal MRI assessment of neuropathology following transient MCAO in the rat: correlations with behaviour. *J Cereb Blood Flow Metab* **20**:563-582

Wagner EK, Guzowski JF, Singh J (1995) Transcription of the herpes simplex virus genome during productive and latent infection. *Prog Nucleic Acid Res Mol Biol* **51**:123-165

Wagstaff M, Collaço-Moraes Y, Aspey BS, Coffin RS, Harrison MJG, Latchman DS, *et al.* (1996) Focal cerebral ischemia increases the levels of several classes of heat shock proteins and their corresponding mRNAs. *Molec Brain Res* **42**:236-244

Wagstaff M, Lilley CE, Smith J, Robinson MJ, Coffin RS, Latchman DS (1998) Gene transfer using a disabled herpes virus vector containing the EMCV IRES allows multiple gene expression *in vitro* and *in vivo*. *Gene Ther* **5**:1566-1570

Wagstaff M, Collaço-Moraes Y, Smith J, de Belleroche JS, Coffin RS, Latchman DS (1999) Protection of neuronal cells from apoptosis by hsp27 delivered with a herpes simplex virus-based vector. *J Biol Chem* **274**:5061-5069

Ward NM, Sharkey J, Brown VJ (1997) Assessment of sensorimotor neglect after occlusion of the middle cerebral artery in the rat. *Behav Neurosci* **111**:1133-1145

Wahl F, Allix M, Plotkine M, Boulu RG (1992) Neurological and behavioral outcomes of focal cerebral ischemia in rats. *Stroke* **23**:267-272

Wegele H, Muller L, Buchner J (2004) Hsp70 and Hsp90-a relay team for protein folding. *Rev Physiol Biochem Pharmacol* **151**:1-44

Wegener S, Gottschalk B, Jovanovic V, Knab R, Fiebach JB, *et al.* (2004) Transient ischemic attacks before ischemic stroke: preconditioning the human brain? *Stroke* **35**:616-621

Weih M, Kallenberg K, Bergk A, Dirnagl U, Harms L *et al.* (1999) Attenuated stroke severity after prodromal TIA: a role for ischaemic tolerance in the brain? *J Cereb Blood Flow Metab* **22**:1283-1296

Weir JP (2001) Regulation of herpes simplex virus gene expression. *Gene* **271**:117-130

Welsh FA, Moyer DJ, Harris VA (1992) Regional expression of heat shock protein-70 mRNA and c-fos mRNA following focal ischemia in rat brain. *J Cereb Blood Flow Metab* **12**:204-212

Whitlock A, Lindsey K, Agarwal N, Crosson CE, Ma JX (2005) Heat shock protein 27 delays Ca^{2+}-induced cell death in a caspase-dependent and -independent manner in rat retinal ganglion cells. *Invest Ophthalmol Vis Sci* **46**:1085-1091

Whittaker GA, Kann M, Helenius A (2000) Viral entry into the nucleus. *Ann Rev Cell Dev Biol* **16**:627-651

Williams KL, Rahimtula M, Mearow KM (2005) Hsp27 and axonal growth in adult sensory neurons *in vitro*. *BMC Neurosci* **6**:1-44

Willis D, Li KW, Zheng JQ, Chang JH, Smit A, Kelly T, *et al.* (2005) Differential transport and local translation of cytoskeletal, injury-response, and neurodegeneration protein mRNA in axons. *J Neurosci* **25**:778-791

Wolfe D, Goins WF, Yamada M, Moriuchi S, Krisky DM, Oligino TJ, *et al.* (1999) Engineering Herpes simplex virus vectors for CNS applications. *Exp Neurol* **159**:34-46

Wood NI, Sopesen BV, Roberts JC, Panbakian P, Rothaul AL, *et al.* (1996) Motor disfunction in a photothrombotic ischaemia model. *Behav Brain Res* **78**:113-120

Wyatt S, Mailhos C, Latchman DS (1996) Trigeminal ganglion neurons are protected by the heat shock proteins hsp70 and hsp90 from thermal stress but not from

programmed cell death following nerve growth factor withdrawal. *Mol Brain Res* **39**:52-56

Xie Y, Mies G, Hossmann KA (1989) Ischemic threshold of brain protein synthesis after unilateral carotid artery occlusion in gerbils. *Stroke* **20**:620-626

Xu L, Giffard RG (1997) HSP70 protects murine astrocytes from glucose deprivation injury. *Neurosci Lett* **224**:9-12

Yamada M, Oligino T, Mata M, Goss JR, Glorioso JC, Fink DJ (1999) Herpes simplex virus vector-mediated expression of Bcl-2 prevents 6-hydroxydopamine-induced degeneration of neurons in the substantia nigra *in vivo*. *Proc Natl Acad Sci USA* **96**:4078-4083

Yamamoto M, Tamura A, Kirino T, Shimizu-Sasamata M, Sano K (1991) Effects of thyrotropin-releasing hormone on behavioral disturbances in middle cerebral artery-occluded rats. *Eur J Pharmacol* **197**:117-123

Yang Y, Nunes FA, Berencsi K, Furth EE, Gonczol E, Wilson JM (1994) Cellular immunity to viral antigens limits E1-deleted adenoviruses for gene therapy. *Proc Natl Acad Sci USA* **91**:4407-4411

Yenari M, Fink SL, Sun GH, Chang LK, Patel MK, Kunis DM, *et al.* (1998) Gene therapy with HSP72 is neuroprotective in rat models of stroke and epilepsy. *Ann Neurol* **44**:584-591

Yenari M, Giffard RG, Sapolsky RM, Steinberg GK (1999) The neuroprotective potential of heat shock protein 70 (HSP70). *Molec Med Today* **5**:525-531

Yenari MA, Dumas TC, Sapolsky RM, Steinberg GK (2001) Gene therapy for treatment of cerebral ischemia using defective herpes simplex viral vectors. *Neurol Res* **23**:543-552

Yenari M (2002) Heat shock proteins and neuroprotection. In: *Molecular Cellular Biology of Neuroprotection in the CNS* (Alzheimer C, ed), Kluwer Academic/Plenum Publishers: London, 281-299

Young JC, Agashe VR, Siegers K & Hartl U (2004) Pathways of chaperone-mediated protein folding in the cytosol. *Nat Rev Mol Cell Biol* **5**:781-791

Zourlidou A, Payne Smith MD, Latchman DS (2004) HSP27 but not HSP70 has a potent protective effect against α-synuclein-induced cell death in mammalian neuronal cells. *J Neurochem* **88**:1439-1448

Zourlidou A (2005) Analysis of mutation in alpha-synuclein and the protective effect of heat shock proteins in a model of alpha-synuclein induced toxicity. Thesis submitted for the degree of Doctor in Philosophy.

Zhang WG, Williams DS, Detre JA, Koretsky AP (1992) Measurement of brain perfusion by volume-localized NMR spectroscopy using inversion of arterial water spins: accounting for transit time and cross-relaxation. *Magn Reson Med* **25**:362-371

Zhang WG, Silva AC, Williams DS, Koretsky AP (1995) NMR measurement of perfusion using arterial spin labeling without saturation of macromolecular spins. *Magn Reson Med* **33**:370-376